CellPress

Matter

Review

Wavelength-selective light-matter interactions in polymer science

Pengtao Lu,[1,5] Dowon Ahn,[1,5] Ruhamah Yunis,[2,3] Laura Delafresnaye,[2,3] Nathaniel Corrigan,[4] Cyrille Boyer,[4,*] Christopher Barner-Kowollik,[2,3,*] and Zachariah A. Page[1,*]

SUMMARY

Light has emerged as a prominent stimulus to both generate and manipulate polymeric materials across multiple length scales. Compared with other external stimuli, light-mediated approaches enable unprecedented control over when and where chemical transformations occur (i.e., spatiotemporal control). To date, the majority of established protocols rely on individual wavelengths of light (∼monochromatic), which does not harness the full potential of light-matter interactions. This review summarizes the nascent progress in utilizing multiple discrete wavelengths of light as a tool to create and alter soft matter. The concepts are structured in an effort to provide a roadmap to foster new directions in light-based polymer materials chemistry. The physical organic nature of wavelength selectivity is first detailed in the introduction to provide key mechanistic insight and lay a foundation for further developments. Next, an overview of chromophores that undergo various light-driven transformations is presented, followed by their utility in polymer platforms for controlled synthesis, property manipulation, and advanced manufacturing. The review concludes with a summary and outlook on the exciting future of wavelength-selective light-matter interactions in polymer science.

INTRODUCTION

Throughout history, there have been several dramatic paradigm shifts in the understanding of light-matter interactions (Figure 1).[1] In the 1700s, Newton passed sunlight through a prism and from this experiment deduced that light was a stream of particles. In the second half of the 19th century, Maxwell described light as electromagnetic waves using a set of elegant equations (Maxwell's equations). In 1905, Einstein built on Planck's theory of energy quanta by categorizing light as quantized (photons) to explain the "photoelectric effect," which is the phenomenon describing the emission of electrons upon interaction with electromagnetic radiation, such as light.[2] This ultimately led to the recognition of the wave-particle duality of light by de Broglie in 1924.[3] Together, these transformative discoveries connected photon energy (E) to the wavelength (λ) of the corresponding electromagnetic wave (Equation 1).

$$E = \frac{hv}{\lambda} \quad \text{(h: Planck's constant; v: speed of light in vacuum)} \qquad \text{(Equation 1)}$$

The practical applications of light date back to 1826, when a discovery by Joseph Nicéphore Niépce resulted in the first permanent image from nature.[4] It was also the first time that light was demonstrated to give control over where and when a chemical reaction occurs (spatiotemporal control). Today, light plays a central role

Progress and potential

Light has provided unparalleled control over when and where chemical transformations take place (spatiotemporal control), yet a third dimension has emerged where the incident color of light can tailor reactivity, termed here spectral control. Wavelength-selectivity in polymer science has been influenced by pioneering reports in light-driven isomerization (photoswitches), deprotection (photocages), coupling (cycloaddition/-reversion), and electron/energy transfer (photoredox/-sensitization), which has enabled both soft matter fabrication and property manipulation (e.g., mechanical, optical, and electrical). Advancing and utilizing wavelength-selective transformations will rely on (1) characterizing photochemical reactions quantitatively as a function of wavelength, (2) introducing new reactive chromophores, (3) expanding the mechanistic scope in manufacturing beyond light-induced radical reactions, and (4) manipulating material properties outside mechanical. Going forward, these transformations will facilitate the design and fabrication of next-generation "smart" materials, which have advanced properties tailored for applications that range from

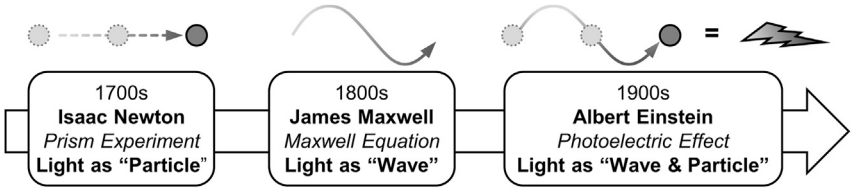

Figure 1. The paradigm shift on the nature of light throughout history

in a myriad of commercialized and emergent technologies, from photography, coatings, and adhesives to microelectronics and three-dimensional (3D) printing.

Since the inception of these everlasting discoveries, light-driven chemistry, or molecular photochemistry, has been the subject of immense research efforts, especially in the development of chromophores, or compounds that demonstrate a distinct interaction (e.g., absorption and/or scattering) with discrete wavelengths of light.[5] Mechanistically, absorption of photons raises chromophores to a higher energy excited state capable of undergoing various chemical transformations (Scheme 1). Compared with other stimuli (redox, heat, pH, and electricity), photoexcitation affords unparalleled spatiotemporal control (Scheme 1), while additionally offering an avenue toward wavelength-selective reactivity, termed here spectral control.[6]

In the last few decades, there have been substantial advances in both the synthesis and characterization of new chromophores. However, the majority of established photochemical protocols utilize a single non-discrete broadband light (i.e., emission across the UV and visible spectra) or near monochromatic light (i.e., emission with a narrow wavelength distribution, such as from a light-emitting diode [LED]).[7–11] To fully exploit the potential of light-matter interactions within soft materials/polymers, it is necessary to establish multi-chromatic processes mediated by different discrete wavelengths (or colors) of light. This may be accomplished by (1) bidirectional photochemical pathways that switch between two states of a single chromophore and/or (2) disparate reaction pathways that are selectively activated by multiple chromophores.

Upon exposure to different wavelengths of light (λ_1 and λ_2), bidirectional photochemical reactions within a single chromophore fall into one of three general categories: (1) *E*/*Z* isomerization (Scheme 2A),[12,13] (2) isomerization by ring opening (Scheme 2B),[14,15] and (3) dimerization (Scheme 2C).[16,17]

Wavelength-orthogonal (no cross-reactivity) activation of multiple chromophores to induce/control distinct reaction pathways (e.g., reactant **A** to product **A** versus reactant **B** to product **B**) is an attractive mode to expand the scope of accessible materials.[5] However, orthogonality between each chromophore remains a formidable challenge (Figure 2A).[18–21] In general, these two rules can guide the design of an orthogonal system comprising two chromophores ($\mathbf{C_a}$ and $\mathbf{C_b}$): (1) selective absorption of incident light and (2) electronic mismatch to preclude electron/energy transfer between chromophores and other reactants that may be present in each photosystem (e.g., co-initiator(s)).[19,22]

By avoiding absorption of photons from a single light source, rule #1 guarantees that the chromophores ($\mathbf{C_a}$ and $\mathbf{C_b}$) are not activated simultaneously (Figure 2B). However, it is also critical to consider the strength of absorption, termed molar

tissue engineering and soft robotics to electronics.

[1]Department of Chemistry, The University of Texas at Austin, Austin, TX 78712, USA

[2]Centre for Materials Science, Queensland University of Technology (QUT), 2 George Street, Brisbane, QLD 4000, Australia

[3]School of Chemistry and Physics, Queensland University of Technology (QUT), 2 George Street, Brisbane, QLD 4000, Australia

[4]Cluster for Advanced Macromolecular Design and Australian Centre for NanoMedicine, School of Chemical Engineering, University of New South Wales, Sydney, NSW 2052, Australia

[5]These authors contributed equally

*Correspondence: cboyer@unsw.edu.au (C.B.), christopher.barnerkowollik@qut.edu.au (C.B.-K.), zpage@cm.utexas.edu (Z.A.P.)

https://doi.org/10.1016/j.matt.2021.03.021

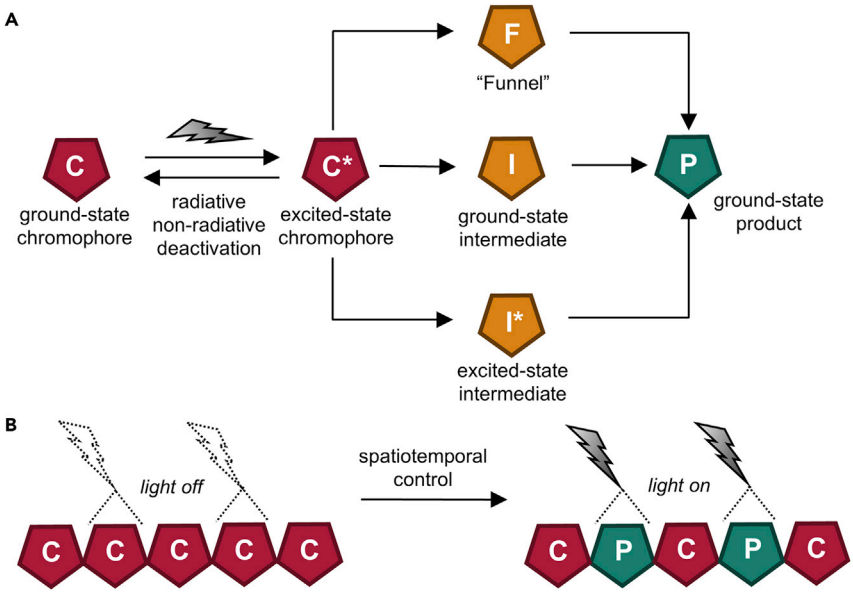

Scheme 1. Facets of photochemistry

General schematics for (A) molecular photochemical pathways in chromophores and (B) spatiotemporal control in a light-mediated process.

absorptivity ε (Equation 2, Beer's law), as well as the quantum yield Φ (Equation 3), of each process.[23]

$$\varepsilon = \frac{A}{l \times c} \quad \text{(A: absorbance; l: optical path length; c: concentration of chromophore)} \qquad \text{(Equation 2)}$$

$$\Phi = \frac{\text{Number of molecules reacted}}{\text{Number of photons absorbed}} \qquad \text{(Equation 3)}$$

Notably, chromophore absorption does not necessarily predict reactivity at a specific wavelength (i.e., the reaction quantum yield), and selecting a wavelength based solely on the absorption spectrum provides only limited guidance. Instead, the optimal excitation wavelength can be identified by employing tunable monochromatic light sources to screen a reaction's conversion as a function of wavelength at a constant photon flux and provide wavelength-dependent photoreactivity spectra, so-called action plots of photoreactivity.[19,24,25]

By mitigating crossover interactions (electron/energy transfer) between chromophores in their ground and excited states (C_a* and C_b, C_a and C_b*, C_a* and C_b*) through careful design, rule #2 is fulfilled to enable orthogonal photochemistry (Figure 2C). An additional consideration is that excited states (C_a* and C_b*) can include either singlet or triplet energy levels, where different modes of electronic cross-communication are possible. Furthermore, several photosystems operating in the visible-to-near-infrared (NIR) region rely on electron/energy transfer to a separate molecule (e.g., co-initiator), and the electronic properties of the oxidized or reduced species for all components involved need to be considered when designing wavelength-orthogonal reactions. Although crossover reactions can be excluded thermodynamically, selecting two chromophores that fully conform to these two rules is anything but trivial.[26] Therefore, kinetic modes of selectively driving photochemical reactions will be discussed, meaning those that do not fully abide by the two rules yet are capable of inducing/controlling distinct

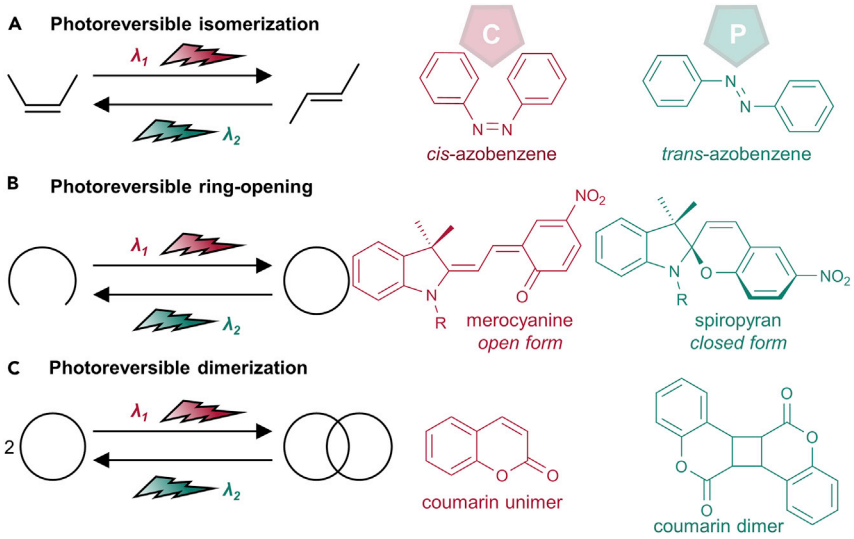

Scheme 2. General schemes of bidirectional photochemical pathways within a single chromophore

(A) Photoreversible isomerization, with azobenzene as an example.

(B) Photoreversible ring opening, with spiropyran as an example.

(C) Photoreversible dimerization, with coumarin as an example (for simplicity, only one isomer of the dimer is shown).

chemical reactions upon exposure to different wavelengths of light in the desired time frame, termed here wavelength-selective. This includes stepwise photomediated processes that are accomplished in a single reaction vessel by toggling an external light source between two different wavelengths, usually from long (lower energy) to short (higher energy) wavelengths (Figure 3).

The development of wavelength-orthogonal/selective photochemistry will undoubtedly augment the toolbox to create more sophisticated polymeric materials and structures, such as those inspired by nature, including materials with elegant hierarchical architectures and fine-tuned multi-functionality. This review highlights recent literature that demonstrates wavelength-selective light-matter interactions in polymer science, both present capabilities and challenges, to inform and invigorate further innovation. The next section provides an overview of the different classes of photochemical transformations to provide readers with a foundation to build-upon for future research, followed by a section that focuses on wavelength-selective protocols that have been developed in photocontrolled polymerization, which permit the synthesis of well-defined polymers through distinct mechanisms. The fourth section turns to wavelength selectivity in manipulating material properties (e.g., optoelectronic, ion-transport, and mechanical), for both synthetic materials and biomaterials. The penultimate section emphasizes wavelength selectivity in materials fabrication through photolithography and light-based 3D printing, and we conclude the review with a perspective on future opportunities in this exciting area.

THE TOOLBOX AND PROTOCOLS FOR WAVELENGTH-SELECTIVE PHOTOCHEMISTRY

The wavelength of incident irradiation is a critical parameter used to alter photoreactivity in chemical transformations. Through careful selection of the incident light source, different classes of wavelength-selective reactions can be triggered, including those

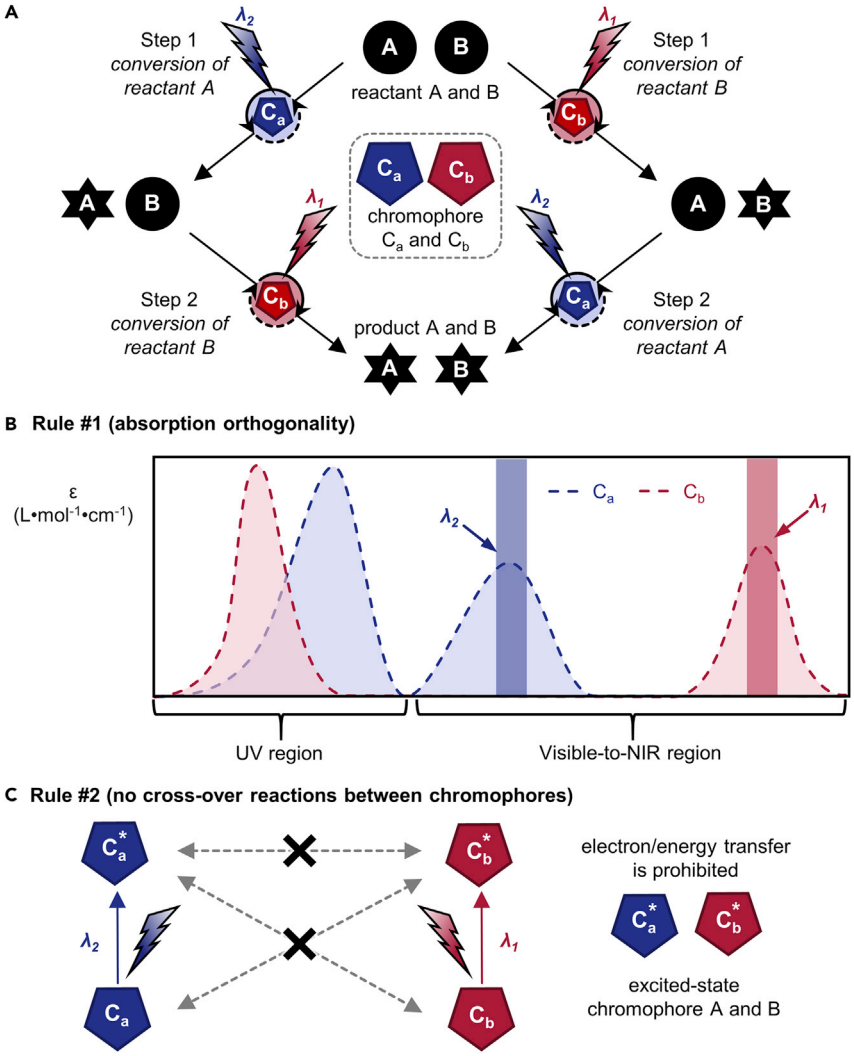

Figure 2. Orthogonal photochemical reactions

(A) Schematic representation for reactions enabled by chromophores C_a and C_b. The orthogonality enables discrete activation of two sequences: reactant **A** to product **A** with blue light and reactant **B** to product **B** with red light in any order (or simultaneously).

(B and C) (B) Overlaid ground-state UV-vis absorption spectra for two arbitrary chromophores (ε: molar absorptivity) C_a and C_b. While C_a and C_b have significant overlap in the UV region, there is little to no overlap in the visible-to-NIR region to follow rule #1 (absorption orthogonality) and (C) possible molecular photochemical pathways between C_a and C_b, where "X" indicates no interaction to follow rule #2 (no crossover reactivity).

containing a single chromophore that switch between different states/isomers and those with more than one chromophore that access different redox states. An absorption profile can be thought of as a unique blueprint intrinsic to chromophores under a particular set of conditions (e.g., matrix polarity and temperature), and the magnitude of absorption (molar absorptivity) at a given wavelength correlates with the likelihood that an incident photon will result in an excitation event. However, an increased likelihood of excitation does not necessarily correlate with reactivity at any given wavelength.[19,24] In this section, a snapshot of wavelength-selective reactions spanning from UV (100–400 nm) to visible (400–780 nm) excitation will be discussed within three overarching classes: photoswitches, photoremovable protecting groups, and light-driven (ir)reversible coupling.

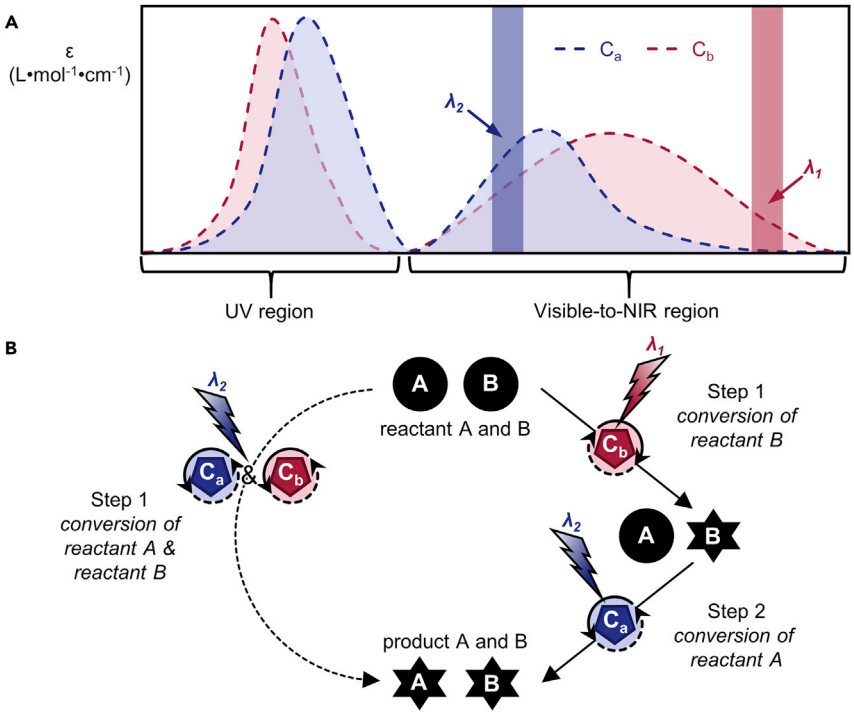

Figure 3. Schematic illustration of a wavelength-selective approach

(A) Overlaid ground-state UV-vis absorption spectra for two arbitrary chromophores (ε: molar absorptivity), C_a and C_b, that possess little to no overlap at long wavelengths (λ_1) but significant overlap at short wavelengths (λ_2), including wavelengths in the UV region. This violates rule #1 (absorption orthogonality).

(B) Schematic showing a wavelength-selective stepwise transformation in going from long-wavelength (red) excitation first, followed by short-wavelength (blue) excitation. However, non-selective, simultaneous photochemical transformations occur with initial exposure to the shorter wavelength of light (blue).

Photoswitches

Molecular photoswitches are small molecules that reversibly isomerize between two or more states upon light irradiation. A photoswitch alters its geometry and π-conjugation through the formation or dissociation of covalent bonds. Accordingly, the photochemical and physicochemical properties of the photoswitches change reversibly by toggling the incident light "ON" and "OFF". Parameters of interest for materials applications that will be mentioned here include rate of reversibility, photochromism (color change), polarity change, fatigue resistance, and operational wavelength range, with emphasis on the latter given its connection to wavelength selectivity. The two main photoisomerization modes that result in these fascinating effects are *cis/trans* (or *Z/E*) isomerization and electrocyclization/ring opening. For a more comprehensive discussion on photoswitches we refer readers to the following published reviews.[13,15,27–30] With respect to the operational wavelength range, early molecular photoswitches were primarily restricted to higher energy UV light (<400 nm), which can be damaging and difficult to distinguish among chromophores due to near universal UV absorption. Recent synthetic efforts have unveiled numerous visible light-activated derivatives, which provides an avenue toward wavelength-selective transformations that can leverage inexpensive and mild LEDs as narrow-band irradiation sources.

Z/E photoisomerization

Stilbenes (1945),[31] azobenzenes (1937),[12] α-bisimines (2014),[32] (thio)indigo dyes (1961),[33] and hydrazones (2009) undergo *Z/E* isomerization upon exposure to

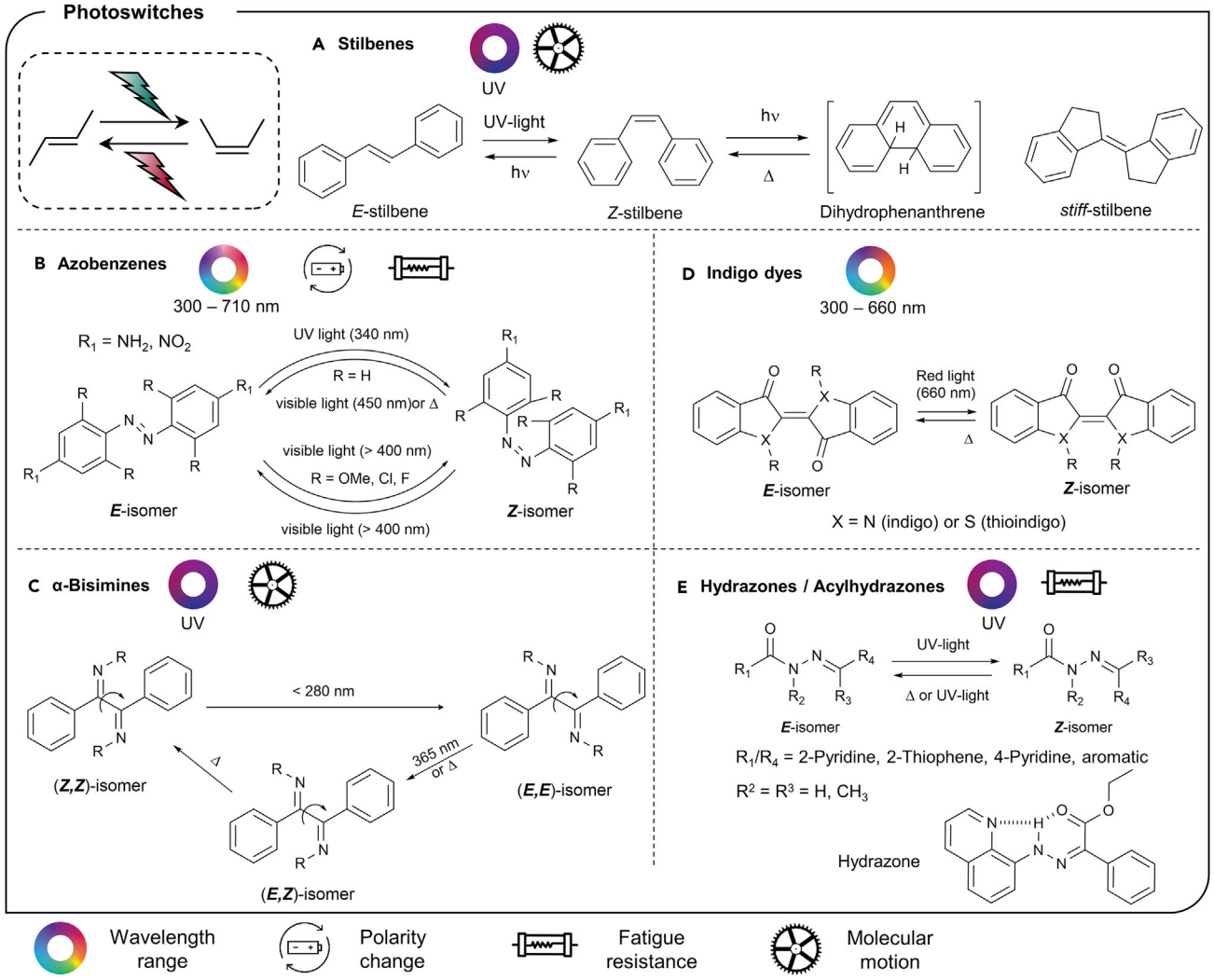

Figure 4. Overview of commonly employed *Z*/*E* photoswitches

(A) Stilbenes switch between *trans*/*cis* isomers upon light irradiation (300–380 nm).

(B) Azobenzene undergoes reversible isomerization with UV or visible light with specific *ortho*-substitution.

(C) α-Bisimine switches between the (*Z*,*Z*), (*E*,*E*), and (*E*,*Z*) isomers with light and heat.

(D) (Thio)indigo dyes photoswitch between *E* and *Z* isomers. (E) (Acyl)hydrazones photoswitch between *E* and *Z* isomers.

light.[34] This mode of isomerization was discovered in 1937 for azobenzenes and has since blossomed into a versatile array of derivatives capable of operating across the UV-to-visible spectrum (300–700 nm) with rapid reversibility, photochromism, polarity changes, fatigue resistance (cycling stability), and molecular motion. These different classes are briefly described below, highlighting absorption windows and how to tailor them for wavelength-selective transformations.

Stilbenes were first synthesized in 1843,[35] but it was not until 1945 that their *Z*/*E* photoisomerization was discovered (Figure 4A).[31] Traditional non-functionalized stilbene derivatives strictly absorb UV light, with peak absorption at 294 nm for *E*-stilbene and 278 nm for *Z*-stilbene.[36] Notably, absorption of UV light by the *Z* isomer not only results in a *Z*-to-*E* isomerization but can also result in cyclization to form dihydrophenanthrene, discussed in photocyclization/-reversion. Cyclization upon

exposure to UV light can be avoided using a fused ring analog (stiff-stilbene),[37] which has additionally been adopted as a structural motif in Feringa-type molecular motors.[38,39]

Azobenzenes, first reported in 1937,[12] are the most widely studied family of photoswitches given their ease of synthesis and versatility. They follow a photoisomerization process similar to that of stilbenes, but the presence of nitrogen results in a notable change in dipole moment and red-shift in absorption relative to analogous stilbene. Irradiation of bare azobenzene with UV light (~340 nm) converts the thermodynamically stable *E* isomer to the less stable *Z* form, which reverts upon irradiation with blue light (~450 nm) (Figure 4B).[40] Since its discovery, an impressive library of azobenzene derivatives have been synthesized and examined in terms of switching kinetics, thermal stability, fatigue resistance, and absorption.[41] Introducing electron-donating amine and withdrawing nitro groups on opposing *para* positions generates "push-pull" azobenzenes and results in an absorption red-shift to ~120 nm for both isomers.[42] Azobenzenes with *ortho*-fluorination can be reversibly addressed using different wavelengths of UV and visible light, providing high photoconversion and remarkably long thermal half-lives in the photostationary *Z* configuration.[43,44] Coordination of BF_2 has also been proved as an effective method to red-shift peak absorption to 710 nm (far-red) for the *Z* isomer.[45,46] Thus, functionalized azobenzenes represent excellent candidates for wavelength-selective photochemistry.

α-Bisimines, first examined by Jean-Marie Lehn in 2014,[32] undergo photochemical/thermal isomerization between three configurations, (*Z*,*Z*), (*E*,*Z*), or (*E*,*E*), due to the rotation around the C=N double bonds (Figure 4C). α-Bisimines are primarily employed for molecular machines. However, isomerization is restricted to UV light, (*Z*,*Z*) to (*E*,*E*) with <280 nm and (*E*,*E*) to (*E*,*Z*) with 365 nm, while (*E*,*E*) to (*Z*,*Z*) can occur thermally. This limits their utility in wavelength-selective photochemistry and presents an opportunity for the development of novel synthetic α-bisimine derivatives.[47]

Indigo dyes were first identified by Mostoslavskii in 1961 (Figure 4D),[33] and are attractive for their low-energy visible light photoisomerization and excellent photostability. For example, hemiindigo dyes (X = N, Figure 4D) with electron-rich aromatic substituents can be photoswitched with yellow-to-red light (~593–633 nm) for both isomers. The utility of visible light has been advantageous for photopharmacological and biological applications, but poor thermal stability has been limiting. To this end, *N*-aryl functionalization and incorporation of electron-withdrawing groups (e.g., CF_3 or CN) have been used to enhance the thermal stability of the *Z* isomer while maintaining absorption of red light.[48]

(Acyl)Hydrazones represent a more recent photoswitch, first developed by Lehn's group in 2011 (Figure 4E).[49] The ease of synthesis, excellent fatigue resistance, negative photochromism (photoinduced decoloration and thermal coloration), large change in absorption (for *Z* versus *E* isomers), tunable thermal half-life, and good quantum yields are among the favorable properties. Additionally, hydrazone derivatives containing a phenyl or quinolinyl group retain their photoswitchability in polar protic solvents, aprotic solvents, and acids and bases. In 2015, Hecht and coworkers synthesized a library of over 40 acylhydrazone photoswitches and investigated the photochromic properties as a function of substitution, finding absorption maxima primarily residing in the long-wave UV region (λ_{max} = 292–403 nm).[50]

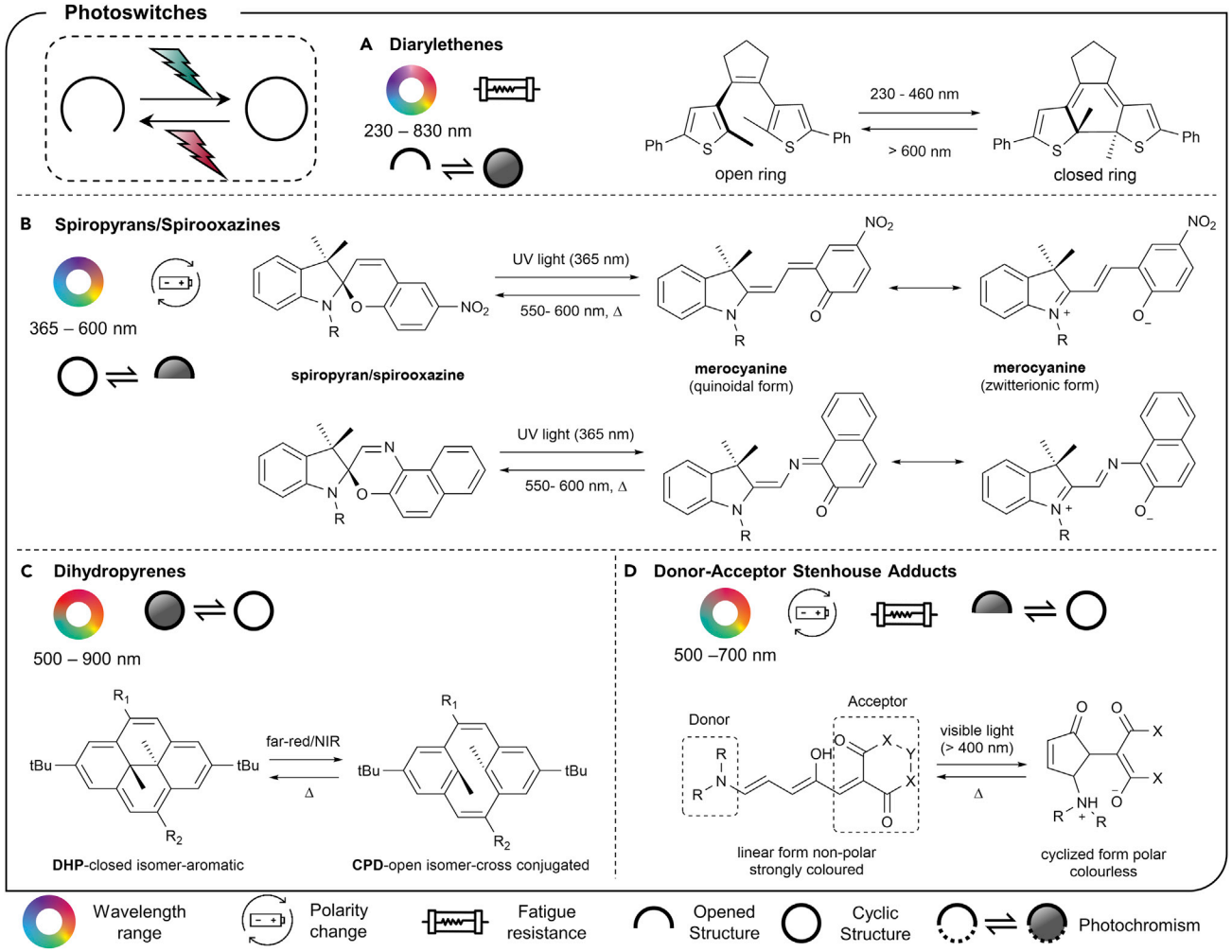

Figure 5. Overview of commonly employed *open/close* photoswitches

(A) Diarylethenes photocyclize and photorevert upon exposure to different wavelengths of light.

(B) Spiropyrans/spirooxazines transform to merocyanines and vice versa in the presence of illumination.

(C) Dihydropyrenes (DHPs) photoswitch between aromatic and cross-conjugated ring isomers with NIR light.

(D) Donor-acceptor Stenhouse adduct (DASA) structures photoswitch between a linear and cyclized form.

Photocyclization/reversion

Diarylethenes (1988),[51] spiropyrans/spirooxazine (1952),[14] dihydropyrene (1965),[52] and donor-acceptor Stenhouse adducts (2014)[53] undergo ring closing/opening upon exposure to light. This mode of isomerization was first noted with spiropyrans in 1952, and has since resulted in a myriad of derivatives capable of operating across the UV-to-visible spectrum (300–700 nm) with rapid reversibility, photochromism, thermal stability, polarity shifts, fatigue resistance, and fluorescence.

Diarylethenes (DAEs) were inspired by dihydrophenanthrenes, which arise from photocyclization of *Z*-stilbenes and result in a distinct red-shift in absorption.[27] However, dehydrogenation in air irreversibly produces phenanthrene, limiting their utility.[54] It was not until 1988 that Irie and coworkers discovered that stable and reversible photochromism resulted when replacing the phenyl rings of stilbene with electron-rich thiophene rings to give diarylethene.[51] DAE photoswitches are known for their thermal stability and fatigue resistance (Figure 5A).[27] Additionally, their derivatives can be bidirectionally switched

between the ring-opened and -closed forms with excellent wavelength selectivity, which can be accomplished in the solid state, facilitating applications in optical data storage devices. Hexafluorocyclopentene dithienylethenes are a class of DAEs that undergo photocyclization with UV to short-wave visible light (230–460 nm, depending on the derivative) to convert from a colorless open form to a stable colorful closed-ring form that reverts back upon exposure to visible light (425–830 nm, depending on the derivative).[55] The large absorption range for closed DAE derivatives has been accomplished by installing a variety of strong donor/acceptor substituents and extending π-conjugation at the 5,5″ position, which enables their utility in wavelength-selective photochemistry.

Spiropyran (SP) represents one of the earliest photoswitches, introduced by Fischer and Hirschberg in 1952.[14] Spiropyran is the name given to the colorless and thermodynamically stable ring-closed isomer that upon irradiation with UV light (~365 nm) opens to form a colored zwitterionic compound called merocyanine, which reverts thermally or with visible light (~550–600 nm) (Figure 5B). These isomers are particularly attractive for their dramatic dissimilarities in physicochemical properties (e.g., volume, absorption, pK_a, and polarity).[56] Operational wavelengths range from 365 to ~600 nm, which is impacted by substitution, associated π-conjugation, and matrix polarity, with non-polar media stabilizing the quinoidal form that red-shifts absorption of merocyanine. Spirooxazines are structurally similar to spiropyrans; however, these photochromic compounds provide unique properties, such as excellent fatigue resistance (>1,000 switching cycles without degradation).

Dihydropyrene (DHP) represents one of the earliest negative photochromes, introduced by Boekelheide in 1965.[52] DHP undergoes a 6π cycloreversion to form decolored cyclophanediene (CPD), which thermally converts back to their fully aromatic form.[57] Recently, Hecht and coworkers applied "donor-acceptor" substitution to the DHP scaffold, shifting the absorption of the parent molecule from the visible to the NIR region (Figure 5C).[58] The donor-acceptor substation of DHPs generally enhances the quantum yield of the ring opening proceeding via the first excited state. Through this strategy, the NIR cross-section has been increased by two orders of magnitude, while the thermal half-lives could be modulated from milliseconds to hours.

Donor-acceptor Stenhouse adducts (DASAs) represent a unique class of photochromic switches introduced in 2014 by Read de Alaniz and coworkers that demonstrate a distinct change in absorption and polarity upon isomerization/cyclization (Figure 5D).[53] In contrast to the majority of photochromic switches, DASAs are negative (or reverse) photochromes, where the thermodynamically stable ring-opened triene state is colored and the photostationary cyclopentenone state is colorless. Negative photochromes are attractive for materials applications that require deep light penetration, which is hindered by high extinction coefficients of standard (not reverse) photostationary states resulting in complete attenuation in the outermost layers of a sample. Moreover, their absorption profiles are highly tunable from green (~500 nm) to far-red (~700 nm) through variations in the donor (amine) and acceptor (carbon-acid) composition, making them excellent candidates for wavelength-selective transformations.

Photoremovable protecting groups

A photoremovable protecting group (PPG) is a light-sensitive compound (also known as a "photocage") that is bound to a leaving group (LG) (e.g., alcohol, thiol, amine, carboxylic acid) to protect ("cage") it from otherwise reactive conditions. Upon exposure to a particular wavelength of light, the PPG reacts (e.g., bond scission) to release ("uncage") the LG to which it was bound. In contrast to photoswitches, PPGs typically go through an irreversible transformation upon irradiation

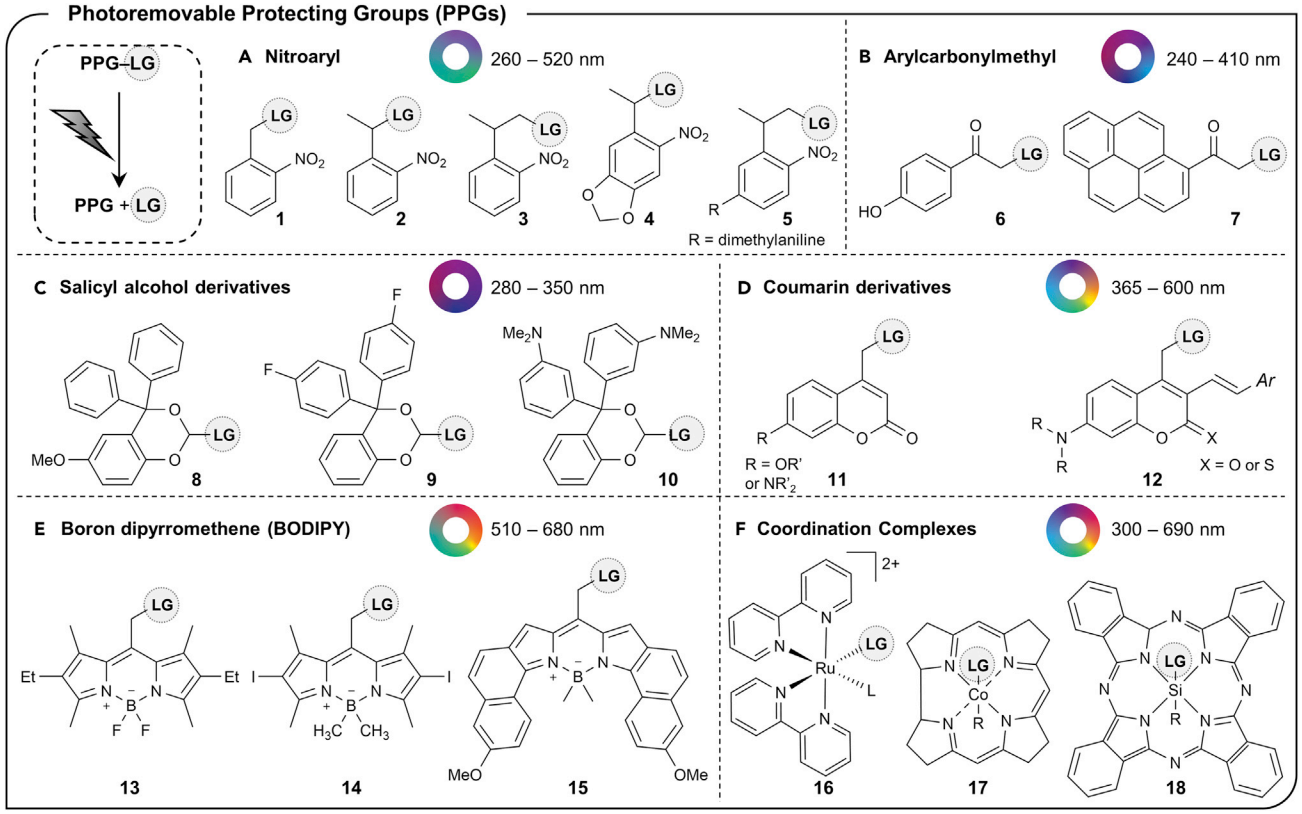

Figure 6. Common photoremovable protecting groups (PPGs) with demonstrated or potential utility in wavelength-selective photochemistry, with wavelength ranges for reported photouncaging

(A–F) (A) Nitroaryl groups, (B) arylcarbonylmethyl groups, (C) salicyl alcohol derivatives, (D) coumarin groups, (E) boron dipyrromethene (BODIPY), and (F) coordination complexes. Color wheels indicate demonstrated wavelengths of light used to induce the chemical reactions shown.

with light. Altering the substitution pattern of the chromophore results in large shifts in absorption maxima (λ_{max}) and photocleavage at corresponding wavelengths. This facilitates wavelength-selective uncaging and utility of PPGs in future materials systems. Significant efforts have been made to expand λ_{max} of various PPGs from UV (<400 nm) to the visible region (<700 nm). The overall efficiency of LG release is evaluated using the quantity $\Phi\varepsilon$, sometimes referred to as the uncaging cross-section, where Φ is the reaction quantum yield and ε is the molar absorptivity. Impressively, subtle compositional changes of PPGs, including variations in substitution, can be used to carefully adjust these critical parameters (λ_{max} and $\Phi\varepsilon$). For each selected PPG family, this section highlights their discovery and operable photolysis, as well as chemical modification to tailor absorption profiles and optimize photolysis efficiency for wavelength-selective reactions. For in-depth reviews of PPGs, readers are directed to two recent comprehensive reviews.[59,60]

Nitroaryl groups were one of the first known PPGs, with photolysis reported by Barton and coworkers in 1962 using dinitrobenzenesulfphenyl esters,[61] followed by Patchornik and coworkers in 1970 who showed that *ortho*-nitrobenzyl (oNB) derivatives could be used as PPGs upon exposure to UV light ($\lambda_{max} \approx 262$ nm, $\varepsilon \approx 5{,}200\ M^{-1}\ cm^{-1}$).[62] Since these discoveries, nitroaryl derivatives have become the most widely utilized PPGs, of which oNB and *ortho*-nitrophenethyl (oNPE) dominate (Figure 6A).[63] Upon exposure to UV light (<365 nm), bare oNB (**1** and **2**) and oNPE (**3**) release an LG and convert into the corresponding *ortho*-nitroso-benzaldehyde and *ortho*-nitrostyrene derivatives,

respectively. Red-shifting peak absorption and reactivity into the visible region have been accomplished through the introduction of electron-donating groups (e.g., -OCH_3) or π-extension, such as derivatives **4** ($\lambda_{max} \approx 351$ nm, $\varepsilon_{365} \approx 3{,}500$ M^{-1} cm^{-1})[64] and **5** ($\lambda_{max} \approx 420$–433 nm, $\varepsilon \approx 30{,}000$ M^{-1} cm^{-1}).[65] One general method that has been employed to improve Φ has been α-methylation (relative to the LG). For example, with pivalate as the LG, compound **1** gave $\Phi \approx 0.13$, while compound **2** gave $\Phi \approx 0.64$.[66] Similar results have also been observed for *o*NPE derivatives.[67]

Arylcarbonylmethyl groups have been used extensively as PPGs, with one of the earliest derivatives, *p*-hydroxyphenacyl (**6**), discovered by Givens and Park in 1996 (Figure 6B).[68] Absorbing in the UV range ($\lambda_{max} \approx 275$ nm), derivatives of **6** release LGs via a photo-Favorskii rearrangement, as demonstrated with phosphates ($\Phi \approx 0.4$),[69] carboxylates ($\Phi \approx 0.3$–0.4),[70–72] phenolates ($\Phi \approx 0.04$–0.11),[73] and thiolates ($\Phi \approx 0.085$).[74,75] Red-shifting the absorption has been accomplished through extending π-conjugation by replacing phenyl with pyrene (**7**), shifting λ_{max} to ~355 nm and enabling efficient photorelease with visible light (410 nm) for both carboxylic acids and alcohols ($\Phi \approx 0.30$–0.41 and 0.17–0.20, respectively).[76]

Salicyl alcohol-based PPGs, developed by Wang and coworkers in 2007, are unique in that they have been utilized for protecting carbonyl functionalities (Figure 6C).[77] Upon irradiation with UV light (<400 nm), ketones and aldehydes have been released with good quantum efficiency ($\Phi \approx 0.11$). While this class of PPGs to date only reacts to UV light exposure, the exact λ_{max} can be tailored with inductive effects, whereby more electron-donating substituents red-shift absorption from ~320 to 350 nm. In 2011, Wang and coworkers demonstrated wavelength-selective sequential photorelease by combining bare compound **8** (absorbing UV light <280 nm) with derivatives **9** and **10** having electron-withdrawing fluorine and donating dimethylamino groups that shifted deprotection wavelengths to <280 nm and >320 nm, respectively.[78]

Coumarin PPGs date back to 1984 when Givens and Matuszewski showed that UV irradiation triggered the release of phosphate from a methoxy-substituted derivative, **11** ($\lambda_{max} \approx 365$ nm, $\varepsilon \approx 17{,}000$ M^{-1} cm^{-1}).[79] Since then, coumarin PPGs have received considerable attention owing to their synthetic versatility, ability to react under visible light (up to 600 nm),[80] and some of the highest photouncaging yields (up to 0.7 for a carboxylate) (Figure 6D).[81] Red-shifted absorption and enhanced quantum yield have primarily been accomplished in three manners, (1) amino (over alkoxy) substitution at the 7-position,[82] (2) thiocarbonyl substitution at the 2-position (thiocoumarin),[83] and (3) extension of π-conjugation with (electron-rich) styryl derivatives at the 3-position.[84] In particular, coumarin derivative **12** with 3-styryl functionality has provided the highest quantum yields to date ($\Phi \approx 0.7$, $\lambda_{max} \approx 515$ nm, $\varepsilon \approx 25{,}000$ M^{-1} cm^{-1}) as a result of rapid intramolecular cyclization that occurs upon photolysis.[81]

Boron dipyrromethene (BODIPY) photocages were first reported independently by Winter and Weinstein in 2015,[85,86] demonstrating efficient visible light reactivity (Figure 6E). Although the original derivative **13** ($\lambda_{max} \approx 544$ nm, $\varepsilon \approx 62{,}000$ M^{-1} cm^{-1}) showed a low photouncaging quantum yield upon exposure to green light (530 nm), with acetate ($\Phi \approx 0.00095$) and nitrophenol-based carbonate ($\Phi \approx 0.0016$) as LGs,[85,86] boron-methylation and pyrrole-halogenation, **14** ($\lambda_{max} \approx 538$ nm, $\varepsilon \approx 60{,}700$ M^{-1} cm^{-1}), resulted in orders-of-magnitude improvement for analogous photorelease of carboxylate ($\Phi \approx 0.28$).[87] The dramatic improvement in Φ was ascribed to a combination of inductive (electron-donating methyl groups) and heavy-atom (halogenation) effects, which increased stability of the photolyzed

ionic product and triplet excited state lifetime, respectively. Furthermore, red light photocleavage (up to 680 nm) has been accomplished with π-extension, whereby conformational restraint, such as in compound **15** ($\lambda_{max} \approx 641$ nm, $\varepsilon \approx 139{,}000$ M^{-1} cm^{-1}), greatly improves quantum yield ($\Phi \approx 0.038$) by blocking undesired excited state relaxation pathways.[88]

Coordination complexes that consist of a central atom or ion with surrounding ligands have been used as visible light active PPGs, where photolysis occurs off the central atom or ion (Figure 6F). For example, Ru(II)bipyridyl derivative, **16** ($\lambda_{max} \approx 489$ nm, $\varepsilon \approx 10{,}000$ M^{-1} cm^{-1}), was first employed in 2003 as a PPG to release 4-aminopyridine ($\Phi \approx 0.02$) upon exposure to a blue laser (473 nm),[89] and subsequently tryptamine ($\Phi \approx 0.018$), tyramine ($\Phi \approx 0.028$), and serotonin ($\Phi \approx 0.023$) upon irradiation with a blue LED (~450 nm).[90] Cobalt(III) complexes, such as **17** (Vitamin B_{12}, $\lambda_{max} \approx 510$ nm, $\varepsilon \approx 8{,}500$ M^{-1} cm^{-1}), have also been employed as PPGs, where bond homolysis releases a radical $LG^{\bullet}$ upon exposure to green ($\Phi_{520\ nm} \approx 0.286$) or red ($\Phi_{660\ nm} \approx 0.074$) light.[91] The farthest red-shifted PPG reported from a coordination complex has been from Si-phthalocyanine macrocycles, **18** ($\lambda_{max} \approx 690$ nm, $\varepsilon \approx 100{,}000$ M^{-1} cm^{-1}), where axial aryloxy ligands undergo homolytic cleavage upon irradiation with red light ($\Phi_{690\ nm} \approx 0.0027$) to form reactive radical anion intermediates.[92]

Although less common, a variety of organic dyes that strongly absorb visible light have been employed as effective PPGs, including xanthenes (<550 nm), cyanines (<700 nm), amino-benzoquinones (<620 nm),[93] benzothiadiazoles (<430 nm), stilbenes (<460 nm), and hydroxyquinolines (<420 nm).[60] The wide range of accessible wavelengths for photouncaging coupled with examples where Φ exceeds 0.1 makes these underexamined derivatives attractive for future wavelength-selective photochemistry.

Photoinduced irreversible and reversible coupling

Photoexcitation can induce changes in the geometric and electronic structure of molecules, which in -turn can unveil reactive pathways that are unavailable in the ground state. Among these reactions, cycloadditions are very efficient and have gained popularity in organic/materials chemistry. The major photoinduced cycloaddition reactions are [2 + 2], [3 + 2], and [4 + 2] whereby two, three, and four carbon atoms are added to an alkene moiety, respectively. These light-driven reactions can either be irreversible or reversible, yet they are primarily restricted to narrow excitation wavelengths in the UV region (<400 nm), presenting an opportunity to expand the photochemical toolbox and leverage these efficient reactions in wavelength-selective transformations.

Photoinduced irreversible coupling

While coupling reactions have been known for decades, it was not until 2001 that Sharpless and coworkers introduced the concept of click chemistry and classified chemical conjugations, which was rapidly extended to photoclick chemistry (also termed photoligation).[94,95]

2-Substituted benzaldehyde derivatives, initially reported in 1961,[96] are among the most popular adducts for photoinduced coupling due to their high efficiency ($\Phi \approx 0.94$), mild reaction conditions, and synthetically accessible chemical structure. The photoenolization of 2-substituted benzaldehydes upon irradiation causes a structural rearrangement in going through a 1,5-sigmatropic hydrogen transfer to produce a dienol that reacts rapidly with a dienophile via a Diels-Alder reaction (Figure 7A).[97] Derivatives bearing an ether functionality *ortho* to the aldehyde have proved useful in photoligation with various dienophiles. Interestingly, the use of

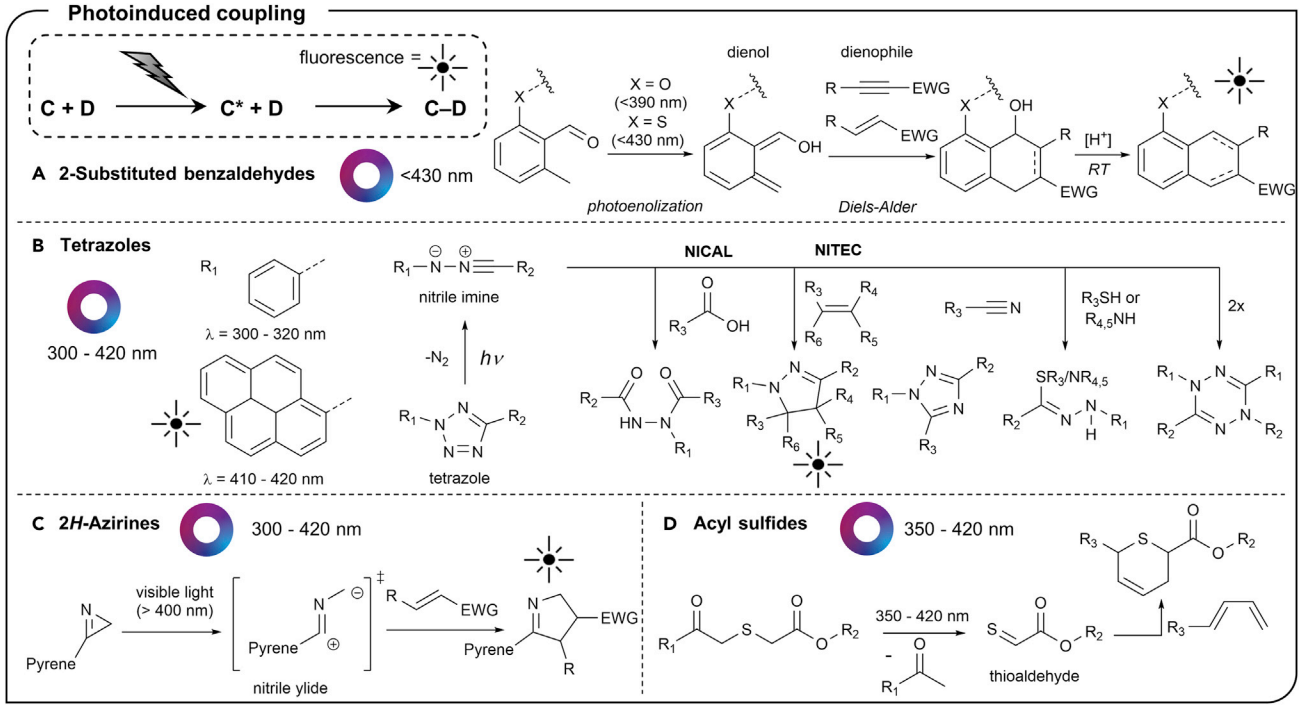

Figure 7. Photoinduced coupling

(A) 2-Substituted benzaldehydes that undergo a photoenolization followed by Diels-Alder cycloaddition.

(B) Tetrazoles that undergo a 1,3-dipolar cycloaddition upon exposure to light.

(C) Acyl sulfides that form reactive thioaldehydes upon exposure to light, followed by a hetero Diels-Alder reaction with a diene (shown) or nucleophile. Color wheels indicate demonstrated wavelengths of light used to induce the chemical reactions shown. EWG, electron-withdrawing group.

electron-deficient alkynes results in Diels-Alder adducts that can be converted to highly fluorescent naphthalenes upon the addition of acid.[98] While these photoligations typically require UV light (<390 nm), a red-shift in absorption toward visible light activation (390–430 nm) has been accomplished by simply replacing the oxygen (in the ether) with sulfur (thioether), expanding their potential utility in wavelength-selective reactions.[99]

Tetrazole derivatives that undergo 1,3-dipolar cycloaddition were first reported in 1967 by Huisgen and Sustmann,[100] and subsequently adopted in 2008 by Lin and coworkers for biorthogonal protein modification.[101] Substitution of tetrazole at the 2- and 5-positions facilitates 1,3-dipolar cycloadditions upon irradiation with UV-visible (UV-vis) light, providing a powerful ligation technique for direct access to a variety of heterocycles (Figure 7B).[102] More specifically, irradiation of the tetrazole releases nitrogen and generates nitrile imines via photolytic cleavage, which then reacts with a dipolarophile, such as a carboxylic acid (nitrile imine-mediated carboxylic acid ligation [NICAL]), alkene, or alkyne to form a fluorescent pyrazoline (nitrile imine-mediated tetrazole-ene cycloaddition [NITEC]), thiols, amines, or itself in the absence of a suitable partner. The reaction is fast (~minutes), efficient, and proceeds under mild, ambient light conditions. Red-shifted absorption has been accomplished by incorporating an electron-rich species at the *N*-substituted position and by extending the tetrazole π-conjugation (shifting from ~300 to ~420 nm).

2*H*-Azirine derivatives were independently discovered by Padwa and Schmid in 1973,[103,104] finding that phenyl-2*H*-azirine undergoes a 1,3-dipolar cycloaddition in the presence of UV light (~300–320 nm) (Figure 7C). Upon irradiation 2*H*-azirines

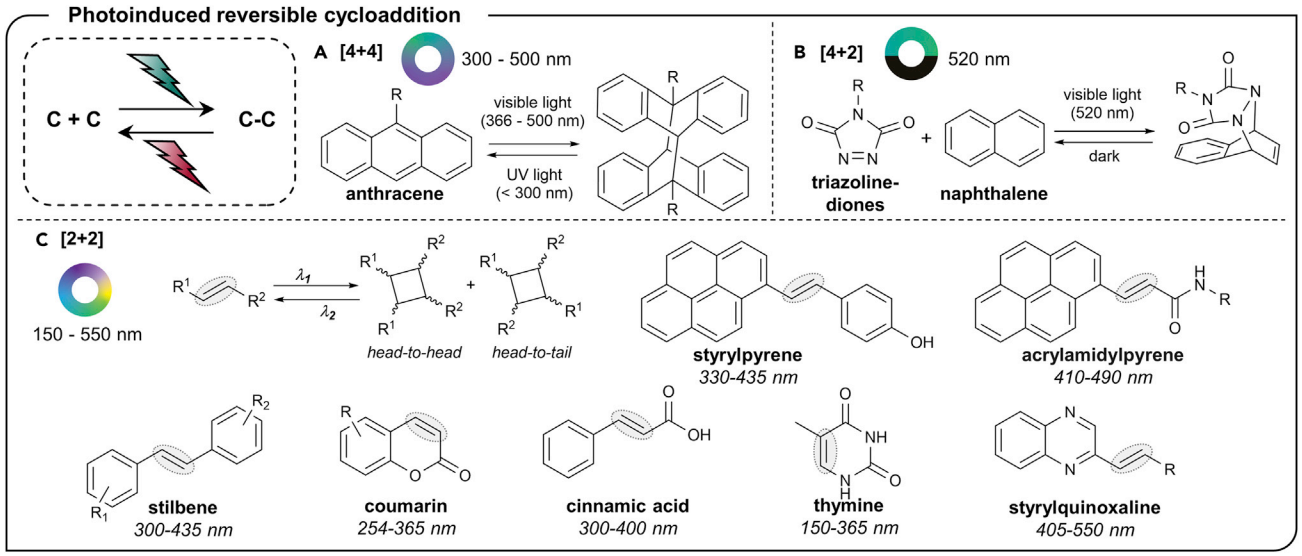

Figure 8. Photoinduced reversible cycloadditions

(A) [4 + 4] dimerization of anthracene.

(B) [4 + 2] cycloaddition between triazoline-diones and naphthalene.

(C) [2 + 2] dimerization of π-conjugated enes. Color wheels indicate demonstrated wavelengths of light used to induce the chemical reactions shown.

form a reactive nitrile ylide intermediate that rapidly undergoes dipolar cycloaddition with an electron-deficient alkene to generate nitrogen containing five-membered heterocycle. Recently, it was discovered that replacing the phenyl with a more π-conjugated pyrene chromophore red-shifts absorption to facilitate cycloadditions with visible light (~420 nm).[105]

Acyl sulfide derivatives have also proved useful in photoinduced coupling reactions since their initial discovery in 1986 (Figure 7D).[106] Irradiation with UV light (~350 nm) converts acyl sulfides into reactive thioaldehydes, which then rapidly undergo a hetero Diels-Alder reaction with nucleophiles (e.g., dienes, amines, aminoxyls, thiols) to form the corresponding heterocyclic sulfide products. Similarly, to tetrazoles, installing pyrene in place of phenyl shifts the reaction from 350 to ~420 nm.

Photoinduced reversible cycloaddition

In general, photoinduced dimerization following a [2 + 2] or [4 + 4] cycloaddition occurs in the UV (300–400 nm) or visible (>400 nm) region while cycloreversion occurs at shorter wavelengths (<250 nm) or thermally in the dark.

This wavelength selectivity depends on the nature of the chromophore and typically leads to many by-products (i.e., head-to-head or head-to-tail products, syn versus anti additions, and so forth). However, certain derivatives provide an avenue toward "clean" reversible cycloadditions, which offers an attractive handle to tune material properties in a reversible manner with the potential for wavelength selectivity.

[4 + 4] anthracene dimerization occurs upon exposure to UV light and is one of the oldest photochemical transformations, pioneered by Fritzche and Prakt in 1867.[107] Specifically, exposure to 365 nm light causes unsubstituted anthracenes to undergo [4 + 4] cycloaddition reactions to form dimers, which dissociate upon irradiation with short-wave UV light (<300 nm) (Figure 8A).[108] Since its inception, it has become widely adopted in materials chemistry with applications in optical storage

devices,[109] drug delivery,[110] and solar cells.[111] Substituting anthracenes (e.g., central electron-withdrawing Br, triazole, or ester groups) have been used as an effective method to red-shift their photodimerization into the visible region (400–500 nm), expanding applicability in wavelength-selective reactions.[102]

[4 + 2] triazolinedione (TAD) cycloaddition with naphthalene occurs upon irradiation with 520 nm light, as first noted by Kjell and Sheridan in 1984 (Figure 8B).[112,113] Interestingly, the photostationary state (during irradiation) can result in a near quantitative yield of the cycloadduct; however, upon removal of light cycloreversion spontaneously occurs at ambient temperature. This provides a unique long-wavelength switch that has been employed in biological applications and photoresists for 3D laser lithography.[114,115]

[2 + 2] π-conjugated ene derivatives are known to undergo dimerization upon exposure to light (Figure 8C). For example, styrylpyrene was originally reported by Kovalenko and coworkers in 1980 to dimerize under violet/blue light (~435 nm) and revert under UV light (~330 nm).[116,117] This photocycloaddition results in 12 different isomers.[118] Similarly, acrylamidylpyrene (~410–490 nm), stilbene (~300–435 nm), coumarin (~254–365 nm), thymine (~150–365 nm), and cinnamic acid (~300–400 nm) also undergo [2 + 2] photocycloaddition reactions upon exposure to UV or visible light irradiation, with details provided in a recent review.[19] Recently, the [2 + 2] photocycloaddition of styrylquinoxaline has extended the operable excitation wavelength to green light (~550 nm), representing the longest wavelength reported to date, with cycloreversion occurring at ~350 nm.[119] Functionalized styrylpyrene derivatives are particularly attractive for wavelength-selective materials applications given their longer wavelength of activation and ability to toggle between monomeric and dimeric states solely with different wavelengths of light.

Toolbox and protocol summary

This section is aimed to introduce molecular photochemistry observed in photoswitches, PPGs, and (ir)reversible cycloaddition reactions with potential applicability in wavelength-selective photochemistry. Particular efforts have been made to shift from high-energy UV light to milder visible and NIR reactive systems, which opens up applications in both a biological and materials context, described in later sections. In addition to these photochemical reactions that constitute a substantial foundation of light-matter interactions in polymer science,[120] photoinitiators[121] and photoredox catalysts[122] represent an alternative route toward wavelength-selective reactivity that will be introduced in the next section.

WAVELENGTH SELECTIVITY IN PHOTOCONTROLLED POLYMER SYNTHESIS

Controlled polymerizations triggered by light have become a major research interest over the last 10 years due to the associated benefits of using a mild, spatiotemporally controlled stimulus.[10,123,124] There are two subcategories of light-mediated polymerizations, those that are (1) photoinduced and (2) photocontrolled (Figures 9A and 9B).[125] A photoinduced polymerization describes the scenario in which light only plays a role during the initiation step and not during propagation. However, photocontrolled propagation is often necessary (for radical mechanisms) to control (de)activation, and minimize unwanted side reactions (e.g., termination and chain transfer) that can yield polymers with ill-defined chain ends and large molecular weight distributions. In contrast, photocontrolled polymerizations rely on light to

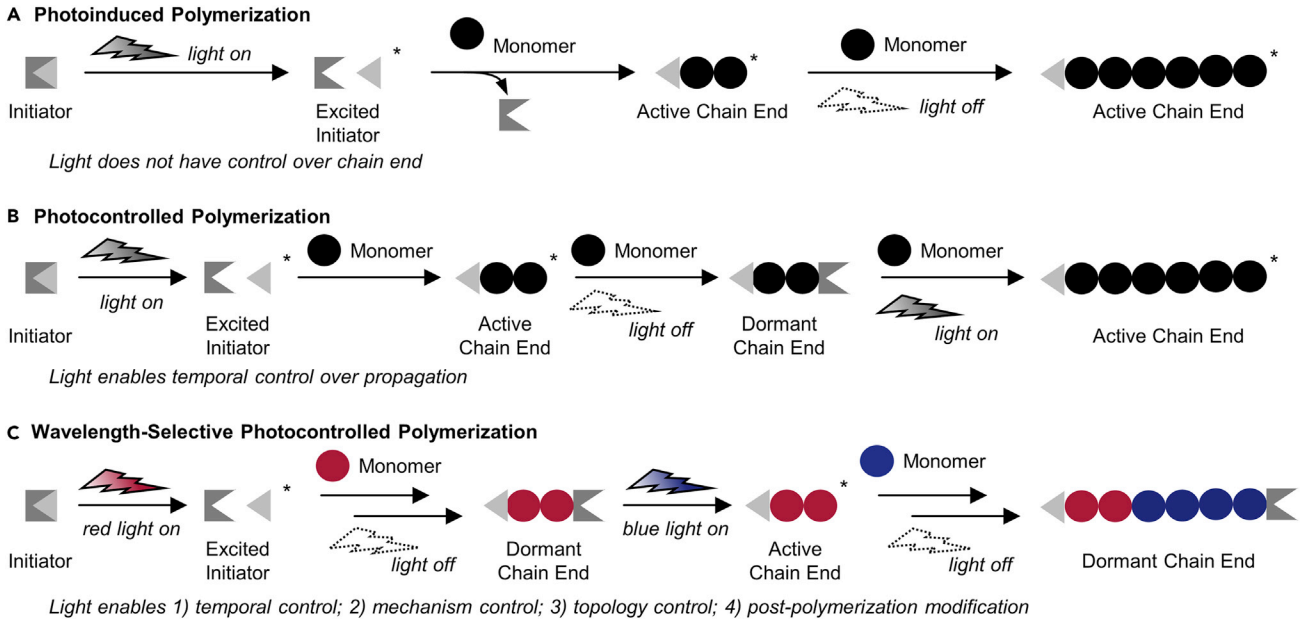

Figure 9. Schematic representation of photoinitiated polymerization, photocontrolled polymerization, and wavelength-selective photocontrolled polymerization

(A–C) In photoinduced polymerizations (A), the initiator is activated upon irradiation with light, leading to an uncontrolled propagation. In photocontrolled polymerizations (B), both initiation and propagation are mediated by light, allowing for temporal control where growth occurs during light "ON" and halts during light "OFF." Wavelength-selective photocontrolled polymerizations (C) are a subcategory of photocontrolled polymerizations where different wavelengths of light are used to control different controlled polymerization processes, as illustrated with a monofunctional initiator here.

both initiate and (de)activate propagation, providing polymers with well-defined chain ends and narrow molecular weight distributions.

To date, a number of photocontrolled polymerizations have been developed, including photo-atom transfer radical polymerization (ATRP, metal[126] versus metal-free[127–129]), photoreversible addition fragmentation chain transfer (RAFT, photoinduced electron/energy transfer RAFT [PET-RAFT],[130,131] photoiniferter RAFT[132,133]), photo-ring-opening polymerization (ROP),[134–136] and photo-ring-opening metathesis polymerization (ROMP, metal[137,138] versus metal-free[139,140]). Notably, these photocontrolled polymerizations demonstrate excellent spatiotemporal control and can be regulated by a wide range of irradiation wavelengths, from UV to visible (Figure 10). By selecting photocontrolled polymerization systems that operate via mechanistically distinct reaction pathways, their successful combination can be achieved using different irradiation wavelengths (Figure 9C). This section describes how wavelength selectivity has been utilized to regulate polymerization mechanisms and polymer topology, and to enable sequential polymerization and coupling. Notably, in nearly all examples to date irradiation with two wavelengths of light has been performed sequentially, with the lower energy (longer wavelength) being used first, followed by the higher energy (shorter wavelength). This presents an opportunity to further improve the wavelength selectivity such that the higher energy wavelength of light can be employed first without activating both light-mediated processes.

Wavelength-selective regulation of polymerization mechanisms

One of the earliest examples of wavelength selectivity in photocontrolled polymerizations was reported by Boyer and coworkers, who combined photoacid-mediated ROP with PET-RAFT polymerization.[135] Here, a dual functional initiator containing

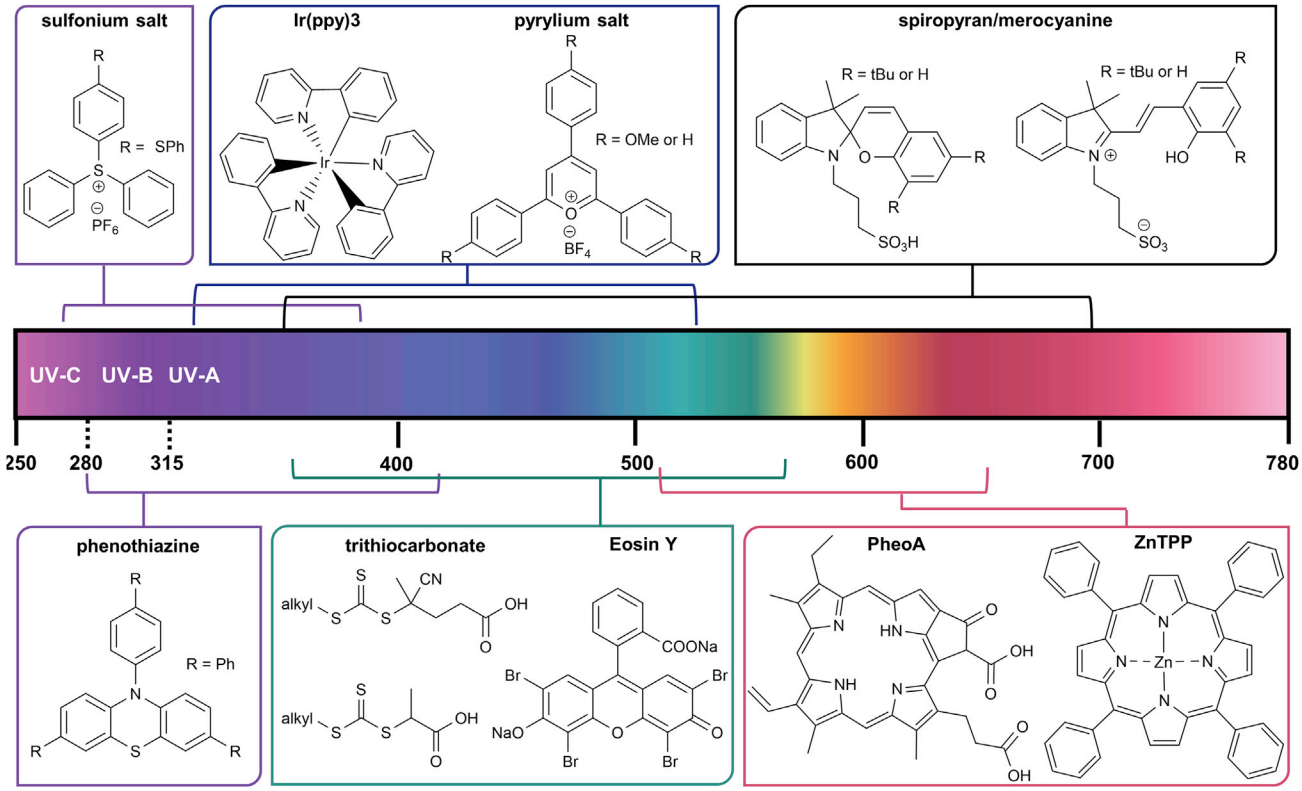

Figure 10. Representative chromophores reported in wavelength-selective photocontrolled polymerizations
Corresponding chemical structures and absorption wavelengths are provided.

both a chain-transfer agent (trithiocarbonate) and an alcohol was synthesized, whereby the alcohol functionality enabled the photoacid-mediated cationic ROP of lactone while poly(acrylate) chains where formed at the trithiocarbonate terminus through PET-RAFT polymerization (Figure 11A). To achieve selectivity, two different catalysts activated by different wavelengths of light were employed. A red light-absorbing photocatalyst, zinc tetraphenyl porphyrin (ZnTPP), was used to control PET-RAFT polymerization,[141] whereas blue light reversibly activated a merocyanine photoacid (PAH). Interestingly, the ZnTPP catalyst, which can be activated under blue light, showed negligible activity during blue light irradiation in the presence of the PAH. As such, blue light irradiation led to the selective ROP of lactones, while red light irradiation allowed the preferential polymerization of acrylate monomers. Similarly, a dual-wavelength-mediated protocol employing a bifunctional initiator for the radical polymerization of methyl methacrylate (MMA) via reversible complexation-mediated polymerization (RMCP) with indole as the photocatalyst under long-wave visible light (550–750 nm) and photoinitiated ROP of lactones using a sulfonium salt under long-wave UV light (350–380 nm) was disclosed by Goto, Kaji, and coworkers (Figure 11B).[142] These examples represent a method to grow block copolymers from a central bifunctional initiator with wavelength selectivity.

Recently, Fors and coworkers demonstrated the ability to toggle between cationic polymerization of vinyl ethers and radical polymerization of acrylates via a novel wavelength-selective approach.[143] Rather than using a dual functional initiator, the authors employed a single trithiocarbonate chain-transfer agent to selectively induce the radical polymerization of acrylates or the cationic polymerization of vinyl

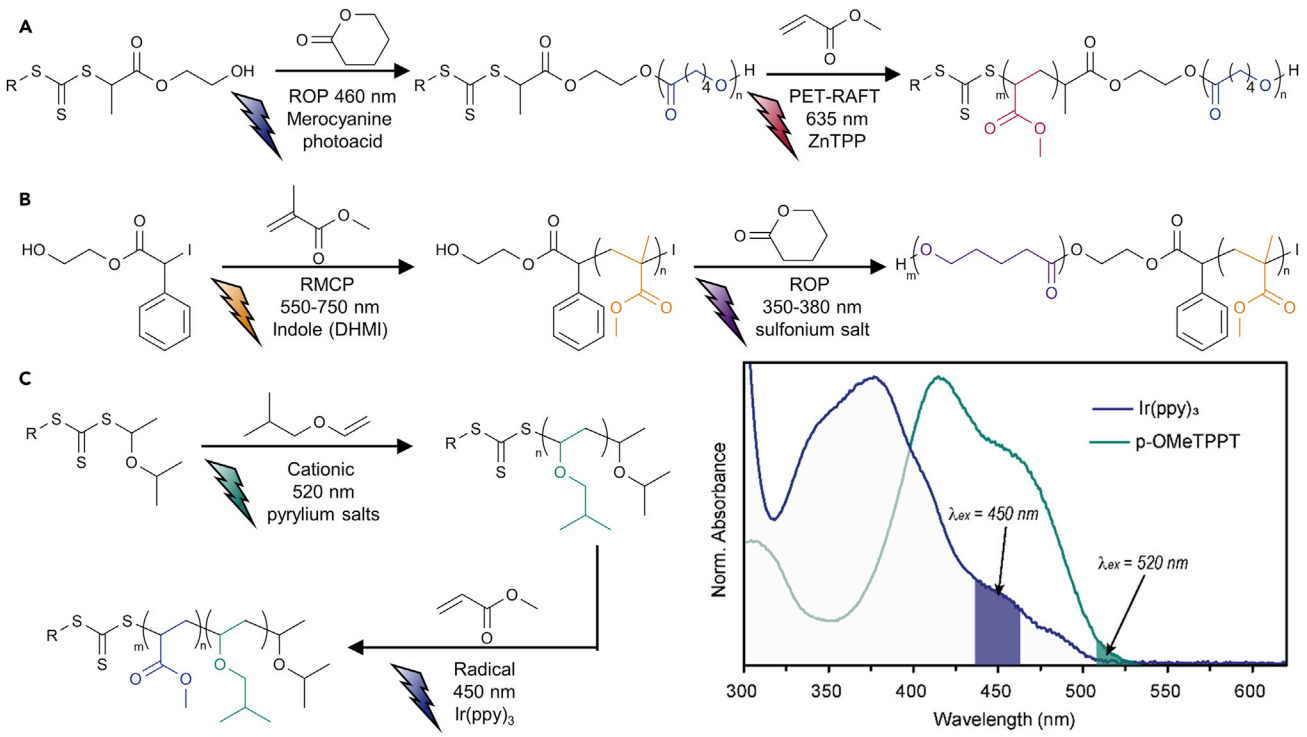

Figure 11. Wavelength-selective regulation of polymerization mechanisms

(A) Dual photoacid-mediated ring-opening polymerization (ROP) under blue light and photoinduced electron/energy transfer-reversible addition fragmentation chain-transfer (PET-RAFT) polymerization under red light.

(B) Dual photoacid-mediated ROP under long-wavelength UV and reversible complexation-mediated polymerization (RCMP) polymerization under visible light.

(C) Interconversion of cationic and radical polymerization via oxidizing (tri-methoxyphenyl pyrylium) and reducing ($Ir(ppy)_3$) photocatalysts. Overlaid UV-vis absorption plots of $Ir(ppy)_3$ and p-OMeTPPT are shown to the right.

ethers. This strategy was possible through a dual photocatalytic system featuring an oxidizing pyrylium photocatalyst (p-OMeTPPT) that was activated under green light irradiation,[144] and a reducing iridium polypyridyl photocatalyst ($Ir(ppy)_3$) that was activated under blue light irradiation (Figure 11C).[145] Critically, polymerization under green light led to the selective incorporation of iso-butyl vinyl ether (IBVE) into the polymer chain via a cationic mechanism, while blue light induced the polymerization of methyl acrylate (MA) via a radical mechanism to form block-like copolymers. Uniquely, this strategy allowed the main-chain units to be switched between IBVE and MA, which is not possible through the dual functional initiator approach. On the other hand, the oxidizing pyrylium and reducing $Ir(ppy)_3$ photoredox catalysts have significant spectral overlap, which necessitates future work on developing new catalysts with more distinct spectral properties.

Wavelength-selective regulation of polymer topology

Apart from switching between mechanistically distinct polymerization processes, wavelength-selective photocontrolled polymerizations can also be used to regulate polymer topology. For example, Boyer and coworkers demonstrated the wavelength-selective photoactivation of different chain-transfer agents (Figure 12A).[146] It was discovered that dithiobenzoates could be activated under red light (690 nm) irradiation in the presence of pheophorbide *a* (PheoA) while trithiocarbonates were not. To exploit this selective activation, a copolymerization of MMA and a trithiocarbonate functionalized methacrylate (BTPEMA) was performed. Upon irradiation with red light (690 nm), PheoA

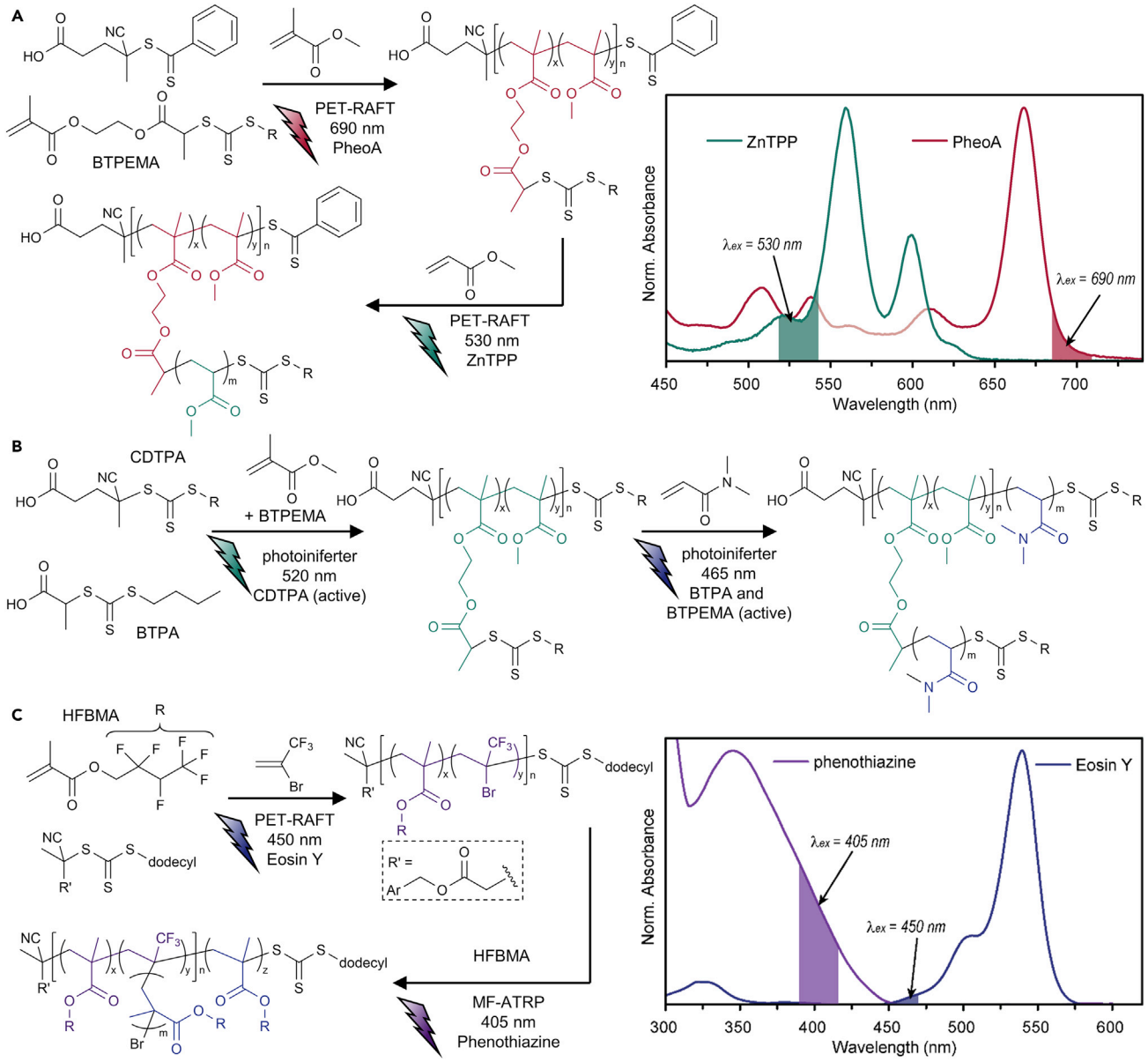

Figure 12. Wavelength-selective regulation of polymer topology

(A) Synthesis of graft copolymers through selective activation of dithiobenzoate and trithiocarbonate under red and green light irradiation, respectively. Overlaid UV-vis absorption plots of ZnTPP and PheoA are shown to the right.

(B) Synthesis of graft copolymers through selective activation of trithiocarbonates under green and blue light irradiation.

(C) Synthesis of graft copolymers through selective activation of PET-RAFT and metal-free ATRP under blue and purple light irradiation, respectively. Overlaid UV-vis absorption plots of phenothiazine and Eosin Y are shown to the right.

resulted in a photocontrolled polymerization of methacrylate, while the BTPEMA inimer (**ini**tiator/mono**mer**) was subsequently activated using ZnTPP and green light irradiation (530 nm) in the presence of acrylates. As a result, well-defined graft copolymers were formed in a mild one-pot two-step process by simply adding acrylate monomer and toggling a light switch.

Matyjaszewski, Boyer, and coworkers have also demonstrated a dual-wavelength-selective photoactivation process using a catalyst-free, photoiniferter (**photo-ini**tiator/trans**fer**

agent/terminator) approach (Figure 12B).[147] In this work, two trithiocarbonate chain-transfer agents with distinct absorption bands were selected: 4-cyano-4-[(dodecylsulfanylthiocarbonyl)sulfanyl]pentanoic acid (CDTPA), having a thiocarbonyl $n \rightarrow \pi^*$ transition with an absorption maximum of ~530 nm (green light) tailing down to ~500 nm, and 2-(n-butyltrithiocarbonate)-propionic acid (BTPA), having a thiocarbonyl $n \rightarrow \pi^*$ transition with an absorption maximum of ~450 nm (blue light) tailing up to ~525 nm. The combination of CDTPA with a BTPA functionalized methacrylate (BTPEMA) thus allowed the formation of graft copolymers through green light irradiation to polymerize MMA, and subsequent blue light irradiation to polymerize dimethyl acrylamide (DMAm) side chains. Matyjaszewski and coworkers have extended this work for the formation of structurally tailored and engineered macromolecular gels, whereby a polymer network is formed under green light irradiation and subsequently expanded under blue light irradiation leading to chain extension with MA or DMAm through the pendant BTPA groups.[148]

Chen and coworkers have presented a dual catalytic system for the wavelength-selective polymerization of linear and branched fluoropolymers (Figure 12C).[149] In this work, eosin Y was used as a photocatalyst under blue light (450 nm) irradiation to selectively activate a trithiocarbonate chain-transfer agent for PET-RAFT polymerization of 2-bromo-trifluoropropene (BTP) and a fluorinated methacrylate monomer (HFBMA). Subsequently, phenothiazine was activated with violet light (405 nm) for photocontrolled metal-free ATRP from the bromide comonomer BTP, which was possible due to the high reduction potential of phenothiazine relative to esoin Y. Additionally, branched architectures could be formed directly under 405 nm irradiation in the presence of phenothiazine given its high reduction potential resulting in activation of both BTP and the chain-transfer agent, causing addition of HFBMA to both the side chain and backbone, resulting in graft copolymers.

As a final example, Barner-Kowollik and coworkers recently demonstrated that different colors of light can produce cyclic or linear topologies during the photocycloreversion of styrylpyrene adducts.[150] Specifically, carboxystyrylpyrene units were introduced at the termini of linear telechelic polyethylene glycol and a step-growth polymerization was induced by blue light (460 nm) irradiation. By increasing the concentration of the polymer, intermolecular reactions are favored over intramolecular cyclization. Subsequently, employing two distinct wavelengths, UV-B (330 nm) or violet light (410 nm), afforded linear or cyclic depolymerization adducts, respectively. The authors hypothesized that violet light triggers the cycloreversion as well, yet dynamically reforms smaller cyclic polymers.

Sequential polymerization and coupling using dual wavelengths

In addition to dual polymerization approaches, photocontrolled polymerizations have been combined with light-driven post-modification coupling reactions by exploiting wavelength selectivity. For instance, Boyer, Yeow, and coworkers demonstrated that wavelength selectivity can be used for photopolymerization-induced self-assembly (photo-PISA) and subsequent photo-crosslinking (Figure 13A).[151] In this work, the initial polymerization and supramolecular self-assembly was accomplished via PET-RAFT polymerization with ZnTPP under orange light (590 nm) irradiation. A coumarin functionalized methacrylate monomer was incorporated into the polymer backbone to enable subsequent photoinduced crosslinking via a [2 + 2] dimerization of coumarin upon irradiation with UV light (365 nm). In a complementary system, photo-PISA and subsequent particle dissociation was also demonstrated.[152] In this work, the initial polymer synthesis was performed using a nitrobenzyl methacrylate monomer and PET-RAFT polymerization under red light irradiation.

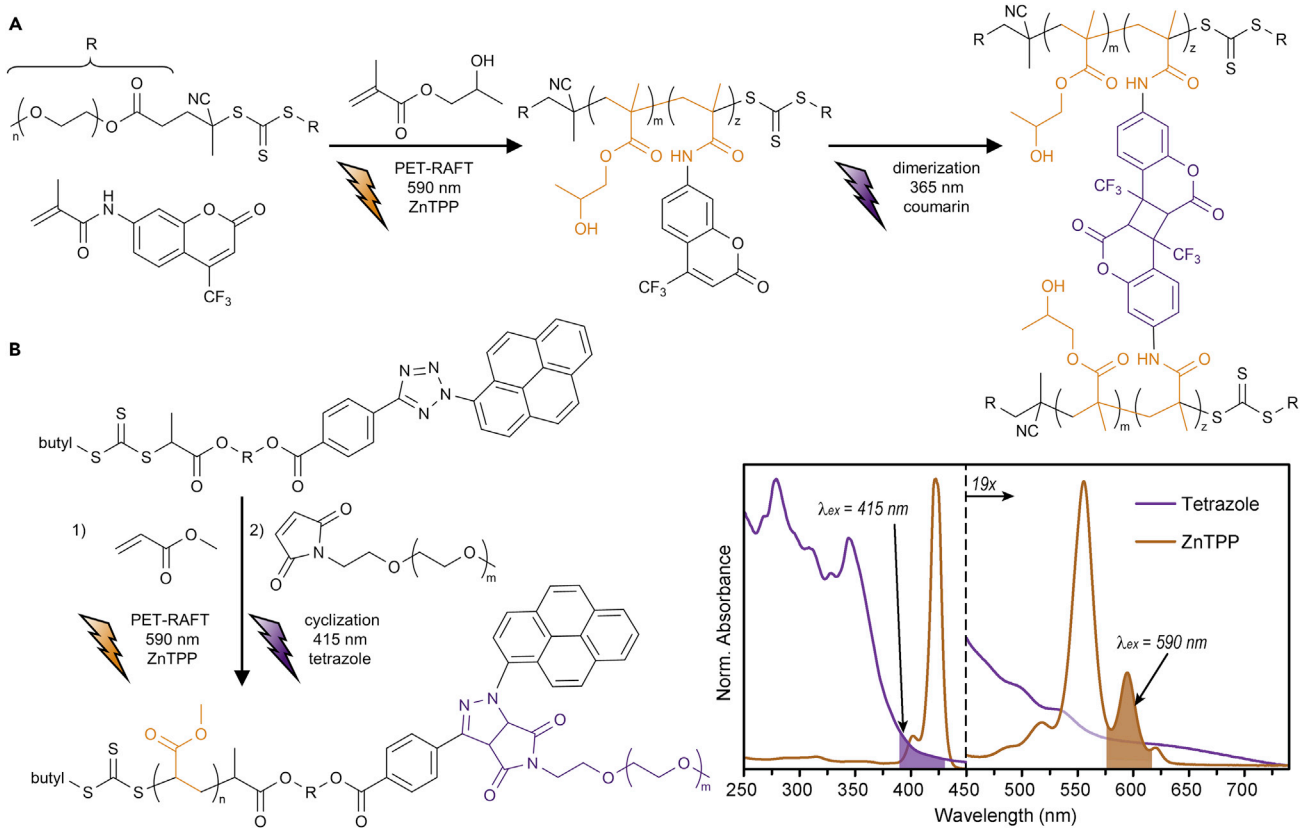

Figure 13. Wavelength-selective sequential polymerization and post-modification

(A) Synthesis of nanoparticles through sequential PET-RAFT and coumarin dimerization under orange and UV light irradiation, respectively.
(B) Synthesis of a block copolymer through sequential PET-RAFT and tetrazole-ene cycloaddition under orange and purple light irradiation, respectively. Overlaid UV-vis absorption plots of ZnTPP and tetrazole are shown to the right.

Following particle formation, irradiation with UV light induced nitrobenzyl cleavage, changing the polarity of the polymer chain and dissociating the polymer particles. Delaittre and coworkers proposed an alternative strategy for the functionalization of polymeric nanoparticles prepared by photo-PISA that relied on visible light-mediated PISA to generate a copolymer bearing a UV-responsive tetrazole functionality.[153] Subsequently, attachment of maleimides via NITEC under UV light was demonstrated as an effective protocol to introduce various functionalities at the polymer nanoparticle surface. This work inspired a more recent protocol by Barner-Kowollik, Boyer, and coworkers that relied on two visible wavelengths of light.[154] Here, PET-RAFT with ZnTPP under orange light (590 nm) irradiation produced an acrylate copolymer from a pyrene-tetrazole functionalized chain-transfer agent, which undergoes a cycloaddition reaction with activated double bonds (e.g., maleimide) upon exposure to violet light (415 nm) (Figure 13B). This was used to prepare a diblock copolymer, given the chain-end functionalization, and presents a mild alternative to fabricating other functional polymeric materials.

WAVELENGTH-SELECTIVE POLYMER PROPERTY MANIPULATION

Photoswitches (e.g., azobenzene, spiropyran, and diarylethene) have been utilized to reversibly manipulate polymeric materials for decades, and as such this section will only emphasize literature from the last decade on wavelength-selective transformations. Additionally, as there exist several comprehensive recent reviews on

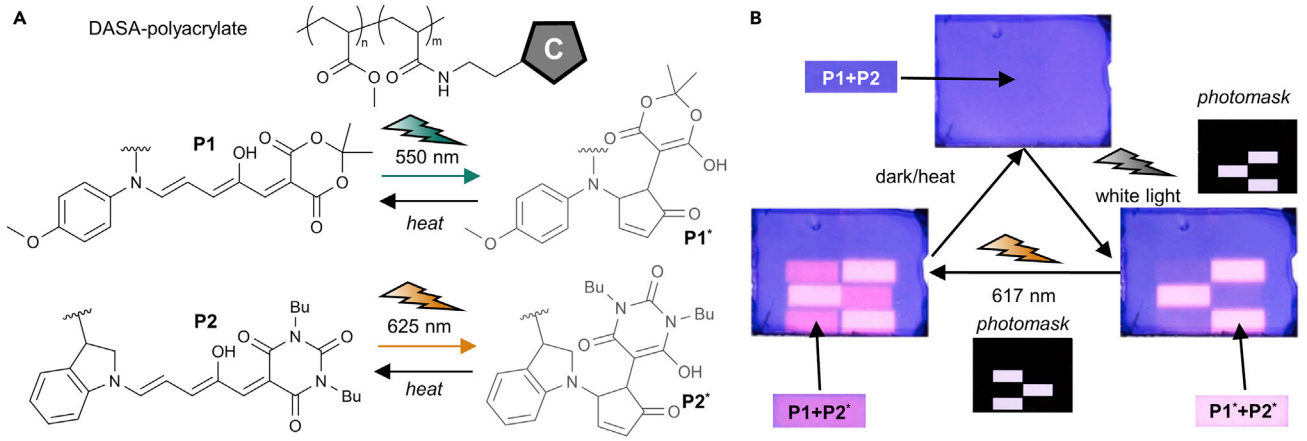

Figure 14. Wavelength-selective patterning of color

(A) Chemical structures of donor-acceptor Stenhouse adduct (DASA) polyacrylates **P1** and **P2**. Visible light irradiation switches both **P1** and **P2** into colorless photostationary states **P1*** and **P2***, while the process is reversed through heating.

(B) Schematic illustration of multicomponent selective photopatterning. In a first step the **P1** + **P2** blended thin film on glass was irradiated with warm white light through a photomask of three alternating transparent rectangles. Subsequently, an inverted photomask from the first was placed on top and irradiated with an orange LED for 5 min. Removal of the photomask revealed a patterned sample with three distinct regions: purple (**P1** + **P2**), pink (**P1** + **P2***), and colorless (**P1*** + **P2***). Heating the sample at 70°C for 5 min in the dark fully erased the pattern and returned the sample to its original state. Image modified with permission from Read de Alaniz and coworkers.[163]

related topics,[56,155–162] the selected references in this section are merely representative. Emphasized herein is the distinction between bidirectional photochemical pathways (single-chromophore systems) and disparate photochemical pathways (multiple-chromophore systems), broken down by the properties under manipulation, including optoelectronic, ion-transport, and mechanical.

Wavelength-selective optoelectronic properties

Photoswitches are well-established motifs for modulating the optoelectronic properties of soft materials.[158] Whether chemically bonded to or physically blended with an optoelectronically active polymer, photoswitches have been demonstrated to enable control over (1) absorption, (2) fluorescence, and/or (3) conductance. These photoresponsive materials are attractive for a variety of applications, such as rewritable data storage, super-resolution bioimaging, and organic light-emitting devices.

Photomediated absorption

Materials with tunable absorption profiles allow for selective photopatterning that is potentially useful in rewritable data storage. This was demonstrated with wavelength-selective bidirectional photochemistry by Read de Alaniz and coworkers using multicomponent films composed of DASA molecules covalently tethered to polymers.[163] Specifically, polyacrylates bearing either a *para*-methoxyaniline-meldrums acid DASA unit, **P1**, or an indoline-barbituric acid DASA unit, **P2**, were synthesized and physically blended to enable wavelength-selective photopatterning (Figure 14A). Photopatterning was accomplished by first irradiating a thin film of the polymer blend through a photomask with white light (warm white 4,000 K, 66 mW/cm^2), switching both DASA components into colorless states. Subsequent irradiation with orange light (617 nm, 72 mW/cm^2) selectively switched **P2**, providing a ternary pattern (purple; pink; colorless). Given the reversibility of photoswitching, the pattern could be completely erased by heating the sample (70°C) above the glass transition temperature of the polymer matrix to provide a new slate for photopatterning (Figure 14B).

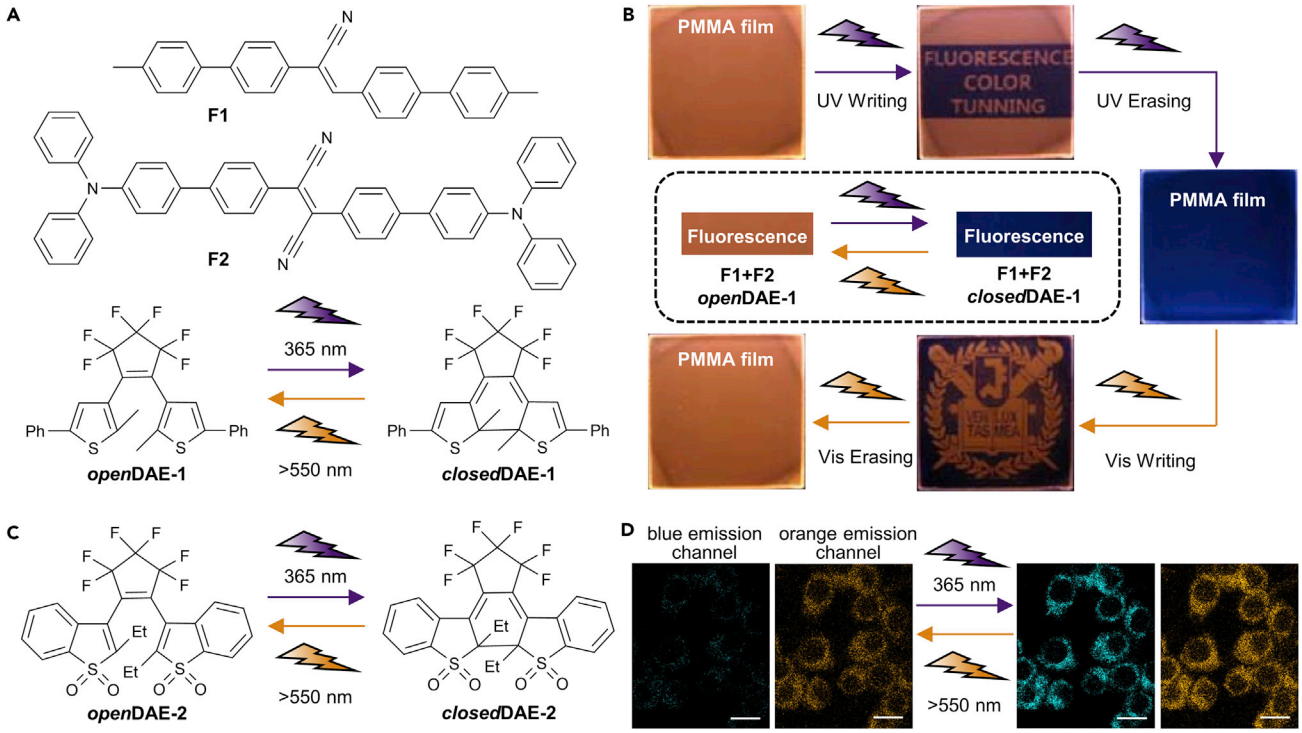

Figure 15. Photomediated fluorescence

(A) Chemical structures of fluorescent molecules: **F1**, **F2**, and photochromic reaction of **DAE-1**.

(B) Photoresponsive reversible fluorescence images of a **F1**/**F2**/**DAE-1** doped PMMA films (λ_{ex} = 365 nm). The orange and blue regions represent areas irradiated with visible and UV light, respectively.

(C) Chemical structure and photochromic reaction of **DAE-2**.

(D) Confocal images of macrophage cells incubated with the polycaprolactone nanoparticles for 1 h (scale bar, 10 μm): blue emission channel (460–500 nm) and orange emission channel (600–780 nm).

Image (B) modified with permission from Park and coworkers.[164] Copyright (2012), American Chemical Society. Image (D) modified with permission from Park and coworkers.[165] Copyright (2019), Springer Nature.

Photomediated fluorescence

DAEs are well-established photoswitches for modulating emission of luminescent polymers due to their (1) large absorption change upon switching and (2) excellent thermal stability and fatigue resistance.[27] Photomediated fluorescence is enabled by Förster resonance energy transfer (FRET) that occurs with the more π-conjugated closed DAE form. For example, Park and coworkers employed poly(methyl methacrylate) films comprising two fluorophores (**F1** and **F2**) with different emission colors (blue and orange) and **DAE-1** (Figure 15A).[164] Critically, the emission of **F1** at ~470 nm overlaps with the absorption of **F2** and **DAE-1** in its closed (colored) form, enabling FRET, but not **DAE-1** in its open (colorless) form. In this mixture, ***closed*DAE-1** acts as a non-radiative acceptor for **F1**, precluding emission from **F2** and resulting in blue fluorescence. However, switching **DAE-1** to the open form allows for FRET between **F1** and **F2**, resulting in orange fluorescence. Therefore, wavelength-selective switching of **DAE-1** from open to closed with UV light (365 nm) and reversal (closed to open) with visible light (>550 nm) enables photomediated fluorescence patterning (Figure 15B). In a subsequent publication, the same group accomplished photomediated fluorescence with a more simplified two-component system embedded in polycaprolactone nanoparticles.[165] The key here was a blue fluorescent ***closed*DAE-2** combined with an orange fluorescent dye (Figure 15C). In this example, irradiation with UV light results in blue + orange emission, while

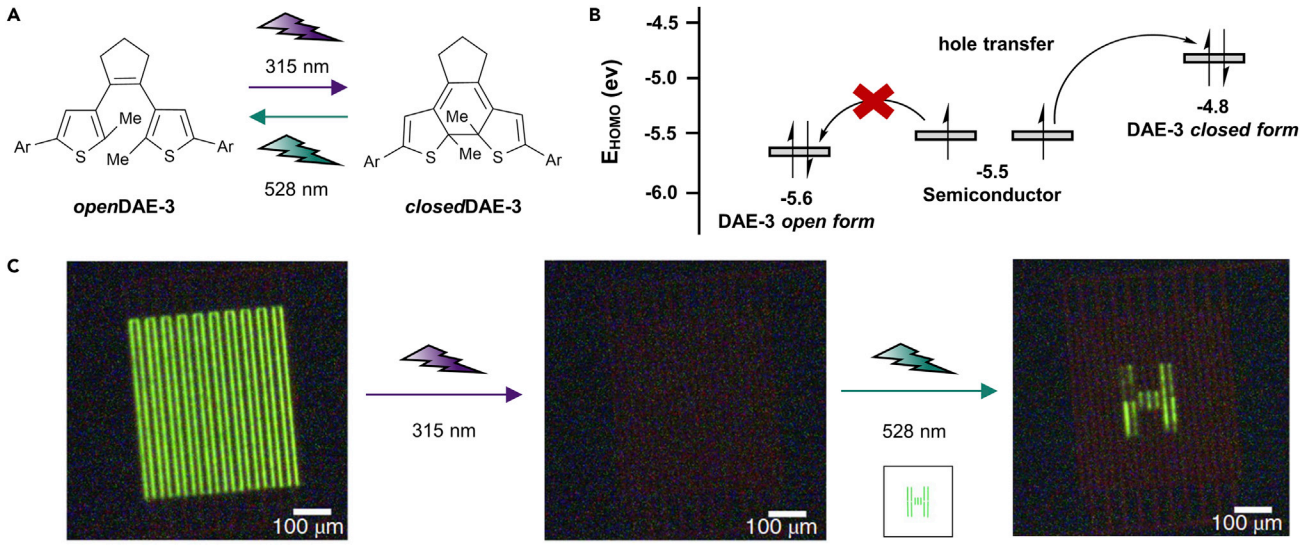

Figure 16. Photomediated charge transfer

(A) Chemical structures of **DAE-3** isomers (both open and closed forms) under UV light (315 nm) and visible light (528 nm).

(B) Energy level diagram showing the proposed switchable charge trapping mechanism.

(C) Images showing the process for rewritable emissive patterns on a single OLET. Image (C) modified with permission from Samorì and coworkers.[171] Copyright (2019), Springer Nature.

visible light irradiation forms *open*DAE-2, turning off fluorescence and leaving only orange emission. This was applied to microscopic bioimaging of macrophage cells with reversible fluorescence switching (Figure 15D).

Photomediated charge transfer

Recently, photoswitchable organic electronics, such as organic LEDs,[166–168] organic thin-film transistors,[169,170] and organic light-emitting transistors (OLETs),[171,172] have gained interest for their utility in next-generation reprogrammable devices. To date, this has been demonstrated by blending semiconducting polymers with photochromic **DAE-3** that act as a bidirectional wavelength-selective charge trap (Figure 16A). In combination with a semiconducting polymer that contains a ground-state energy level between those of the two isomeric DAE states, the DAE can act as a hole trap in the closed state (UV irradiated) and not in the open state (visible irradiated) (Figure 16B). This has been applied to OLETs by Samorì and coworkers, where both current and luminescence were reversibly modulated by irradiation cycles with UV (315 nm) and visible light (528 nm).[171] The spatiotemporal control offered by light was elegantly demonstrated in these OLETs by generating rewritable emissive patterns on a single device (Figure 16C). Recently, the same group has identified guidelines for fabricating high-performance optically switchable devices: (1) weak interactions between polymer matrix and DAE; (2) low-percentage crystallinity in the polymer matrix for homogeneous mixing; (3) polymer HOMO (highest occupied molecular orbital) level close to the closed DAE for higher device mobility or close to the open DAE for higher on/off current ratio.[172]

Wavelength-selective ion transport

Similar to the optoelectronic properties discussed previously, the ion-transport properties of polymeric materials can also be tuned with the aid of photoswitches. Unlike the dependence on photoswitchable energy transfer in previous examples, the following systems rely on the bidirectional wavelength-selective ion affinity of

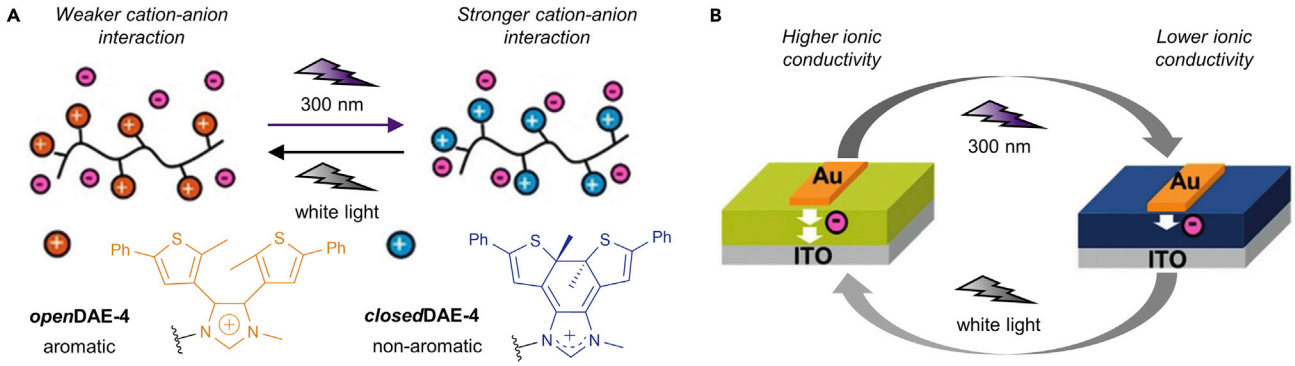

Figure 17. Photomediated aromaticity

(A) Polyionic liquid bearing a photoswitchable DAE to tailor ionic interactions (chemical structures of open and closed **DAE-4** shown).

(B) Device architecture used to measure ionic conductivity of thin photoswitchable films. Image modified with permission from Read de Alaniz and coworkers.[173]

photoswitches. To date, two established photomediated mechanisms governing the strength of ion affinity have been demonstrated: (1) aromaticity and (2) acidity/basicity.

Photomediated aromaticity

Ion-transport modulation has been accomplished by Read de Alaniz and coworkers using a wavelength-selective polymer ionic liquid containing positively charged DAE units (**DAE-4**).[173] The key was tuning the cationic character of the imidazolium bridging group upon photoswitching (Figure 17A). Specifically, ***open*DAE-4** (obtained upon irradiation with visible light) molecules are aromatic and delocalize the positive charge, weakening the ionic interactions. In contrast, irradiation with UV light triggers the formation of ***closed*DAE-4**, leading to a non-aromatic imidazolium with greater localization of the positive charge, strengthening the binding with mobile ions. Thus, reversible modulation of ionic binding strength resulted in tailored ionic conductivity (Figure 17B). The influence of different counterions (I^- versus BF_4^- versus $TFSI^-$) was further investigated, which revealed that anions featuring stronger cation-anion interaction (I^-) and higher ratios of ring-closed photostationary states have a greater impact on photomediated ionic conductivity.[174] More recently, the same group integrated these photochromic molecules with self-healable polymer electrolytes, illustrating potential applications in "smart" electronics.[175]

Photomediated acidity

Apart from DAEs, SPs have also been used as photoswitches to control ionic transport across polymeric membranes. Here, modulation relies on a decrease in acidity (increase in pK_a) in going from the "closed" SP to the "open" merocyanine (MC) state. Bakker and coworkers utilized this pK_a shift for proton exchange membranes comprising SP and a cation exchanger (Borate R^-), where ion selectivity was dependent on the state ("open" or "closed").[176] The proton gradient was generated across a membrane by irradiating one side with UV light and the other with visible light. In a 0.1 M HCl solution, the change in electrochemical potential resulted in the generation of a photocurrent, with proton transport aided by Borate R^- (Figure 18). Furthermore, reversibility was demonstrated by cycling between UV and visible light irradiation, which induced an alternating current.

Wavelength-selective mechanical property tuning

The mechanical properties of a polymeric material (e.g., stiffness, hardness, storage/loss modulus, tensile strength) are critical in determining its suitability for a particular

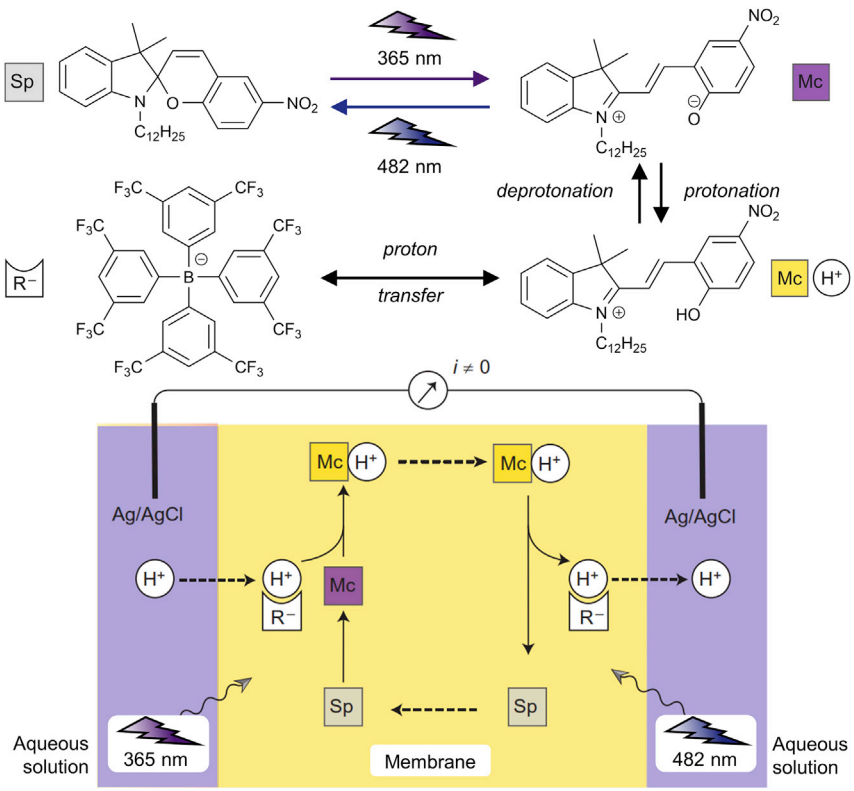

Figure 18. Photomediated acidity

The left side of the membrane is illuminated with UV light (365 nm) and the right with visible light (482 nm). The membrane contains spiropyran (SP), a cation exchanger, a lipophilic salt (tetradodecylammonium tetrakis(4-chlorophenyl)borate), and nitrophenyloctylether (NPOE) as the solvent. For simplicity, the lipophilic salt and NPOE are not shown. Image modified with permission from Bakker and coworkers.[176] Copyright (2014), Nature Publishing Group.

application.[177] The ability to manipulate mechanical properties with spatiotemporal control will pave the way for next-generation functional plastics. To date, wavelength-selective transformations have facilitated the preparation of materials with disparate mechanical properties in two fashions: (1) photoisomerization and (2) making and breaking covalent bonds.

Photoisomerization

Unique to mechanical property manipulation of polymers with photoswitches is the ability to do so through altering non-covalent interactions, such as solid-state packing of polymer chains.[178] In this regard, azobenzene has been extensively examined due to the dramatic change in molecular properties that occurs upon switching between *trans* and *cis* configurational isomers, including end-to-end distance (9.0–5.5 Å, respectively) and dipole moment (0–3 D, respectively).[13] To maximize the impact that azobenzene photoswitches have on mechanical properties, it is important to select a polymer matrix that will undergo a macroscopic shift in response to a microscopic change (e.g., isomerization). For example, Wu and coworkers demonstrated that a polyacrylate bearing azobenzene side chains converts from an ordered solid (**P3-*trans*AB**, $T_g \sim 48°C$) to an isotropic liquid (**P3-*cis*AB**, $T_g \sim -10°C$) upon irradiation with UV light (~365 nm, 67 mW/cm^2), and reverts back to a solid (**P3-*trans*AB**) upon exposure to visible light (~530 nm, 5 mW/cm^2) (Figure 19A).[179] This reversible transformation in physical appearance is accompanied

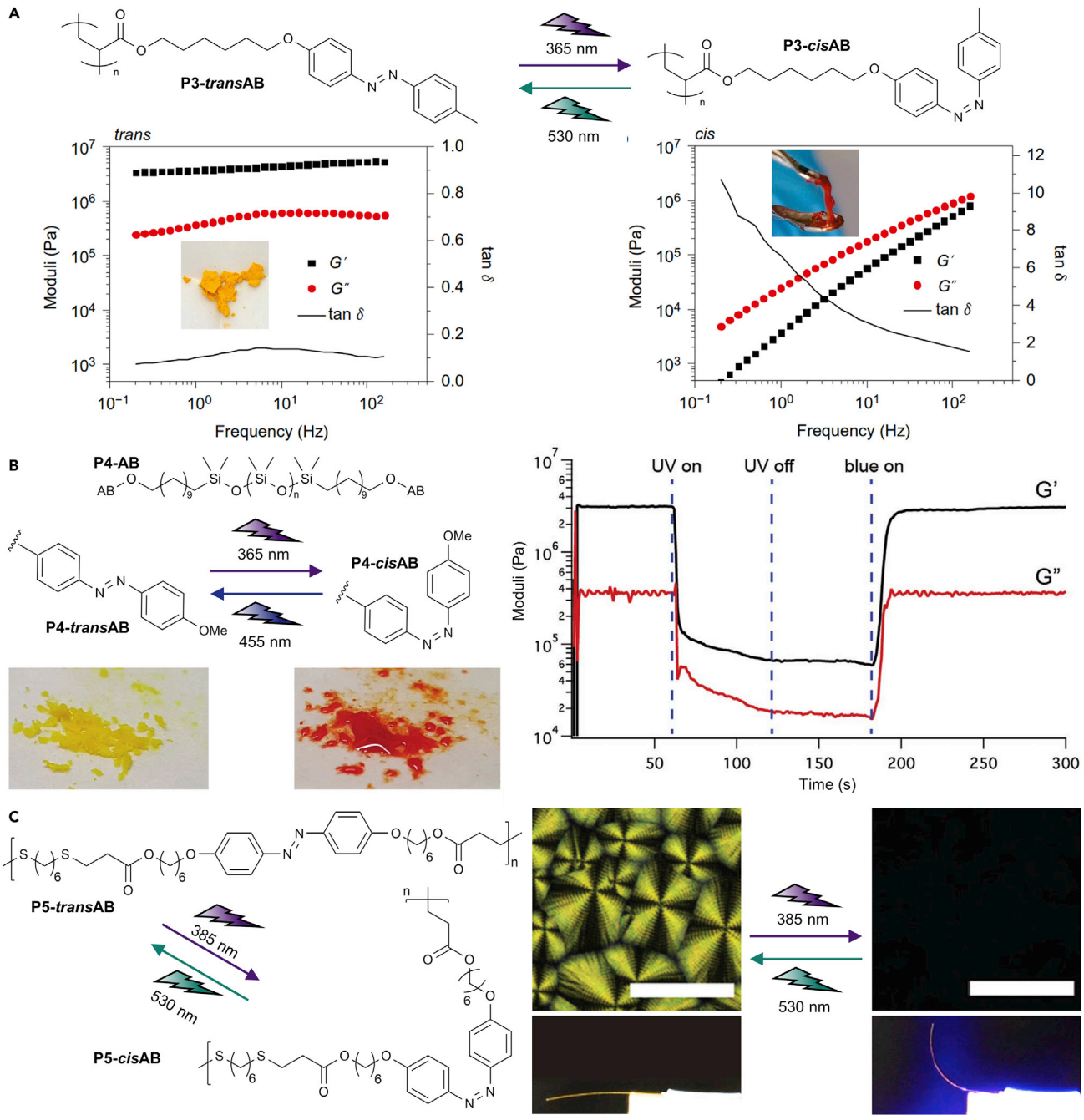

Figure 19. Photoisomerization to tailor mechanical properties through non-covalent solid state packing interactions

(A) Chemical structures of P3-azobenzene isomers under UV light (365 nm, 67 mW/cm^2) and visible light (530 nm, 5 mW/cm^2), with corresponding photorheology data highlighting *G′*, *G″*, and tan*δ*. Insets are pictures showing the transformation from a solid to liquid form upon isomerization from P3-*trans*AB to P3-*cis*AB.

(B) Chemical structures for **P4-AB** isomers (*trans* and *cis* forms) under UV light (365 nm, 200 mW/cm^2) and visible light (455 nm, 200 mW/cm^2), with corresponding photorheology data highlighting the wavelength selectivity and temporal control over *G′* and *G″*.

(C) Chemical structures of P5-azobenzene isomers under UV light (385 nm, 100 mW/cm^2) and green light (530 nm), with corresponding polarized optical microscopy images (top) and actuation (scale bar, 100 μm).

Image (A) modified with permission from Wu and coworkers.[179] Copyright (2016), Nature Publishing Group. Image (B) modified with permission from Meijer and coworkers.[180] Copyright (2017), Wiley-VCH. Image (C) modified with permission from Hayward and coworkers.[181] Copyright (2020), American Chemical Society.

by stark changes in mechanical properties, such as storage and loss moduli (G' and G'') measured using photorheology that shows solid-like behavior for **P3-*trans*AB** ($G' > G''$) and liquid-like for **P3-*cis*AB** ($G' < G''$).

In contrast to polymers with azobenzene side chains, main-chain incorporation of azobenzene has also enabled wavelength-selective manipulation of mechanical properties. For example, Meijer and coworkers prepared linear homotelechelic poly(dimethylsiloxane) derivatives end-capped with azobenzene units (**P4-AB**) and demonstrated reversible conversion from solid to liquid upon irradiating with UV light (365 nm, 200 mW/cm^2), and back again with visible light (455 nm, 200 mW/cm^2).[180] Monitoring G' and G'' via *in situ* rheology revealed a significant drop in both moduli upon exposure to UV light, and a near full recovery upon switching to blue light (Figure 19B). These materials are attractive as photoswitchable adhesives. Additionally, main-chain poly(azobenzene)s have been used to convert photon energy into mechanical work (photomechanical actuation). In a recent report by Hayward and coworkers,[181] this was demonstrated using semicrystalline main-chain poly(azobenzene)s, prepared by thiol-Michael addition. Bidirectional wavelength-selective reversible melting and recrystallization upon irradiation with UV light (385 nm, 100 mW/cm^2) to **P5-*cis*AB** and green light (530 nm) to **P5-*trans*AB**, respectively, led to photoactuation with shape memory applications (Figure 19C).

Photoisomerization to modulate mechanical properties via bidirectional wavelength selectivity has also been accomplished by tuning the rate and degree of dynamic crosslinking using functionalized photoswitches with configurationally dependent reactivity. For example, Kalow and coworkers prepared tetra-armed poly(ethylene glycol) (PEG) with either a boronic acid functionalized azobenzene (**P6-AB**) or diol as end groups (Figure 20A).[182] It was experimentally observed (and theoretically computed) that the boronic acid on **P6-AB** was more reactive with diol (to form boronic esters) when the azobenzene was in a *cis* form (**P6-*cis*AB**), which was leveraged to toggle between a sol and gel state by irradiating with different wavelengths of light. Specifically, exposure to UV light (365 nm, 3.6 mW/cm^2) resulted in *trans*-to-*cis* isomerization and gel formation, while exposure to blue light (470 nm, 900 lux) resulted in reversion back to sol. The authors extended this work to a more thermally stable and purely visible light-controlled system (blue, 470 nm and green, 525 nm) by using *ortho*-difluoro-azobenzene derivatives. The resultant hydrogels can serve as promising candidates to probe mechanobiology, which examines the effect of dynamic mechanics on cell behavior.[183]

In addition to azobenzene crosslinkers with wavelength-selective reactivity, DAE photoswitches have also been examined. One example was a dialdehyde-DAE by Hecht and coworkers, which had configurationally dependent amine condensation reaction kinetics.[184] Irradiation with UV light (313 nm) resulted in the ring-closed form that was shown to be more electrophilic and thus reactive toward primary amines by ~1 order of magnitude relative to the ring-open, less electron-delocalized form that occurred upon exposure to visible light (579 nm) (Figure 20B). Reacting the dialdehyde-DAEs with a multi-functional amine-containing polysiloxane resulted in the formation of a dynamic covalent polyimine network capable of self-healing with a rate controlled by the wavelength of light (UV = faster healing relative to visible light). The same group developed another strategy based on a photomediated Diels-Alder reaction, where a DAE-bearing furan acted as a diene in the open form (upon irradiation with visible [460 nm] light) capable of undergoing thermally reversible Diels-Alder reactions.[185,186] However, irradiation with UV light

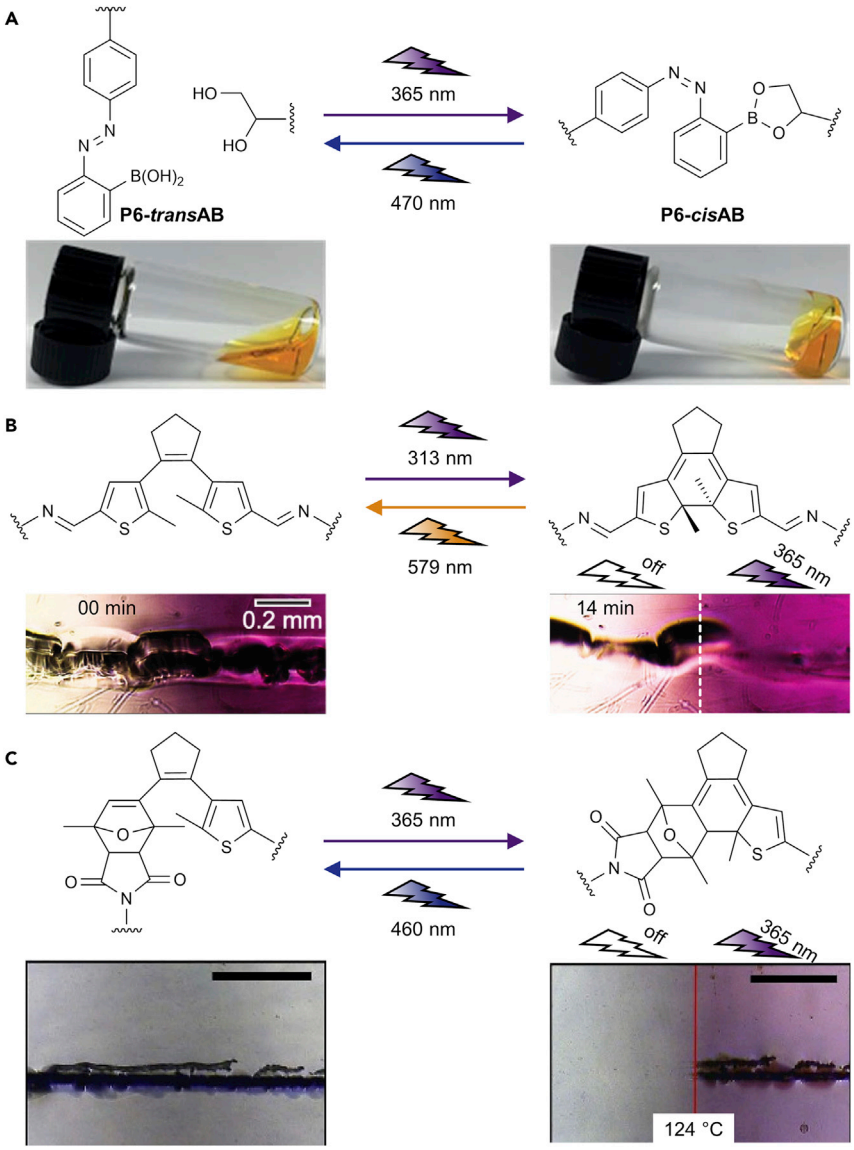

Figure 20. Photoswitch-based crosslinkers to modulate the rate and equilibrium of dynamic covalent bonds within polymer networks

(A) Photoreversible boronic ester formation under alternating UV (365 nm, 3.6 mW/cm^2) and visible (470 nm, 900 lux) light irradiation to convert between a sol and gel (shown in the corresponding images).

(B) UV-light-accelerated imine exchange used for self-healing that is faster in UV-light-exposed areas (right) as compared with non-exposed areas (left).

(C) A Diels-Alder adduct that shows accelerated thermal reversibility (retro-Diels-Alder) in the open form relative to the closed form. Corresponding microscopy images of a scratched film that heals upon heating in the non-exposed region (left), and not the UV-light exposed region (right).

Image (A) modified with permission from Kalow and coworkers.[182] Copyright (2018), Royal Society of Chemistry. Image (B) modified with permission from Hecht and coworkers.[184] Copyright (2016), Wiley-VCH. Image (C) modified with permission from Hecht and coworkers.[185] Copyright (2016), Springer Nature.

closed the ring and eliminated the diene unit necessary for the Diels-Alder reaction. This wavelength-selective reactivity was demonstrated to tailor the mechanical properties and self-healing behavior of a polymer network bearing maleimide functionality poised for Diels-Alder reactions with the furan-functionalized DAE crosslinkers (Figure 20C).

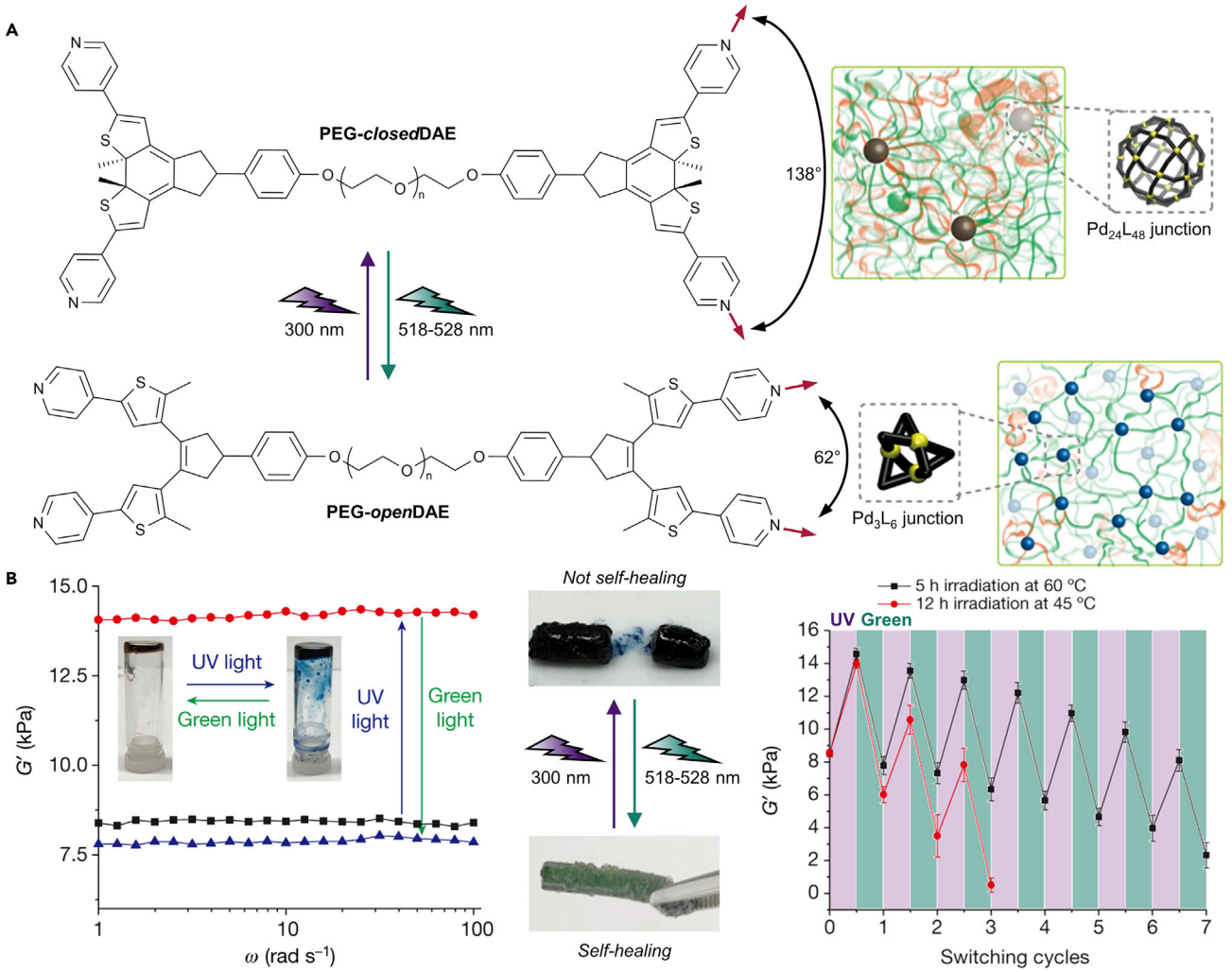

Figure 21. Wavelength-selective switching of polymer metal organic cage networks.

(A) Schematic illustration of photomediated interconversion between two different network topologies. Photoresponsive MOCs are introduced as junctions within polyMOCs. Under UV irradiation (300 nm), the MOCs convert from Pd_3L_6 to $Pd_{24}L_{48}$, which can be reversed with green light (518–528 nm).

(B) Impact of photoswitchable network topology on storage modulus (*G*′) (left) and self-healing (center) properties, and associated fatigue as a function of irradiation time per cycle (right).

Image modified with permission from Johnson and coworkers.[187] Copyright (2018), Macmillan Publisher Ltd.

Recently, Johnson and coworkers demonstrated a unique strategy to tailor the topology and associated mechanical properties of polymer metal-organic cage (polyMOC) networks using a bidirectional wavelength-selective photoswitch.[187] In this example, the polymer chains were crosslinked via a bifunctional PEG end capped with pyridyl functionalized DAE photoswitches (PEG-DAE). The photoswitches facilitated reversible metallosupramolecular assembly of discrete metal-organic cages (MOCs) by altering the bond angle between the pyridines (and associated bite angle in the presence of a metal) upon converting between open (62°) and closed (138°) states.[188] Thus, mixing PEG-DAE with Pd^{2+} afforded polyMOC gels with nanosized $metal_x ligand_y$ (M_xL_y) cages as crosslink junctions that could be switched from small (Pd_3L_6) to large ($Pd_{24}L_{48}$) MOCs upon irradiation with UV light (300 nm) and back again when exposed to green light (518–528 nm) (Figure 21A). The larger junctions from **PEG-*closed*DAE** were found to be less dynamic than the smaller ones from **PEG-*open*DAE** and, as such, irradiation with UV light increased the storage modulus (*G*′) from ~8 to 14 kPa, which was partially reversible upon exposure to green light

(Figure 21B). Furthermore, self-healing was shown to occur only in the small junction gels, PEG-*open*DAE, after UV irradiation. However, fatigue was observed for the gels with extended irradiation, as noted by a decrease in storage modulus upon repeated irradiation cycles.

Making and breaking covalent bonds

Photoreversible cycloadditions provide thermosets capable of making and breaking covalent bonds upon exposure to light of a selective wavelength. Sumerlin and coworkers designed water-soluble linear polymers bearing coumarin side chains that, upon exposure to long-wavelength UV light (365 nm, 7 mW/cm^2), crosslinked via dimerization to form hydrogels (Figure 22A).[189] However, upon irradiation with short-wavelength UV light (254 nm) these hydrogels could be reverted to soluble polymer precursors. To overcome the limitations of short-wavelength UV light, particularly for biomedical applications, Truong, Forsythe, and coworkers reported wavelength-selective coupling and decoupling of polymers via the photoreversible cycloaddition of styrylpyrene (StyP) mediated by visible (410–460 nm, cycloaddition) and long-wavelength UV light (365 nm, cycloreversion) irradiation (Figure 22B).[190] Leveraging this bidirectional wavelength-selective reversible transformation, the mechanical properties of the resultant hydrogels (4arm-StyP-StyP-PEG) could be modulated. Furthermore, self-healing was demonstrated by irradiating fractured hydrogels with UV light followed by visible light. This was taken one step further by combining styrylpyrene with a more red-shifted derivative, acrylamidylpyrene (AP), which enabled the formation of a hydrogel (4arm-StyP-AP-PEG) with disparate wavelength-selective stiffness (Figure 22B).[191] These hydrogels can serve as a promising platform to probe mechanobiology.

Combining two orthogonal photochemical reactions with wavelength-selective activation has also been used to control the mechanical properties of polymer networks. Anseth and coworkers demonstrated this by combining PPGs with a free radical photopolymerization.[192] In this example, a hyaluronic acid hydrogel was fabricated with photodegradable *o*NB crosslinks and polymerizable methacrylates. Sequential exposure to UV light (365 nm, 10 mW/cm^2) in the absence of a photoinitiator and visible light (400–500 nm, 10 mW/cm^2) in the presence of lithium phenyl-2,4,6-trimethylbenzoylphosphinate (LAP) as a photoinitiator resulted in photodegradation to soften (14.8 to 3.5 kPa) and polymerization to stiffen (3.5 to 27.7 kPa) the hydrogel, respectively (Figure 23A). Furthermore, the degree of each photochemical transformation was dependent on the total light dosage, which facilitated mechanical property tuning, and each was shown to be cytocompatible, making it an attractive method for tissue engineering applications.

In a later example, Barner-Kowollik and coworkers designed a strategy that eliminated the need to add photoinitiator in a separate step by combining disparate reactions that could be activated first with visible light followed by UV light.[193] Specifically, in one pot, a dimethacrylate crosslinker bearing a central disulfone unit was copolymerized with butyl acrylate using a photoinitiator (Ivocerin) reactive to visible light (400–520 nm), while also including an *o*NB protected cyclohexylamine that remained intact under these initial conditions (Figure 23B). Subsequently, exposure to UV light (355–390 nm) resulted in release of the photogenerated amine that then reacted with the disulfone crosslinks and softened the polymer network, ultimately resulting in a transformation from solid to liquid after ~4 h.

Wavelength-selective polymerization and manipulation of mechanical properties has also been accomplished using photoinduced dynamic covalent bond exchange

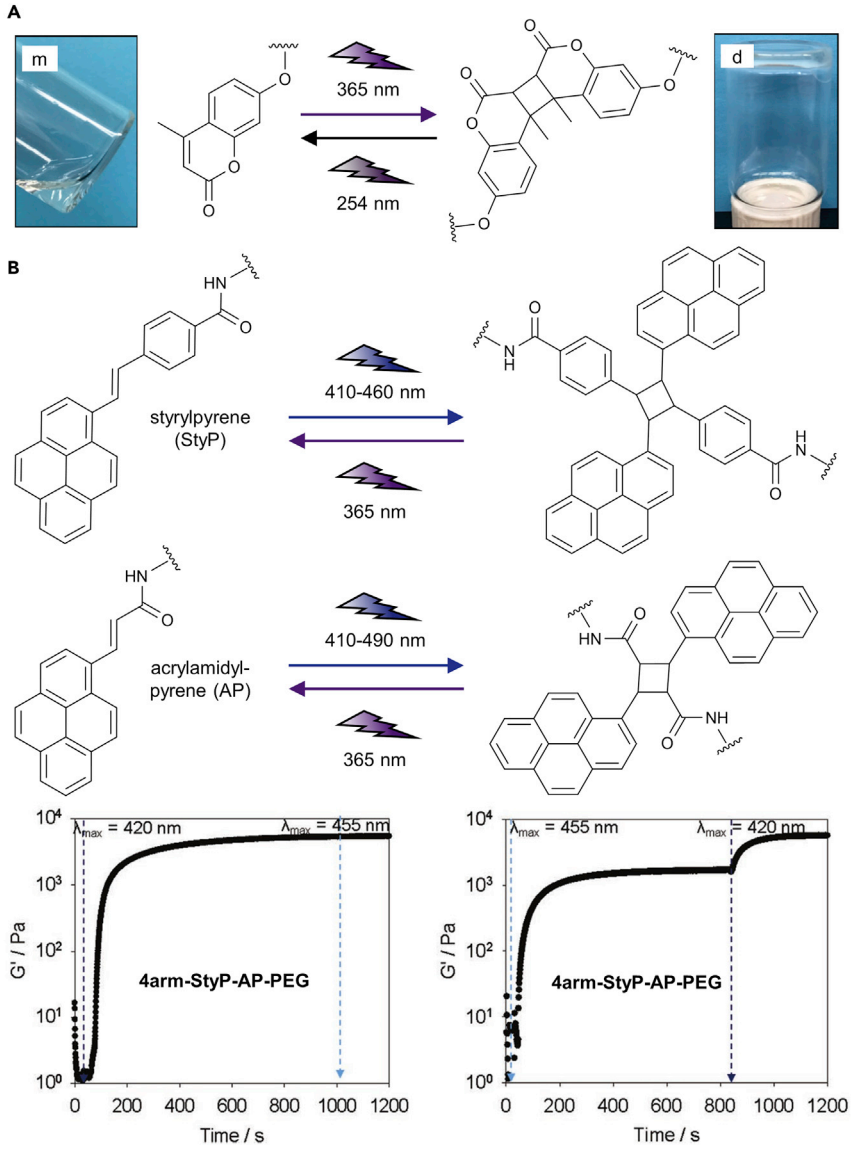

Figure 22. Photoreversible cycloaddition reactions to enable wavelength-selective mechanical modulation of hydrogels

(A) Coumarin crosslinked hydrogels using reversible photodimerization. Left: solution of polymer in water (5 wt %); right: hydrogel formed after irradiation of 5 wt % polymer solution with 365 nm light (7 mW/cm^2).

(B) Styrylpyrene (StyP) and acrylamidylpyrene (AP) photodimerization. Left plot: irradiation of 4arm-StyP-AP-PEG at λ = 420 nm (20 mW/cm^2) triggered gelation increasing the storage modulus to 4.8 kPa, with no change upon increasing the wavelength to 455 nm; Right plot: irradiation of 4arm-StyP-AP-PEG with light at λ = 455 nm (20 mW/cm^2) resulted in gelation and a maximum storage modulus of 1.74 kPa, which could be further increased to 5.4 kPa upon irradiating with 420 nm light. Image (A) modified with permission from Sumerlin and coworkers.[189] Copyright (2018), American Chemical Society. Image (B) modified with permission from Truong and coworkers.[191] Copyright (2020), Wiley-VCH.

in networks by Bowman and coworkers .[194] In a first step the thermoset network was generated using visible light (400–500 nm, 10 mW/cm^2) to activate an acylphosphine oxide photoinitiator (I-819) that reduced a Cu(II) precatalyst ($CuCl_2$/PMDETA) and led to Huisgen 1,3-dipolar cycloadditions between a multi-functional alkyne

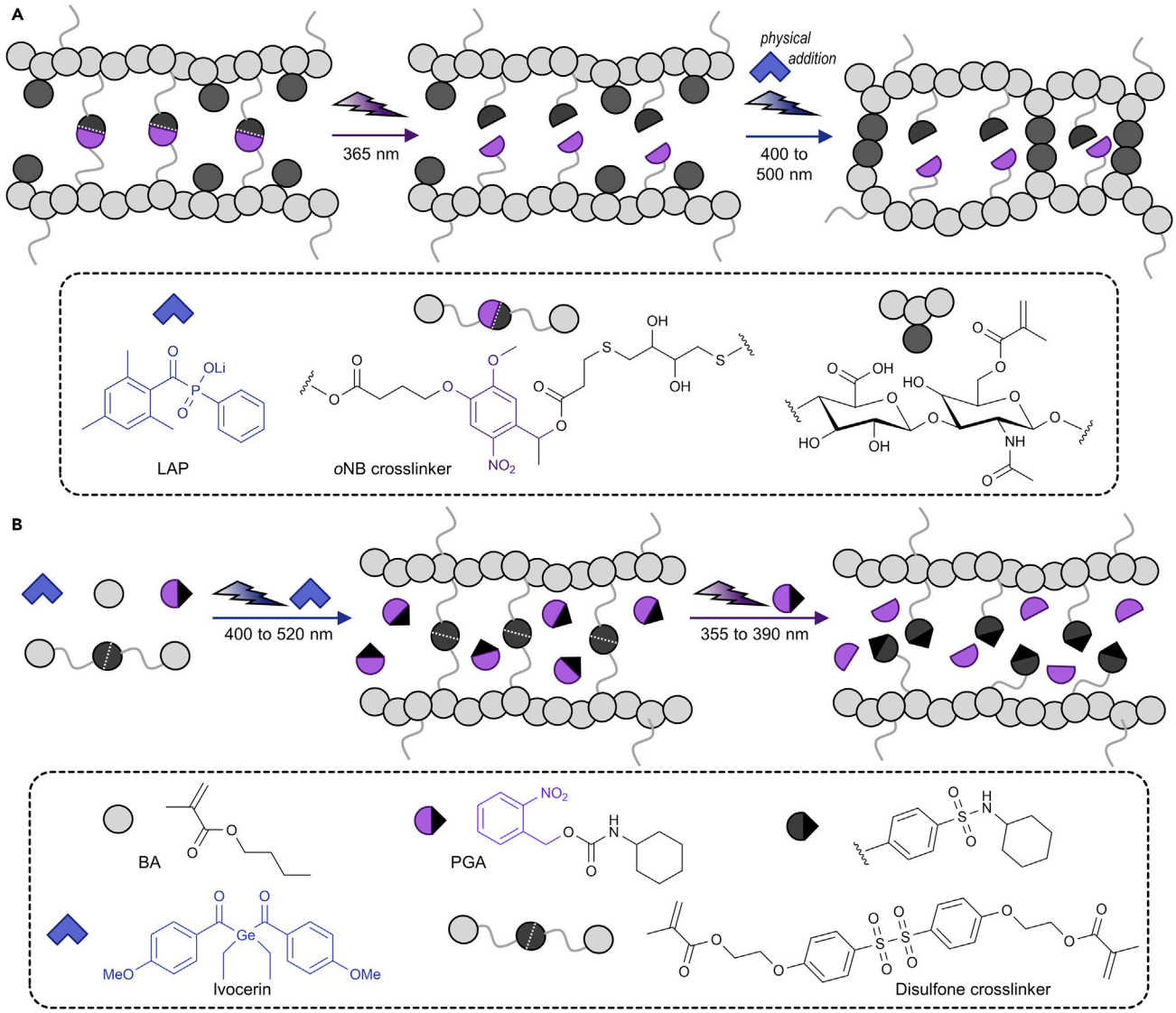

Figure 23. Schematic representation of stepwise photoreactions for controlling mechanical properties

(A) The initial hydrogel was irradiated with UV light (365 nm, 10 mW/cm^2) first. After the addition of photoinitiator lithium phenyl-2,4,6-trimethylbenzoylphosphinate (LAP), the materials were irradiated by visible light (400–500 nm, 10 mW/cm^2).

(B) The thermoset was prepared by photopolymerization through visible light (400–520 nm). The photodegradation happened after the light source was changed to UV light (355–390 nm).

Image (A) modified with permission from Anseth and coworkers.[192] Copyright (2017), Wiley-VCH. Image (B) modified with permission from Barner-Kowollik and coworkers.[193] Copyright (2017), American Chemical Society.

(Tri-AK and AS-AK) and azide (BZ-N_3) (Figure 24A).[195] Subsequently, UV light irradiation (365 nm, 8 mW/cm^2) was used to generate radicals from the photoinitiator dimethoxy-2-phenylacetophenone, which prompted dynamic covalent bond exchange of AS-AK, the allyl sulfide repeat units that were embedded in the main chain (Figure 24B). The authors demonstrated that the photoinduced dynamic bond exchange could be used for stress relaxation, even in the glassy thermosets. Stress relaxation was demonstrated by irradiating a thick polymer sample under tension from one side, where partial light penetration manifested as curling once tension was released, as shown in Figure 24A. Furthermore, UV irradiation of samples during

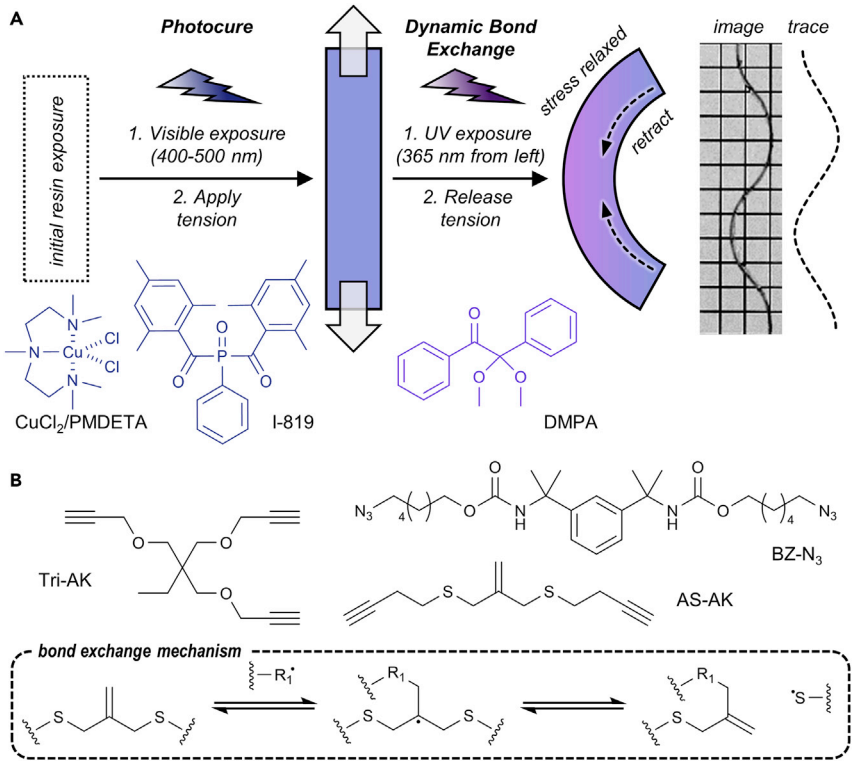

Figure 24. Wavelength-selective photocuring and photoactivated bond exchange

(A) Schematic of process used to create and manipulate dynamic polymer networks with light. In the first step, visible light is used to activate Cu-catalyzed alkyne-azide cycloaddition (CuAAC), followed by irradiation under tension to active stress relaxation via allyl sulfide bond exchange. Chemical structures of visible light initiator I-819 (Irgacure 819), copper catalyst ($CuCl_2$/PMDETA), and UV initiator DMPA (2,2-dimethoxy-2-phenylacetophenone) are shown beneath the corresponding arrow. The image on the right shows a film that was irradiated from alternating sides through a photomask under tension, resulting in a wave (indicated by the dashed line trace).

(B) Chemical structures of the primary resin components, a difunctional azide monomer (BZ-N_3), trifunctional alkyne crosslinker (Tri-AK), and allyl sulfide-based difunctional alkyne monomer (AS-AK). The bond exchange mechanism is shown in the box at the bottom.

Image (A) modified with permission from Bowman and coworkers.[194] Copyright (2006), Wiley-VCH.

Image (B) modified with permission from Bowman and coworkers.[195] Copyright (2020), Wiley-VCH.

mechanical loading resulted in a 50% improvement in elongation to break and 40% improvement in toughness when compared with the same network without photoinduced bond exchange during the measurement.

More recently, Bowman and coworkers developed a method to modify mechanical properties by combining thiol-ene crosslinking with photobase generation to activate dynamic covalent thioester bond exchange (Figure 25A).[196] In the first step, visible light (455 nm, 30 mW/cm^2, 1 min) exposure of a hexaarylbiimidazole (HABI) photoinitiator induced thiol-ene crosslinking between pentaerythritol tetra(3-mercaptopropionate) and a difunctional thioester-based crosslinker, while in the presence of an *o*NB protected tetramethyl guanidine (TMG) photobase. Subsequent irradiation with UV light (365 nm, 40 mW/cm^2, 10 min) released TMG, a base capable of deprotonating thiols, which converted the originally solid static network into a liquid-like dynamic network through rapid bond exchange with the thioester crosslinks. The inverse conversion from fluid to solid was also demonstrated by including TMG in the formulation to create an initially dynamic network, followed by activation

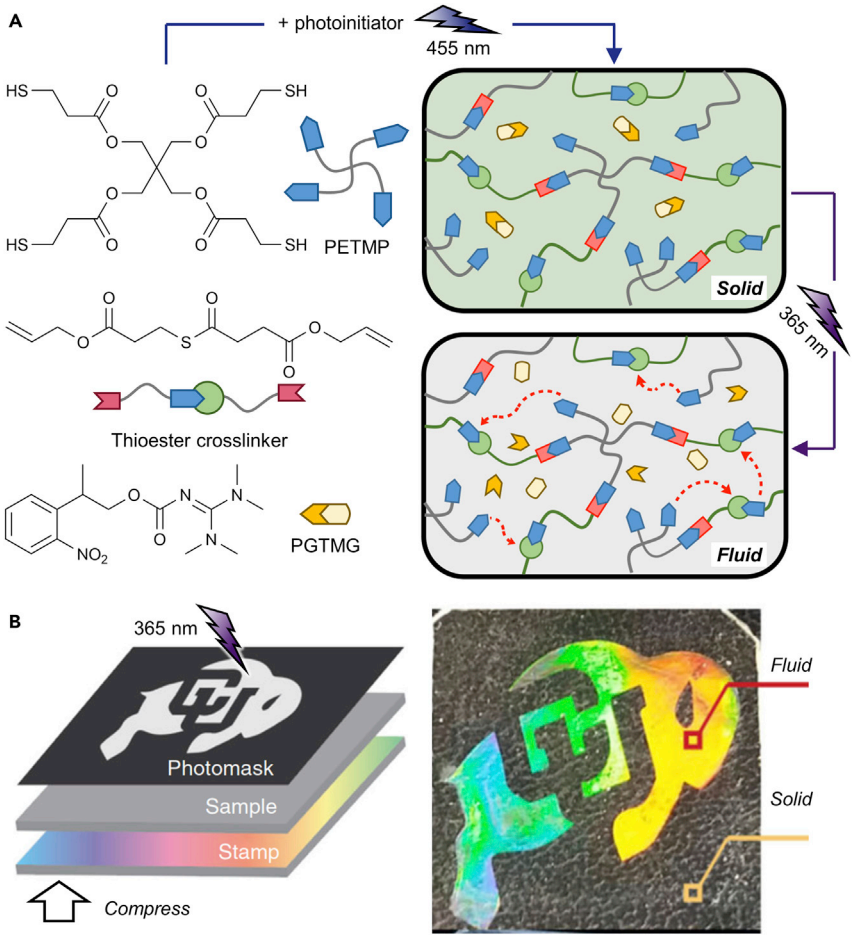

Figure 25. Wavelength-selective photoswitchable states of matter

(A) Schematic representation with chemical structures showing thiol-ene polymerization under visible light (455 nm) to create a solid polymer network followed by photobase generation with UV light (365 nm) to induce dynamic bond exchange that resulted in fluid-like behavior.

(B) Imprint lithography with spatial control over the state of matter. A nanoscaled pattern (noted by the color) was transferred from a stamp to the sample via compression.

Image modified with permission from Bowman and coworkers.[196] Copyright (2018), Springer Nature.

of a photoacid (oNB protected benzoic acid) with UV light to quench the TMG and halt bond exchange. This method was applied to imprint lithography with spatiotemporal control over the dual-wavelength network formation and photorelease of base or acid (Figure 25B).

Wavelength selectivity to control property-function relationships in biomaterials

Photochemical transformations to create and manipulate biomaterials have gained considerable attention in the last couple of decades, in particular with respect to applications in regenerative medicine.[120,197] The utility of photoresponsive units in biomaterials (e.g., hydrogels, proteins, DNA) has enabled spatiotemporal control over chemical transformations to locally modulate both the chemical and physical environment.[198,199] For example, bioactive ligands (i.e., proteins, cells, and peptides) have been reversibly incorporated through photochemical means and used to direct cell proliferation, migration, and differentiation. Additionally, mechanical

properties (e.g., stiffening/softening) have been manipulated with light irradiation, which has proved useful in disease models and delivery of therapeutics. Recently, a few examples of wavelength-selective photochemistry using multiple chromophores have been demonstrated in the realm of biomaterials, bringing synthetic analogs one step closer to accurately mimicking those found in nature.

In 2013, Anseth and coworkers reported one of the first examples of wavelength-selective photochemistry in biomaterials to facilitate sequential release of small molecules.[200] Disparate reactivity was accomplished by employing *o*NB and coumarin methylester (CM) as photocleavable units to selectively release dyes (rhodamine and fluorescein) and proteins (bone morphogenic proteins, BMP-2 and BMP-7) at different times (Figure 26A). It was found that CM resulted in selective photorelease upon exposure to violet light (405 nm) relative to *o*NB, while *o*NB was shown to react faster than CM when exposed to UV light (365 nm). The utilization of these two photoprotecting groups enabled sequential release of multiple proteins, which was used to increase human mesenchymal stem cell differentiation in a temporal manner. In 2017, Forsythe and coworkers developed novel photodegradable hydrogels incorporating multiple photolabile linkers to selectively release cells from synthetic hydrogels.[201] Functionalized *o*NB derivatives (**P1**–**P6**), 7-(diethylamino) coumarin (**P7**), and perylene (**P8**) were employed in the photodegradable hydrogels, and degradation kinetics of resultant polymer networks upon UV and broad-spectrum visible LEDs (i.e., 365, 420, 455, 470, and 530 nm) were monitored (Figure 26B). Consequently, selective release of different proteins/cells from biomaterials was demonstrated upon irradiation with different wavelengths of light, where both the **P7** and **P8** derivatives provided the greatest sensitivity to visible light.

The native extracellular matrix (ECM) is a highly dynamic environment consisting of complex heterogeneous microenvironments. To date, synthetic biomaterials have not been able to effectively mimic the ECM, although wavelength-selective photopatterning has proved to be one of the most promising routes to this end. In 2012, DeForest and Anseth utilized two biorthogonal photochemical reactions to demonstrate the reversible presentation of a biological cue with spatial control.[202] The hydrogels were fabricated using copper-free, strain-promoted azide-alkyne cycloaddition click chemistry, which incorporated alkenes as anchor points for functionalization of biochemical cues (Figure 27). Eosin Y was then used as a visible light photoinitiator (490–650 nm) to covalently attach *o*NB-containing fluorescently labeled peptides via thiol-ene chemistry. Subsequently, UV light irradiation (365 nm) triggered the scission of *o*NB groups, releasing the attached fluorescently labeled peptides from the hydrogels, as observed using fluorescence microscopy.

Photochemical reactions have been commonly utilized to fabricate optically controlled, nanoscale biomaterials with applications in nanomedicine, DNA nanotechnology, and more.[199] Recently, wavelength-selective transformations have enabled more sophisticated control over these materials. For instance, Famulok, Valero, and coworkers reported reversible control over DNAzyme activity by incorporating two distinct photoswitches, 2′,6′-dimethylazobenzene (DM-Azo) and *N*-methyl-arylazopyrazole (AAP).[203] In the *trans* configurations, which were present when exposed to blue light (450 nm) for DM-Azo and orange light (590 nm) for AAP, DNA hybridization was allowed (Figure 28A). However, irradiation with UV light (<400 nm) hindered hybridization due to steric constraints that arise from the *cis* isomers. Impressively, the application of three different colors of light (UV, blue, and orange) enabled reversible switching in DNAzyme activity. In 2019, the Famulok group utilized azobenzene derivative to mimic the movement of biological motors

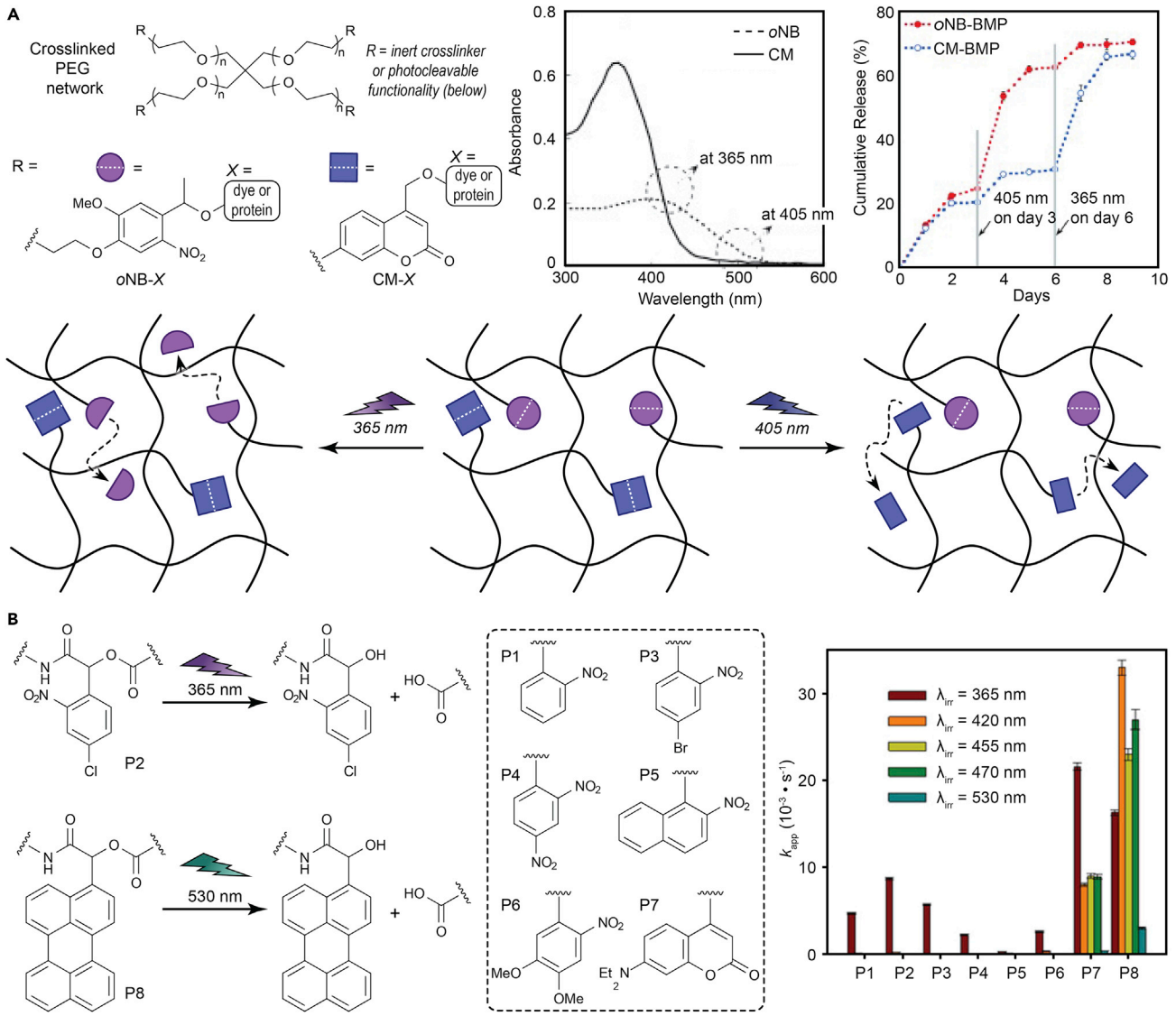

Figure 26. Photodegradable hydrogels containing multiple photolabile compounds to release biologically active species

(A) Chemical structures for the crosslinked PEG network containing *o*NB and CM photocages. Absorption spectra of the two photocleavable compounds and utility in sequential release of bone morphogenic proteins (BMP-2 and BMP-7) using UV (365 nm) and visible (405 nm) light. (B) Representative photocleavage of compounds P2 (*o*NB) and P8 (pyrene-based) and chemical structures for the remaining six photocleavable linkers (in the dashed box). Plot of degradation rate constants for hydrogels containing different photolabile linkers upon irradiation with different wavelengths of light, showing selectivity.

Image (A) modified with permission from Anseth and coworkers.[200] Copyright (2013), Wiley-VCH. Image (B) modified with permission from Forsythe and coworkers.[201] Copyright (2017), American Chemical Society.

(i.e., DNA walkers).[204] Two azobenzene derivatives, 2′,6′-dimethy-4′-(methylthio) azobenzene (S-DM-Azo) and DM-Azo, were utilized to demonstrate entirely light-induced molecular walking that relied on a precise coordination of strand displacement that occurred when cycling between *cis*/*trans* states (Figure 28B). Again, irradiation with UV light (365 nm) induced *trans*-to-*cis* isomerization, hindering DNA hybridization, while exposure to visible light (450 nm) converted the azobenzene photoswitches to their *trans* state and strengthened hybridization. As a final example, in 2020, Asanuma and coworkers reported orthogonal photocontrol of hybridization between serinol nucleic acid (SNA) and ribonucleic acid (RNA) by

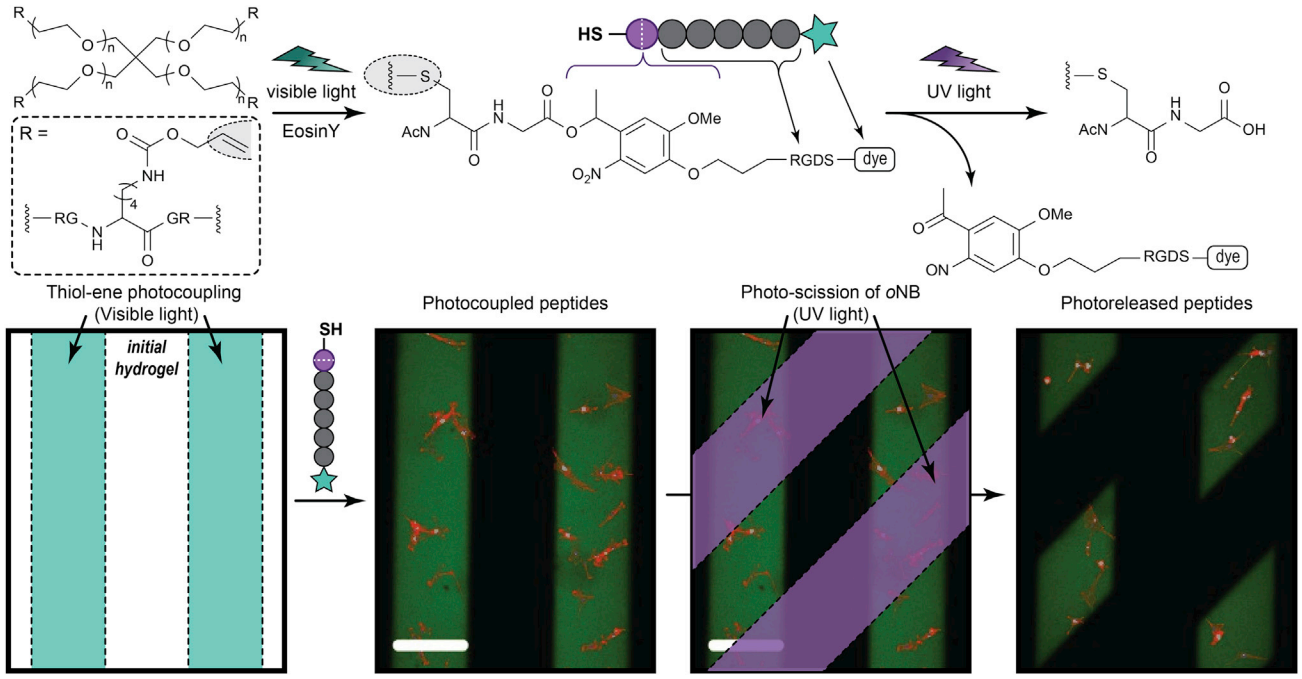

Figure 27. Photoreversible patterning of biomolecules

In a first step, visible light was used to functionalize hydrogel via thiol-ene chemistry, incorporating a photolabile, fluorescently labeled, peptide sequence (RGDS). Subsequently, exposure to UV light resulted in photocleavage of *o*NB to release the biological cues. Fluorescence microscopy of photopatterned hydrogels showed selective adhesion of mouse embryonic fibroblast (NIH 3T3) cells in regions functionalized with RGD, along with selective detachment in regions subsequently irradiated with UV light that cleaved the RGD sequence. Green, RGD; red, F-actin; blue, nuclei. Scale bar, 200 μm. Image modified with permission from Anseth and coworkers.[202] Copyright (2012), Wiley-VCH.

incorporating vinyladenine moieties that undergo reversible cycloaddition/-reversion upon exposure to different wavelengths of light (Figure 28C).[205] These two novel vinyladenine derivatives, 8-naphthylvinyl adenine (^{NV}A) and 8-pyrenylvinyl adenine (^{PV}A), enabled intrastrand photocrosslinking that destabilized SNA/RNA duplexes and resulted in dissociation into single strands. Both homo- and hetero-[2 + 2] photocyclization were demonstrated, whereby cyclization occurs upon exposure to long-wave UV light (340–405 nm) for ^{NV}A and visible light (405–460 nm) for ^{PV}A, and both cyclorevert upon exposure to UV light ($\leq$300 nm and $\leq$340 nm for ^{NV}A and ^{PV}A, respectively), which facilitates duplex formation.

WAVELENGTH-SELECTIVE ADVANCED MANUFACTURING

Photochemical reactions have been vital in several manufacturing processes from two-dimensional (2D) optical lithography for microelectronics to additive manufacturing (or 3D printing). Besides traditional synthetic polymers, biocompatible materials, such as hydrogels, have also received widespread attention due to their implications in medicine (e.g., tissue engineering and drug delivery). Traditionally, high-energy UV light has been employed to initiate photochemical reactions via direct photolysis, owing to the myriad of reactive molecules that absorb UV light to impart rapid chemical transformations along with the associated spatiotemporal control. However, the recent commercialization of LED technology has enabled a broader palette of colors to be explored to carry out organic and polymer synthesis, particularly using visible-to-NIR light that is more benign in a biological context. Also empowered by this advancement is wavelength-selective photochemistry for the fabrication of next-generation multi-functional materials. In this section, we highlight

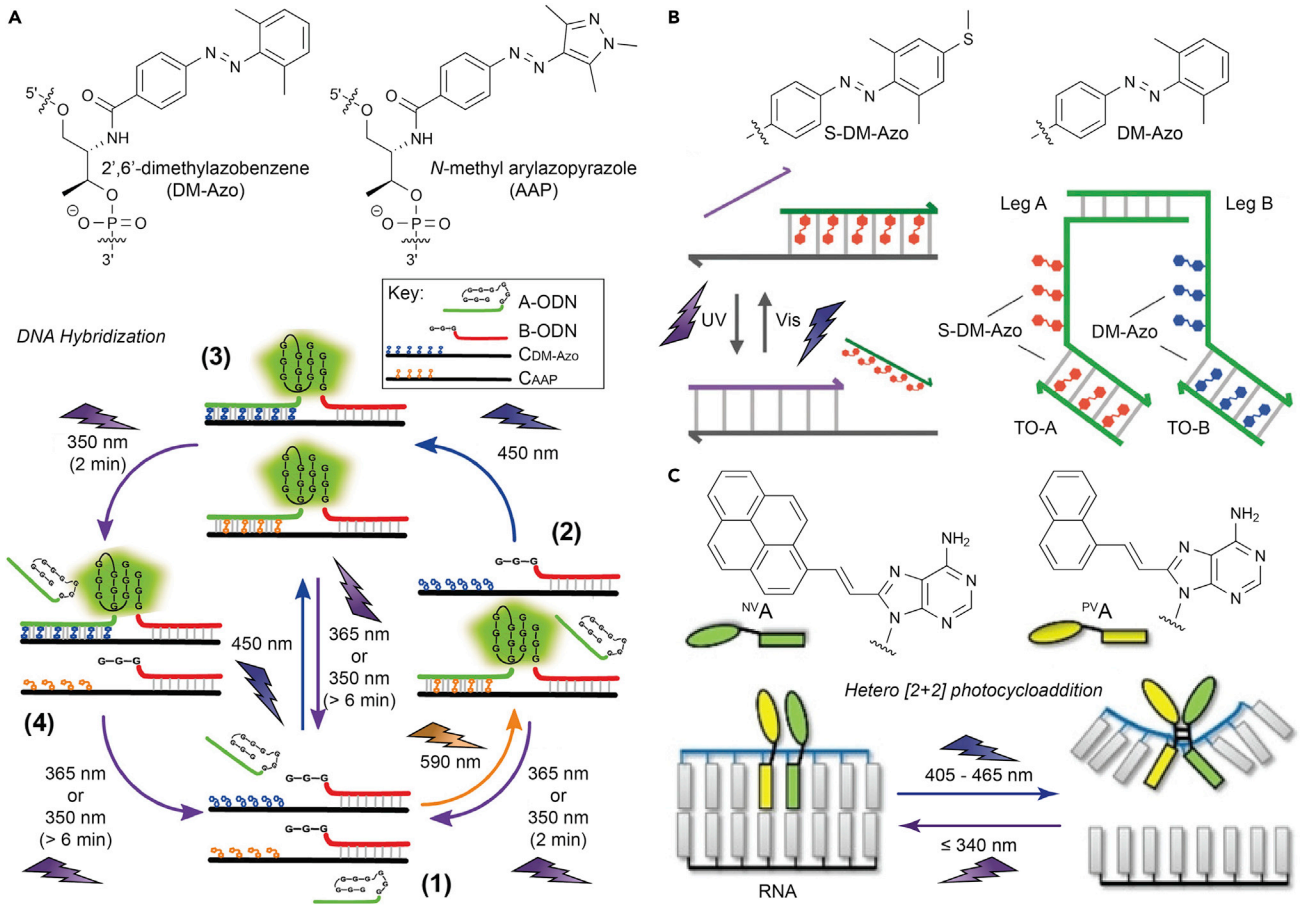

Figure 28. Photoresponsive nanoscale biomaterials

(A) Chemical structure of DM-Azo and AAP. Wavelength-selective photoswitchability upon exposure to three different colors of light (UV, blue, and orange) was used to modulate the activity of DNAzyme for hybridization.

(B) Chemical structure of 2′,6′-dimethy-4′-(methylthio)azobenzene (S-DM-Azo) and 2′,6′-dimethylazobenzene (DM-Azo) used to photocontrol strand displacement and DNA walking.

(C) Chemical structure of 8-naphthylvinyl adenine (^{NV}A) and 8-pyrenylvinyl adenine (^{PV}A) for photocontrolled SNA/RNA duplex dissociation and formation.

Image (A) modified with permission from Famulok and coworkers.[203] Copyright (2018), American Chemical Society. Image (B) modified with permission from Famulok and coworkers.[204] Copyright (2019), Wiley-VCH. Image (C) modified with permission from Asanuma and coworkers.[205] Copyright (2020), Wiley-VCH.

recent examples where wavelength-selective photochemistry has been used for photolithography and light-based 3D printing of polymeric materials/objects that are seemingly unattainable with only a single wavelength of light.

Photolithography

Over the last 60 years, light-responsive polymers (e.g., photoresists) have played an essential role in the preparation of well-defined 2D surfaces via lithography, which has led to the boom of modern microelectronics found in everyday appliances from phones to televisions and computers. However, in contemporary photolithography the smallest feature size (resolution) is diffraction limited (roughly $\approx \lambda/2$), which has led to the use of expensive and harmful light sources with shorter wavelengths into the deep UV (<200 nm). Moreover, when resins can only react through a single light-driven chemical transformation, only monolithic (single component) objects are possible. However, in the last decade innovative methods that employ

multiple wavelengths of light have been developed to go beyond diffraction limited resolution and introduce multiple materials/functionality.

Super-resolution two-color photolithography

Photopatterning with multiple colors of light has enabled super-resolution lithography, which goes beyond the diffraction limit. In 2009, this was demonstrated by three independent groups, where one color of light activates a chemical transformation and the second color deactivates it.[206–208] In one example, McLeod and coworkers utilized two distinct wavelengths of light to facilitate wavelength-selective photoinitiation and photoinhibition.[206] Specifically, a two-component photoinitiation system, camphorquinone (CQ) and ethyl 4-(dimethylamino)benzoate (EDAB), were used to initiate a radical photopolymerization under blue light (473 nm), while thiuram disulfide (TED) terminated polymerization when irradiated with UV light (364 nm) (Figure 29A). By focusing a UV light beam into a Gauss-Laguerre (GL) "doughnut" shape surrounding the primary visible light beam, features down to 64 nm were achieved ($\sim\lambda/7.5$).

In the same year, Fourkas and coworkers, developed a novel two-color photolithographic technique referred to as resolution augmentation through photoinduced deactivation (RAPID) lithography.[207] This process relies on two-photon absorption of 800 nm light for excitation and subsequent radical polymerization and a second 800 nm laser beam that inhibits the polymerization (Figure 29B). The concept of RAPID lithography was inspired by stimulated emission depletion fluorescence microscopy, which utilizes a second laser pulse to deactivate the excited molecules through stimulated emission. In this report, a single molecule, malachite green carbinol base, acted as both the photoinitiator and photoinhibitor upon the first and second laser beam exposures, respectively. With this technique, features down to 40 nm ($\sim\lambda/20$) were obtainable.

In a third example, Menon and coworkers invented a technique termed absorption modulation lithography, whereby a photochromic dye was used to modulate the absorption of photoresists upon two-color irradiation.[208] In this process, a thin layer of photochromic molecules was placed on top of the recording photoresist layer (Figure 29C). To create the nanoscale patterns, the photochromic layer was exposed to an interference pattern that overlaps peaks at 325 nm with nodes at 633 nm. Regions exposed to UV light resulted in isomers transparent at that wavelength; however, in the regions exposed to red light, the layer efficiently absorbs the UV irradiation and protects the photoresist. Therefore, only the regions exposed to little to no red light elicited the UV-activated photochemical reaction, resulting in subwavelength resolution modulated by the intensity ratio of red/UV light, ultimately yielding a resolution of ~36 nm ($\sim\lambda/10$).

Since these three pioneering examples appeared just over a decade ago, there have been exciting advancements in multicolor lithography. For example, based on the initial contribution from the McLeod group, Gu and coworkers systematically examined the influence of the inhibiting laser power and its exposure time on feature size, demonstrating a resolution limit of 40 nm ($\sim\lambda/12$ the initiating laser) at higher inhibitor laser intensities (Figure 30Ai).[209] In 2013, the same group developed a two-photon photoinitiation (800 nm) and one-photon photoinhibition (375 nm) mechanism, with 2,5-bis(p-dimethylaminocinn amylidene)-cyclopentanone as the photoinitiator and TED as the photoinhibitor, revealing feature sizes down to 9 nm ($\lambda/42$ relative to the inhibition beam) (Figure 30Aii).[210]

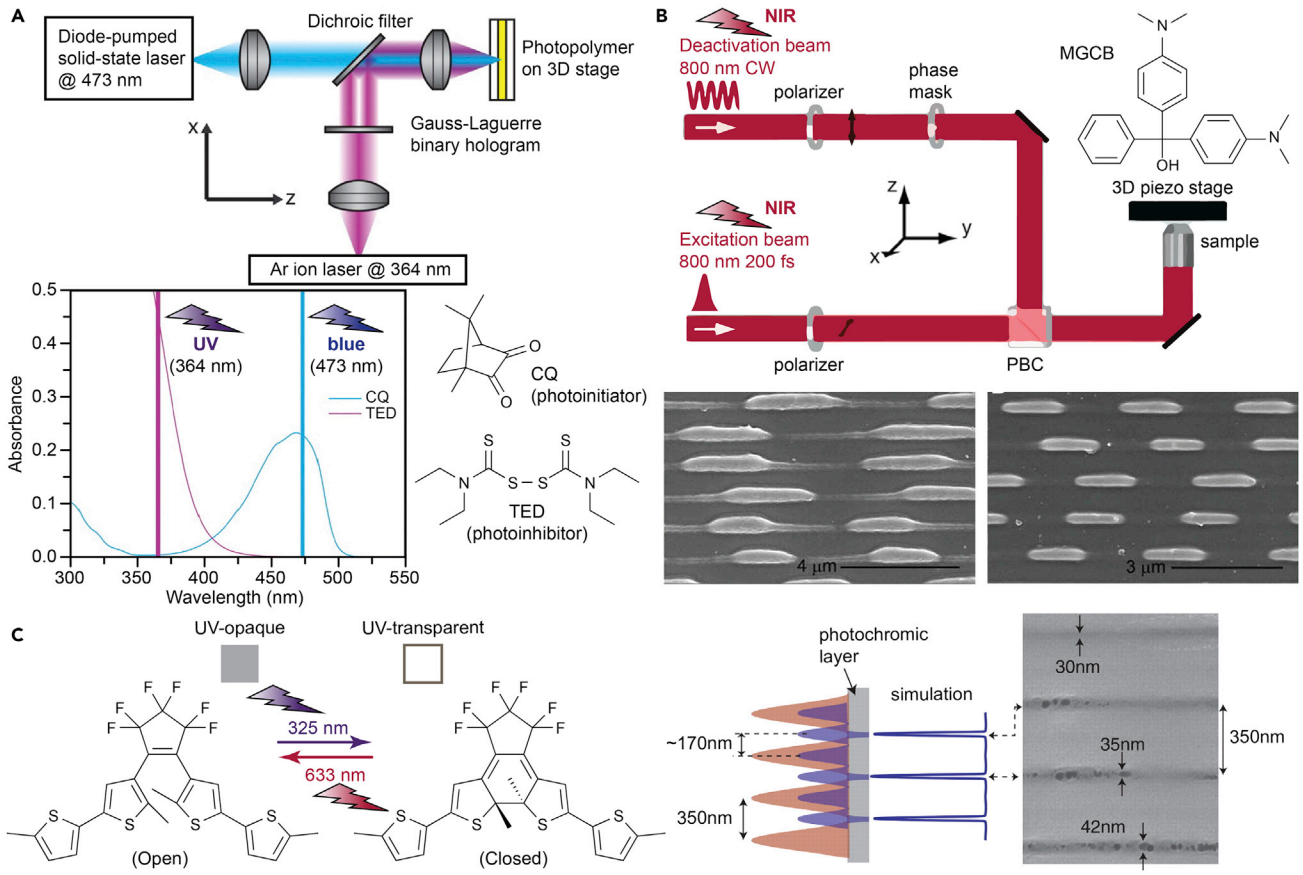

Figure 29. Two-color photopatterning to achieve resolution beyond the diffraction limit

(A) Schematic setup of two-color direct-write photolithography. Camphorquinone (CQ) and thiuram disulfide (TED) were utilized for orthogonal photoinitiation and photoinhibition given their non-overlapped absorbance at visible (473 nm) and UV (364 nm) light, respectively.

(B) Experimental setup for resolution augmentation through photoinduced deactivation (RAPID) lithography. Schematic of the process with the chemical structure shown for the photoinitiator/inhibitor, malachite green carbinol base (MGCB), and associated scanning electron microscopy (SEM) images of written lines.

(C) Photoisomerization of a thermally stable photochromic diarylethene derivative upon two-color irradiation, used for subwavelength patterning via absorbance modulation.

Image (A) modified with permission from McLeod and coworkers.[206] Copyright (2009), American Association for the Advancement of Science. Image (B) modified with permission from Fourkas and coworkers.[207] Copyright (2009), American Association for the Advancement of Science. Image (C) modified with permission from Menon and coworkers.[208] Copyright (2009), American Association for the Advancement of Science.

In addition to two-color activation/deactivation of polymerizations, this has also been applied effectively to directly photocontrol individual bond formation reactions (e.g., coupling and crosslinking chemistry). For example, in 2017, Wegener, Barner-Kowollik and coworkers utilized direct laser writing to generate photoenol isomer intermediates (*E*-enol versus *Z*-enol) from α-methyl benzaldehyde (Figure 30B).[211] Two-photon absorption with far-red light (700 nm) resulted in the formation of the *E*-enol, capable of acting as a diene in Diels-Alder reactions. However, irradiation of the *E*-enol with blue light (440 nm) converts it to the non-reactive *Z*-enol that undergoes rapid relaxation back to the original benzaldehyde derivative. This photoswitchable coupling chemistry was used to pattern polymerization initiators onto the surface of glass, providing surface-bound brushes with a lateral resolution of 100 nm post polymerization. Recently, Blasco, Wegener, Barner-Kowollik, and coworkers utilized photoswitchable spirothiopyran (820 nm versus 640 nm) that crosslinks via supramolecular interactions after exposure to NIR light (820 nm)

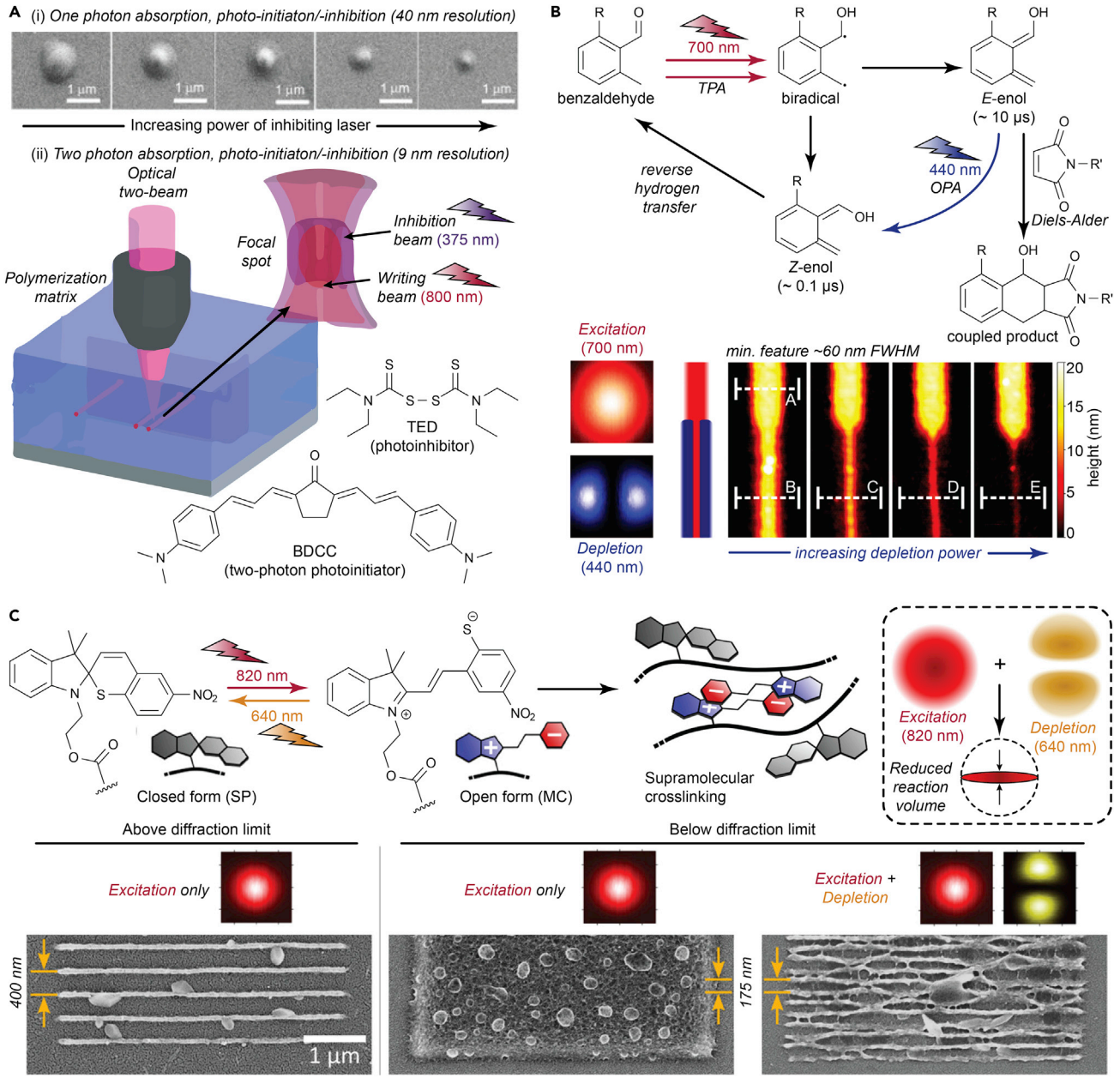

Figure 30. Recent advancements in two-color super-resolution photolithography

(A) One-photon (i) and two-photon (ii) absorption methods of photoinitiation/photoinhibition to generate sub-diffraction-limited patterns. SEM images of cured spots fabricated using different inhibition laser powers with one-photon absorption only (i) and schematic of the two-photon absorption process with corresponding chemical structures for photoinhibitor and photoinitiator.

(B) Photocontrolled Diels-Alder reactions using excitation of α-methyl benzaldehyde via two-photon absorption (TPA) with far-red light (700 nm) to generate a reactive *E*-enol (diene) and depletion with a Gauss-Laguerre beam to convert the *E*-enol to an unreactive *Z*-enol via one-photon absorption (OPA) with blue light (440 nm). Atomic force microscopy images of surface-bound polymer brushes (bottom) with varying depletion light intensity.

(C) Photoswitchable spirothiopyran for supramolecular crosslinking. TPA by the closed spiropyran (SP) with NIR light (820 nm) results in the reactive open merocyanine (MC) form, while irradiation with red light (640 nm) reverts to the unreactive SP form. Excitation and depletion focus was used to generate sub-diffraction features, as seen in the SEM images (bottom).

Image (A) (i) modified with permission from Gu and coworkers.[209] Copyright (2011), The Optical Society. Image (A) (ii) modified with permission from Gu and coworkers.[210] Copyright (2013), Springer Nature. Image (B) modified with permission from Wegener and coworkers.[211] Copyright (2017), American Chemical Society. Image (C) modified with permission from Blasco and coworkers.[212] Copyright (2019), American Chemical Society.

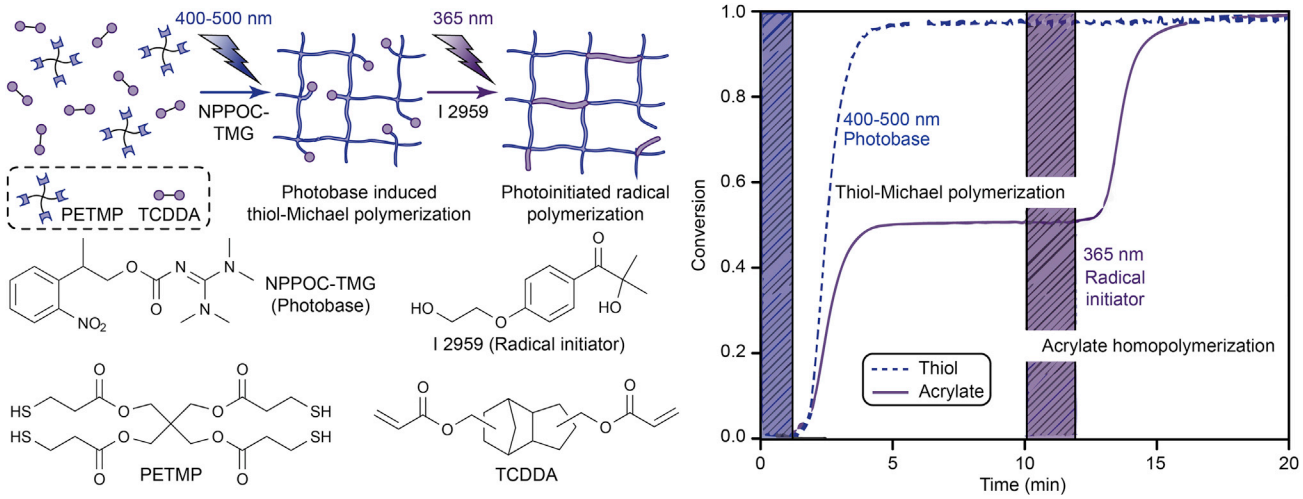

Figure 31. Wavelength-selective polymer network formation via dual polymerization

Sequential reactions were accomplished through thiol-Michael addition induced by a photobase generator, 2-(2-nitrophenyl)propyloxycarbonyl tetramethyl guanidine (NPPOC-TMG) activated with visible light (400–500 nm), and radical acrylate homopolymerization using 2-hydroxy-4′-(2-hydroxyethoxy)-2-methylpropiophenone (I 2959), a UV-activated photoinitiator (355 nm). The selected monomers are pentaerythritol tetra(3-mercaptopropionate) (PETMP) and tricyclodecane dementhanol diacrylate (TCDDA). Image modified with permission from Bowman and coworkers.[213] Copyright (2017), American Chemical Society.

to give the open MC form, while irradiation with red light (640 nm) reverted it to the uncrosslinked SP form. With this photoswitchable transformation, two-color super-resolution patterning was accomplished using a GL depletion beam (640 nm) surrounding the primary beam (820 nm) to yield linewidths down to 31 nm (Figure 30C).[212]

Wavelength-selective photoresists and related processes

The formation and degradation of polymer networks with multiple colors of light has been exploited in advanced photoresist applications, including the formation of multi-material/functional patterns. In one of the first examples, Bowman and coworkers integrated a photobase generator, 2-(2-nitrophenyl)propyloxycarbonyl tetramethyl guanidine (NPPOC-TMG), and a photoradical initiator, 2-hydroxy-4′-(2-hydroxyethoxy)-2-methylpropiophenone (I 2959), for sequential wavelength-selective polymerizations.[213] Upon exposure to visible light (400–500 nm), a base (tetramethyl guanidine) was released to initiate an anionic thiol-Michael polymerization, while radicals were subsequently generated for a second-stage acrylate polymerization at an independent wavelength (365 nm) (Figure 31). Through manipulating the thiol/acrylate ratio, the properties of both the intermediate and final networks could be tuned. For example, when the thiol/acrylate ratio was changed from 1:1 to 1:2, the modulus of the intermediate network decreased slightly from 8 MPa to 2 MPa while that of the final network increased substantially from 8 MPa to 23 MPa.

In 2019, Barner-Kowollik and coworkers developed a photoresist that combined a photoinduced radical polymerization with self-dimerization of photocaged dienes (Figure 32A).[214] The polymerization was conducted with visible light (>400 nm) using phenylbis(2,4,6-trimethylbenzoyl)phosphine oxide (Irgacure 819), followed by non-radical crosslinking via uncaging and [4 + 4] dimerization of *o*-methylbenzaldehyde (*o*-MBA) with UV light (330 nm). Leveraging wavelength selectivity, the hardness profiles within the same material could be adjusted spatially from 30 MPa to almost 300 MPa (as determined with nanoindentation). More recently, the Barner-Kowollik

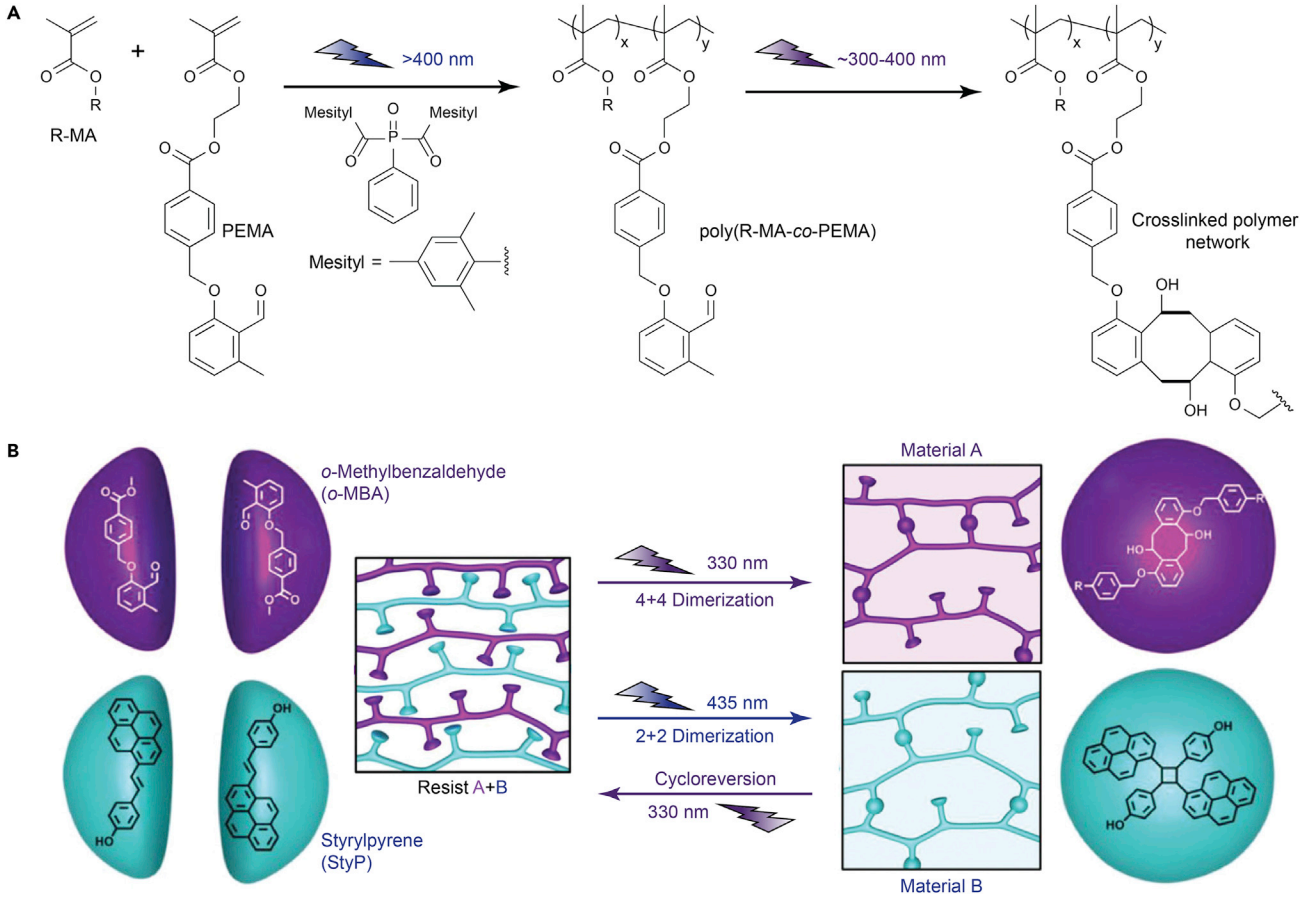

Figure 32. Wavelength-selective polymer network formation via dimerization

(A) Free radical polymerization of methacrylate (R-MA) and photoenol methacrylate (PEMA) with visible light (>400 nm), followed by non-radical photodimerization with UV light (300–400 nm).

(B) Wavelength-selective dimerization of *ortho*-methylbenzaldehyde (*o*-MBA) upon exposure to UV light (330 nm) to produce material A and styrylpyrene (StyP) upon exposure to blue light (435 nm) to produce material B. Image (B) modified with permission from Barner-Kowollik and coworkers.[215] Copyright (2019), Wiley-VCH.

group demonstrated disparate multi-material photoresists consisting of UV-sensitive *o*-MBA and blue light-active styrylpyrene (StyP) (Figure 32B).[215] Here, UV light exposure selectively resulted in dimerization of *o*-MBA while simultaneously reverting StyP cycloadducts that could be formed selectively using blue light irradiation (435 nm) through a [2 + 2] dimerization, enabling independent curing based solely on the wavelength of incident light. Recently, material property manipulation, including Young's modulus and swelling ratio, of this multi-material photoresist was thoroughly examined while maintaining spatiotemporal control.[216]

Light-based 3D printing

Recently, 3D printing (or additive manufacturing) has drawn widespread attention as an inexpensive and less wasteful alternative to traditional (e.g., subtractive) manufacturing processes.[217] While a number of sophisticated 3D-printing methods exist, stereolithography, or light-based additive manufacturing, offers some of the fastest build rates, highest feature resolution, and widest materials scope.[218] However, multi-material stereolithography remains elusive,[219] yet highly attractive given the potential to fabricate 3D objects consisting of multiple components with discrete functionality/properties (e.g., mechanical, optical, electronic, thermal, and spin).

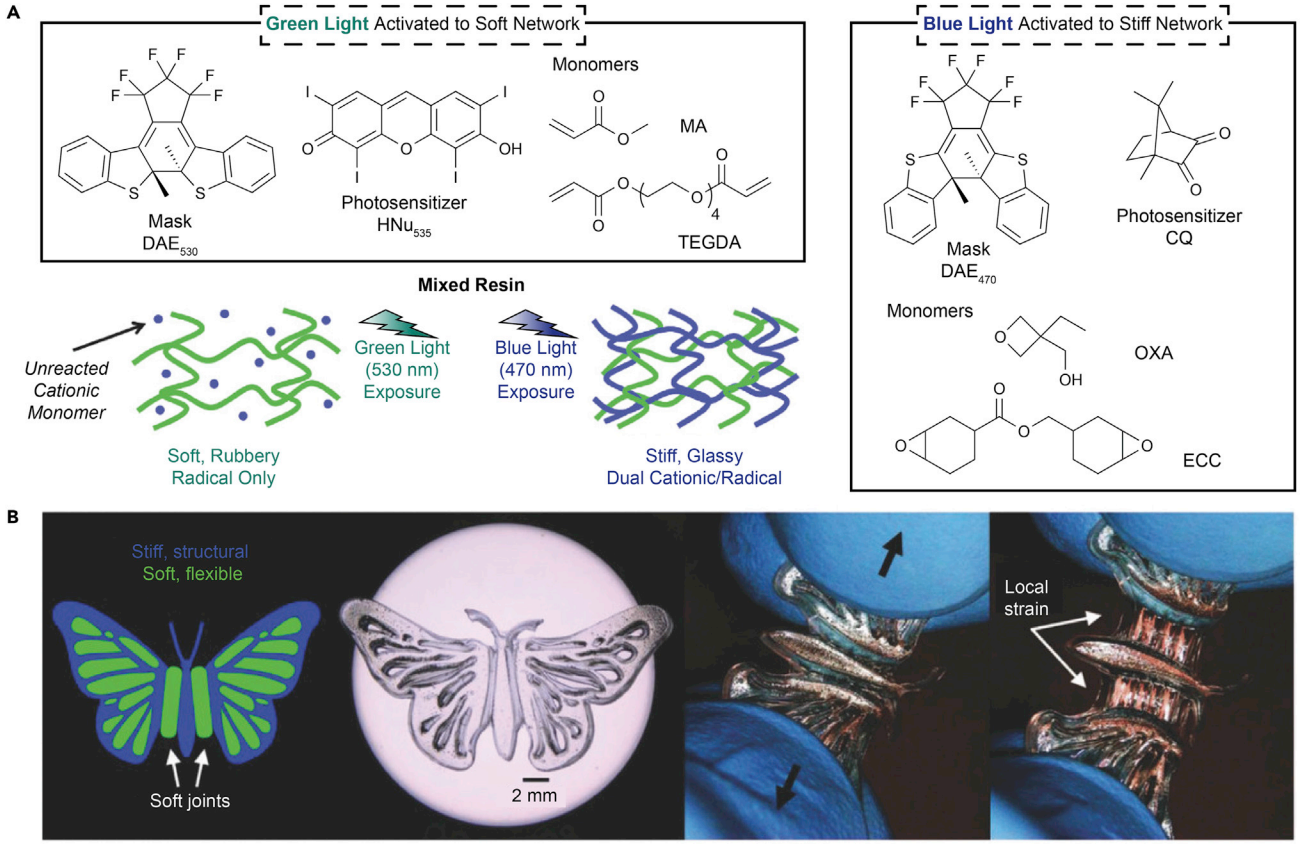

Figure 33. Wavelength-selective multi-material additive manufacturing

(A) Reaction components for green (diarylethene [DAE_{530}], 2,4,5,7-tetraiodo-3-hydroxy-6-fluorene [HNu_{535}], methyl acrylate [MA], and tetraethylene glycol diacrylate [TEGDA]) and blue (diarylethene [DAE_{470}], camphorquinone [CQ], 3-ethyl-3-hydroxymetyloxetane [OXA], and 3,4-epoxycyclohexylmethyl 3,4-epoxycyclohexanecarboxylate [ECC]) light active resins, along with representative network structures formed under green and blue light.

(B) Digital butterfly image (left) and corresponding object (right) with soft joints separating stiff segments.

Image modified with permission from Hawker and coworkers.[222] Copyright (2018), Wiley-VCH.

The simplest approach for multi-material stereolithography has been to manually change the photoreactive liquid (resin) during the printing process. However, this is an extremely energy- and time-intensive process that requires expensive equipment and reduces the precision and associated resolution.[220,221] As a recent alternative, wavelength-selective photochemistry has been developed and applied to stereolithography for multi-material fabrication from a single resin.

In 2018, Hawker and coworkers reported a methodology termed solution mask liquid lithography (SMaLL) that utilized wavelength-selective photochemistry to fabricate optically governed 3D objects composed of both stiff and soft domains.[222] In this work, diarylethene photochromic masks (DAE_{530} and DAE_{470} for green and blue light, respectively) were combined with a green and blue light-activated radical and cationic polymerization, respectively (Figure 33A). The photochromic masks facilitated a photobleaching front such that photocuring could occur through the depth of the resin while remaining confined to the irradiation zones. The dual photocatalysts employed for wavelength-selective photocuring were a xanthene green light absorbing dye (HNu_{535}), used to produce the soft domains via radical polymerization of an acrylic, and a blue light absorbing CQ photosystem to initiate both the radical acrylate and cationic epoxy

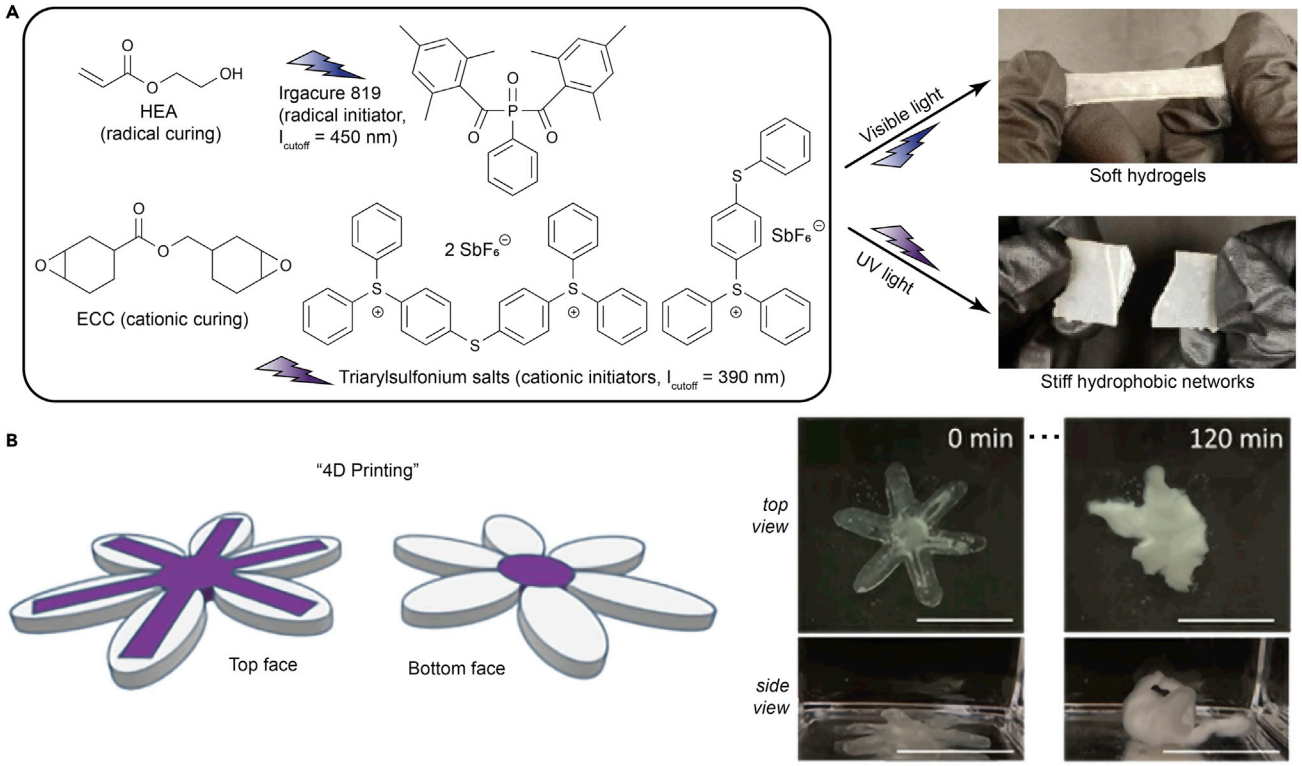

Figure 34. Wavelength-selective, one-photon stereolithographic multi-material 3D printing

(A) UV (3,4-Epoxycyclohexylmethyl 3,4-epoxycyclohexanecarboxylate [ECC] and triarylsulfonium salts) and visible (hydroxyl ethyl acrylate [HEA] and phenylbis(2,4,6-trimethylbenzoyl)phosphine oxide [Irgacure 819]) light-sensitive photoinitiating systems and resins employed.

(B) Digital models of 3D-printed sea star (left) and the swelling-induced actuation of the corresponding 3D-printed object (right). Image modified with permission from Boydston and coworkers.[225]

polymerizations to produce domains composed of stiff interpenetrating polymer networks (Figure 33B). Recently, this strategy was extended to fabricate resilient multi-material, polymer-polymer composite objects containing a spatially resolved stiff exterior shell and a soft core with well-defined pore arrays,[223] along with a detailed examination of the resultant multi-material interfaces.[224]

In 2019, Schwartz and Boydston showed a similar concept using a combined UV and visible light stereolithographic approach, demonstrating the ability to produce 3D objects beyond optically governed shapes.[225] In this work, a visible light-sensitive photoinitiator (Irgacure 819, λ_{cutoff} = 450 nm) was used for radical curing of a soft and hydrophilic acrylate and a UV-sensitive triarylsulfonium salt (TAS, λ_{cutoff} = 390 nm) induced both the radical acrylate curing and cationic epoxy curing to form a stiff and hydrophobic material (Figure 34A). Furthermore, the 3D-printed objects were shown to be stimuli responsive through swelling-induced actuation, commonly referred to as "4D printing" (Figure 34B).

In 2020, Barner-Kowollik and coworkers prepared photoresists comprising anthracene dimers for direct laser writing (DLW) using two-photon absorption with NIR light (780 nm). This was used to fabricate microscopic "4D-printed" objects with locally tailorable mechanical properties by irradiation with a second light source (Figure 35).[226] A boxing ring provided the exemplary 3D structure, where DLW (16 mW, 3,000 $\mu m \cdot s^{-1}$) was used iteratively to first prepare the frames out of

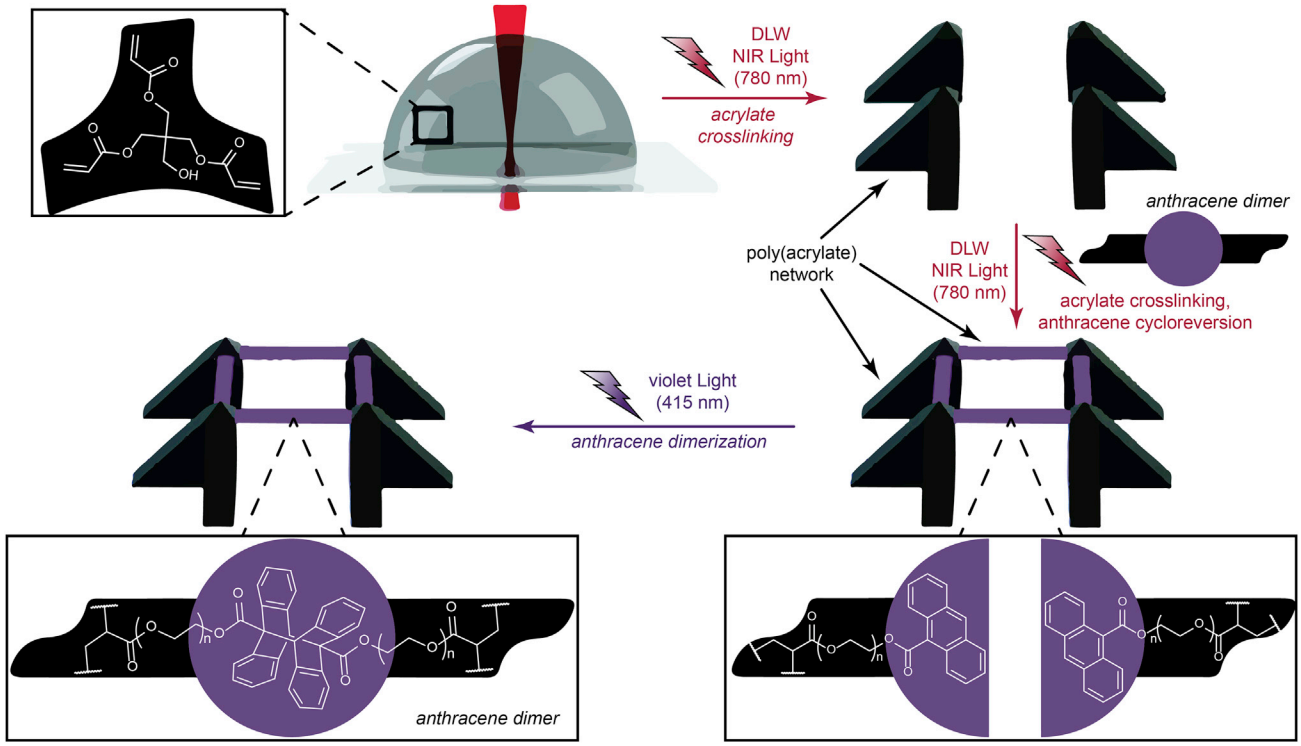

Figure 35. Preparation of a multi-material 3D microstructure with locally adaptive mechanical properties

A "boxing ring" was prepared in a multistep fashion using direct laser writing (DLW) with NIR light (780 nm) to cure an acrylic resin followed by dimerization of pendent anthracene units with violet light (415 nm) to exclusively enhance bridge stiffness.

Image modified with permission from Barner-Kowollik and coworkers.[226] Copyright (2020), Royal Society of Chemistry.

non-adaptive resin, primarily consisting of pentaerythritol triacrylate. DLW (10 mW, 200 $\mu m \cdot s^{-1}$) was then used to print bridges from an anthracene dimer-containing resin, during which some fraction of the anthracene dimers cleaved into monomers, softening the bridges. Subsequent irradiation with violet light (415 nm) induced anthracene dimerization, increasing the mechanical stiffness of the bridges from 5 MPa to 45 MPa (as determined by nanoindentation).

The concept of wavelength-selective photochemistry in stereolithography has also been applied to enhance the rate of printing, which is quite relevant for industrial/commercial applications. In traditional bottom-up stereolithography, photopolymerization occurs in a static layer-by-layer fashion, whereby a mechanical stage raises and lowers the resin between each successive curing step to construct the 3D object. The recoating and repositioning processes that occur between each layer greatly increases the total print time. This was first addressed by DeSimone and coworkers using continuous liquid interface production (CLIP),[227] which creates a thin layer at the window/resin interface (bottom of the vat) where no polymerization occurs due to the presence of oxygen that diffuses through the window. This inhibition region, called the "dead zone," enables the build platform to be continuously raised out of the resin bath during irradiation as fresh resin flows underneath, greatly enhancing the build rate. However, the thickness of the dead zone is a critical parameter that impacts both maximum speed and resolution, making it difficult to scale for the rapid production of very large objects. To address this, wavelength-selective photoinitiation and photoinhibition was developed and employed in an analogous stereolithography process by Scott and coworkers (Figure 36A).[228] Unlike CLIP, a two-color irradiation process was used,

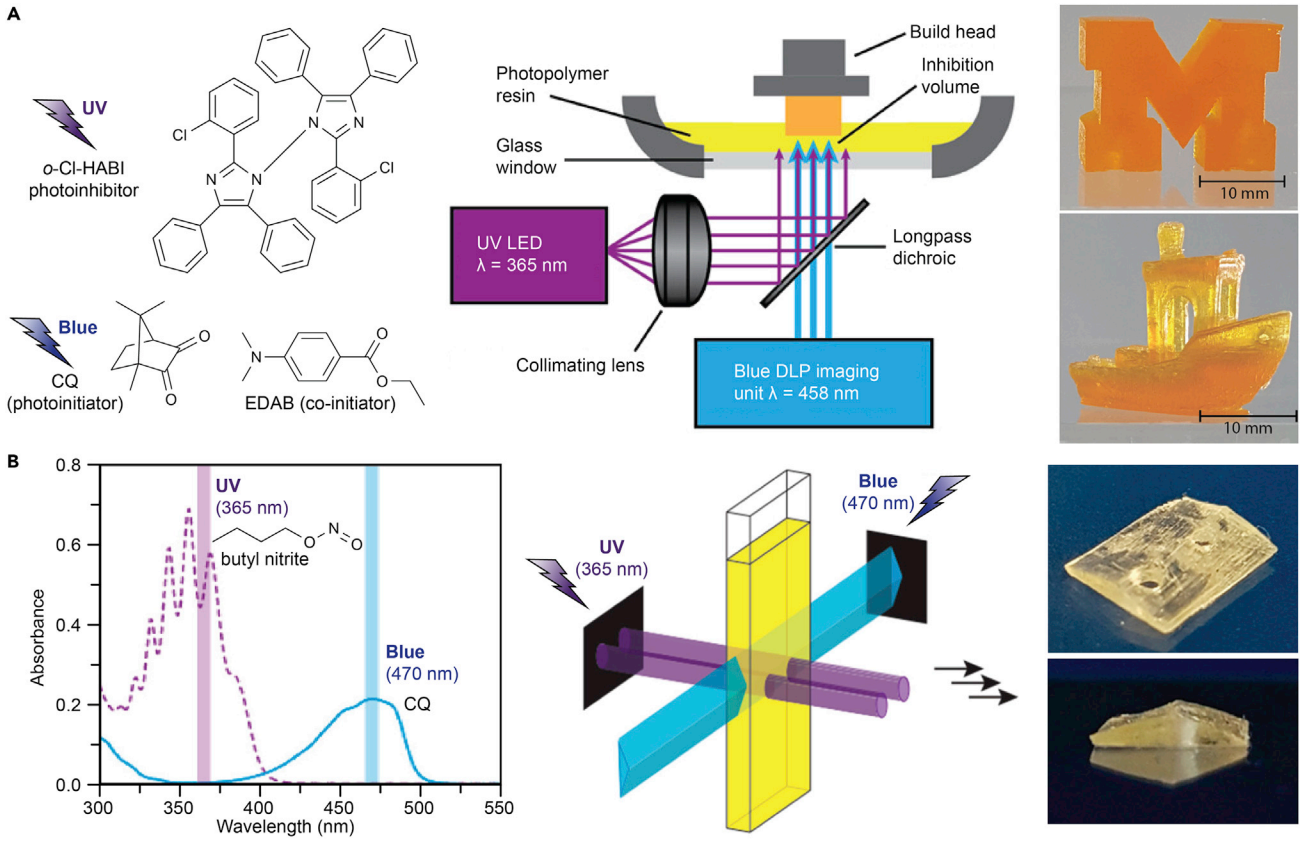

Figure 36. Wavelength-selective photoinitiation and photoinhibition for rapid 3D printing

(A) Optical setup for two-color stereolithographic process with digital light projection (DLP) (left) and example objects printed with this method at a rate of 500 and 350 mm/h, respectively.

(B) Schematic of optically governed volumetric 3D printing that uses perpendicular blue (470 nm) and UV (365 nm) irradiation for photoinitiation and photoinhibition, respectively (left), and an example object (prism) containing two circular holes from UV light inhibition (right).

Image (A) modified with permission from Scott and coworkers.[228] Copyright (2019), American Association for the Advancement of Science. Image (B) modified with permission from Scott and coworkers.[229] Copyright (2019), American Chemical Society.

whereby a resin formulation containing CQ and EDAB undergoes photopolymerization upon irradiation with blue light (458 nm) while bis[2-(*o*-chlorophenyl)-4,5-diphenylimidazole] (*o*-Cl-HABI) acts as a radical inhibitor upon irradiation with UV light (365 nm). With this approach, a blue image was created via digital light projection while UV light was irradiated uniformly throughout the build area. The inhibition volume thickness was controlled by the incident initiating (blue) and inhibiting (UV) light intensities along with the inclusion of blue and UV absorbing dyes (called passive absorbers or opaquing agents) to attenuate the incoming light without activating a chemical transformation. This resulted in print speeds of ~2 m/h, which is ~100 times faster than conventional static stereolithography processes. The same group also demonstrated volumetric photopolymerization confinement by utilizing a similar protocol of wavelength-selective photoinitiation and photoinhibition (Figure 36B).[229] In this example, butyl nitrite was used as the UV-active photoinhibitor, activated at 365 nm, and CQ + EDAB as the blue light reactive photocuring system to produce optically governed shapes.

As a final example, in 2020, Regehly, Hecht, and coworkers introduced xolography as a novel dual-color volumetric 3D-printing technique that relies on a photoswitchable photoinitiator that is only active at the intersection of UV and visible

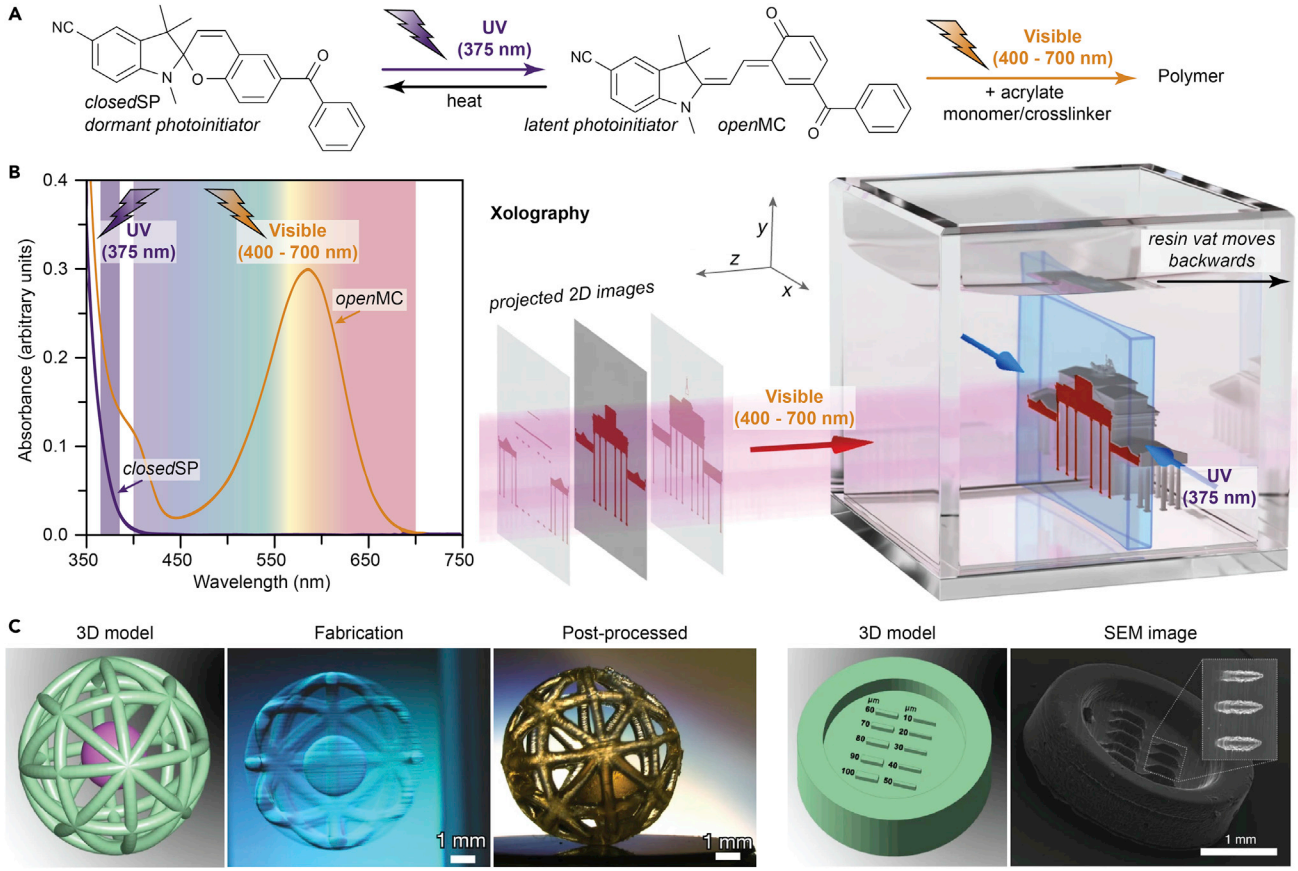

Figure 37. Dual-color volumetric 3D printing (xolography)

(A) Chemical structures and mechanism for photoswitchable photoinitiator.

(B) UV-vis absorption plot overlaying the dormant spiropyran benzophenone (*closed*SP) and active photostationary merocyanine (*open*MC) (left), along with a 3D rendition of the xolography setup.

(C) Representative models and images of 3D prints with a free-floating ball in a spherical cage (left) and a resolution print showing the smallest achievable feature size in the SEM image (right). All scale bars represent 1 mm.

Image modified with permission from Hecht and coworkers.[230] Copyright (2020), Springer Nature.

light beams.[230] The photoswitchable photoinitiator is a benzophenone functionalized spiropyran, adding to the small library of photoswitchable photopolymerization initiators.[231,232] In this case, the spiropyran is dormant in its closed thermodynamic state (*closed*SP), with little to no visible light absorption (Figure 37A). Irradiation with UV light (375 nm) results in ring opening to the photostationary merocyanine (*open*MC) that strongly absorbs visible light, which activates the benzophenone and can induce radical polymerization. To gain 3D spatial control a UV light sheet is passed along the width of a resin vat (x axis), while a projected visible image (400–700 nm) is incident orthogonal (z axis) to the plane of the UV light sheet (Figure 37B). Using a mechanical stage, the resin vat is moved away from the visible projection source while simultaneously displaying new 2D slices to reconstruct the 3D object in a continuous fashion. This method boasts an unmatched combination of resolution (~25 μm in x and y and ~50 μm in z), around ten times higher than state-of-the-art volumetric printing methods, and speed (55 mm^3 s^{-1}), four to five orders of magnitude faster volume generation than two-photon photopolymerization, while enabling the fabrication of free-floating objects (Figure 37C).

CONCLUSION AND OUTLOOK

Light as an energy source to create and manipulate soft matter (e.g., polymers) has demonstrated unmatched spatiotemporal control, which has enabled numerous applications from microelectronics to medicine. In the last decade, the ability to leverage different colors of light as discrete packets of energy to selectively activate distinct chemical transformations, or spectral control, has unveiled exciting potential to access next-generation materials, such as stimuli responsive ("smart") plastics and multi-functional 3D objects. Given the potential, it is anticipated that the next decade is likely to witness a considerable rise in both fundamental designs and commercial applications of wavelength-selective photochemistry in polymer science to affording high-performance materials with an unprecedented combination and regulation of properties. This review, based on specific examples, provides a roadmap to foster the objective of improved spectral control by detailing a distinction and associated requirements for both bidirectional photochemical pathways (single-chromophore systems) and disparate photochemical pathways (multiple-chromophore systems). These two photochemical pathways are highlighted through various chromophores that react to light in unique manners, including photoswitches, PPGs, and compounds that undergo photoinduced irreversible/reversible coupling. To guide the next generation of wavelength-selective reactions in polymer science these chromophores, along with photosensitizers for energy transfer and photoredox compounds for electron transfer, are placed into context through recent examples of (1) photocontrolled polymerization, (2) photoswitchable materials, and (3) advanced manufacturing. These advances lay the foundation for future discoveries, with some prospects outlined below following the order of sections in this review:

The toolbox and protocols for wavelength-selective photochemistry

Several established photochemical reactions exist that now span the electromagnetic spectrum from UV through visible (up to red light, ~700 nm). However, improving the reactivity and selectivity in this region is necessary to advance the efficiency and capabilities of wavelength-selective photochemistry. Furthermore, fewer reactions have been driven by far-red (700–780 nm) and NIR (~780–1700 nm) light, presenting an opportunity to harness these smaller packets of energy (longer wavelengths of light) to create and manipulate soft materials. This is particularly enticing for biological applications (e.g., sensing, imaging, and tissue engineering), as many are sensitive to UV light through scattering, absorption, and/or degradation, which may be mitigated by red-shifting photochemical transformations. Specifically, a combination of novel analytical characterization and powerful computational modeling will undoubtedly improve our understanding of light-matter interactions as a function of wavelength and accelerate efforts in the design and synthesis of optimal chromophores and photosystems.

Wavelength selectivity in photocontrolled polymer synthesis

Photocontrolled polymerizations encompass versatile mechanisms based on reactive intermediates that include radical, cation, and metal alkylidene, yet photocontrolled anionic polymerization methods remain elusive. Access to such anionic protocols with spatiotemporal control will expand the monomer scope and provide an orthogonal toolset to use in wavelength-selective controlled polymerizations. Additionally, improving wavelength selectivity of existing polymerization mechanisms will enable more facile and economical one-pot preparation of custom macromolecular materials with predefined architectures and sequences that rival the functionality found in nature.

Wavelength-selective polymer property manipulation

The vast majority of methods to modulate polymer properties (e.g., optoelectronic, ion-transport, and mechanical) with wavelength selectivity have relied on the use of a single bidirectional photoswitch. This presents an opportunity to examine systems with multiple switches to improve the sophistication (or "smarts") of polymeric materials by granting access to more than two metastable states. However, it is also important to consider the associated "return on investment" in terms of the time and energy that goes into creating such complex materials and how that translates to potential commercialization. Apart from bidirectional photoswitches, disparate wavelength-selective protocols have been restricted to manipulating mechanical properties, providing an opportunity to tailor additional facets of soft materials through dual (or more) photochemical pathways.

Wavelength-selective advanced manufacturing

The utility of multiple light sources in fabrication through light-induced chemical crosslinking (photocuring) has enabled photolithographic patterning beyond the diffraction limit of light and stereolithographic 3D printing of multi-functional/material objects or geometrically complex objects at incredible speeds. The next steps include (1) merging the resolution demonstrated in 2D patterning with the production speed and scale of 3D printing and (2) introducing multiple functionalities beyond alteration of mechanical properties into 3D objects. To the latter objective, improved wavelength selectivity will be paramount.

The current review attempts to educate, engage, and exhilarate the scientific community on wavelength-selective light-matter interactions in polymer science through describing the basic design rules, current photochemical toolbox, and state-of-the-art demonstrations with two wavelengths of light in controlled polymer synthesis, property manipulation, and advanced manufacturing. While impressive feats have been accomplished to date, the full potential of wavelength-selective photochemistry has yet to be unlocked. As we continue to learn more, exciting opportunities to create and manipulate soft materials will present themselves, and in this regard we end with a question: why stop at two wavelengths of light?

ACKNOWLEDGMENTS

The authors thank Prof. Mao Chen for providing original UV-vis absorption data. Z.A.P. thanks the Robert A. Welch Foundation (F-2007) and the Center for Dynamics and Control of Materials: an NSF MRSEC (DMR-1720595) for financial support. C.B.-K. acknowledges funding from the Australian Research Council in the form of a Laureate Fellowship (FL170100014) underpinning his photochemical research program. Further, C.B.-K. acknowledges continued support from QUT and its Center for Materials Science. C.B. thanks the Australian Research Council (DP 210100094 and DP 180102540) for financial support.

AUTHOR CONTRIBUTIONS

Conceptualization, P.L., D.A., and Z.A.P.; Writing – original draft, P.L., D.A., R.Y., L.D., N.C., and C.B.; Writing – review & editing, all authors; Project design and supervision, project funding acquisition, C.B., C.B.-K., and Z.A.P.

REFERENCES

1. Feynman, R.P., Leighton, R.B., and Sands, M.L. (2011). The Feynman Lectures on Physics New Millennium (Basic Books).
2. Einstein, A. (1905). Über einen die Erzeugung und Verwandlung des Lichtes betreffenden heuristischen Gesichtspunkt. Ann. Phys. *322*, 132–148.
3. Broglie, L.de (1924). XXXV. A tentative theory of light quanta. Lond. Edinb. Dublin Philos. Mag. J. Sci. *47*, 446–458.

4. Willson, C.G., Dammel, R.R., and Reiser, A. (1997). Photoresist materials: a historical perspective. In Proc. SPIE 3051, Optical Microlithography X, G.E. Fuller, ed. (SPIE). https://doi.org/10.1117/12.275984.

5. Turro, N.J., Ramamurthy, V., and Scaiano, J.C. (2010). Modern Molecular Photochemistry of Organic Molecules (University Science Books).

6. Aubert, S., Bezagu, M., Spivey, A.C., and Arseniyadis, S. (2019). Spatial and temporal control of chemical processes. Nat. Rev. Chem. *3*, 706–722.

7. Corrigan, N., Shanmugam, S., Xu, J., and Boyer, C. (2016). Photocatalysis in organic and polymer synthesis. Chem. Soc. Rev. *45*, 6165–6212.

8. Xiao, P., Zhang, J., Dumur, F., Tehfe, M.A., Morlet-Savary, F., Graff, B., Gigmes, D., Fouassier, J.P., and Lalevée, J. (2015). Visible light sensitive photoinitiating systems: recent progress in cationic and radical photopolymerization reactions under soft conditions. Prog. Polym. Sci. *41*, 32–66.

9. Zivic, N., Kuroishi, P.K., Dumur, F., Gigmes, D., Dove, A.P., and Sardon, H. (2019). Recent advances and challenges in the design of organic photoacid and photobase generators for polymerizations. Angew. Chem. Int. Ed. *58*, 10410–10422.

10. Dadashi-Silab, S., Doran, S., and Yagci, Y. (2016). Photoinduced electron transfer reactions for macromolecular syntheses. Chem. Rev. *116*, 10212–10275.

11. Tuten, B.T., Wiedbrauk, S., and Barner-Kowollik, C. (2020). Contemporary catalyst-free photochemistry in synthetic macromolecular science. Prog. Polym. Sci. *100*, 101183.

12. Hartley, G.S. (1937). The cis-form of azobenzene. Nature *140*, 281.

13. Bandara, H.M.D., and Burdette, S.C. (2012). Photoisomerization in different classes of azobenzene. Chem. Soc. Rev. *41*, 1809–1825.

14. Hirshberg, Y., and Fischer, E. (1954). Photochromism and reversible multiple internal transitions in some spiropyrans at low temperatures. Part I. J. Chem. Soc. (Resumed) *297*, 3129–3137.

15. Kortekaas, L., and Browne, W.R. (2019). The evolution of spiropyran: fundamentals and progress of an extraordinarily versatile photochrome. Chem. Soc. Rev. *48*, 3406–3424.

16. Ström, K.T. (1904). Polymere cumarsäuren. Berichte Dtsch. Chem. Ges. *37*, 1383–1386.

17. Kaur, G., Johnston, P., and Saito, K. (2014). Photo-reversible dimerisation reactions and their applications in polymeric systems. Polym. Chem. *5*, 2171–2186.

18. Corrigan, N., Yeow, J., Judzewitsch, P., Xu, J., and Boyer, C. (2019). Seeing the light: advancing materials chemistry through photopolymerization. Angew. Chem. Int. Ed. *58*, 5170–5189.

19. Frisch, H., Marschner, D.E., Goldmann, A.S., and Barner-Kowollik, C. (2018). Wavelength-Gated dynamic covalent chemistry. Angew. Chem. Int. Ed. *57*, 2036–2045.

20. Corrigan, N., Ciftci, M., Jung, K., and Boyer, C. (2021). Mediating reaction orthogonality in polymer and materials science. Angew. Chem. Int. Ed. *60*, 1748–1781.

21. Corrigan, N., and Boyer, C. (2019). 100th anniversary of macromolecular science viewpoint: photochemical reaction orthogonality in modern macromolecular science. ACS Macro Lett. *8*, 812–818.

22. Hansen, M.J., Velema, W.A., Lerch, M.M., Szymanski, W., and Feringa, B.L. (2015). Wavelength-selective cleavage of photoprotecting groups: strategies and applications in dynamic systems. Chem. Soc. Rev. *44*, 3358–3377.

23. San Miguel, V., Bochet, C.G., and del Campo, A. (2011). Wavelength-selective caged surfaces: how many functional levels are possible? J. Am. Chem. Soc. *133*, 5380–5388.

24. Menzel, J.P., Noble, B.B., Lauer, A., Coote, M.L., Blinco, J.P., and Barner-Kowollik, C. (2017). Wavelength dependence of light-induced cycloadditions. J. Am. Chem. Soc. *139*, 15812–15820.

25. Menzel, J.P., Noble, B.B., Blinco, J.P., and Barner-Kowollik, C. (2021). Predicting wavelength-dependent photochemical reactivity and selectivity. Nat Commun *12*, 1691.

26. Lerch, M.M., Hansen, M.J., Velema, W.A., Szymanski, W., and Feringa, B.L. (2016). Orthogonal photoswitching in a multifunctional molecular system. Nat. Commun. *7*, 12054.

27. Irie, M., Fukaminato, T., Matsuda, K., and Kobatake, S. (2014). Photochromism of diarylethene molecules and crystals: memories, switches, and actuators. Chem. Rev. *114*, 12174–12277.

28. Lerch, M.M., Szymański, W., and Feringa, B.L. (2018). The (photo)chemistry of Stenhouse photoswitches: guiding principles and system design. Chem. Soc. Rev. *47*, 1910–1937.

29. Crespi, S., Simeth, N.A., and König, B. (2019). Heteroaryl azo dyes as molecular photoswitches. Nat. Rev. Chem. *3*, 133–146.

30. Fihey, A., Perrier, A., Browne, W.R., and Jacquemin, D. (2015). Multiphotochromic molecular systems. Chem. Soc. Rev. *44*, 3719–3759.

31. Waldeck, D.H. (1991). Photoisomerization dynamics of stilbenes. Chem. Rev. *91*, 415–436.

32. Greb, L., and Lehn, J.-M. (2014). Light-driven molecular motors: imines as four-step or two-step unidirectional rotors. J. Am. Chem. Soc. *136*, 13114–13117.

33. Izmail'skii, V.A., and Mostoslavskii, M.A. (1961). Absorption spectra of 3- oxo-2,3-dihydrothianaphthene and its derivatives. II. Isomerism of 2- benzylidene-3-oxo-2,3-dihydrothionaphthene. Ukr. Khem. Zh. 234–237.

34. Harris, J.D., Moran, M.J., and Aprahamian, I. (2018). New molecular switch architectures. Proc. Natl. Acad. Sci. U S A *115*, 9414–9422.

35. Laurent, A. (1843). Mémoire sur la série stilbique [Memoir on the stilbene series]. Comptes Rendus *16*, 856.

36. Suzuki, H. (1952). The spatial configurations and the ultraviolet absorption spectra of the stilbene derivatives. Bull. Chem. Soc. Jpn. *25*, 145–150.

37. Oelgemöller, M., Frank, R., Lemmen, P., Lenoir, D., Lex, J., and Inoue, Y. (2012). Synthesis, structural characterization and photoisomerization of cyclic stilbenes. Tetrahedron *68*, 4048–4056.

38. van Leeuwen, T., Lubbe, A.S., Štacko, P., Wezenberg, S.J., and Feringa, B.L. (2017). Dynamic control of function by light-driven molecular motors. Nat. Rev. Chem. *1*, 0096.

39. Kassem, S., van Leeuwen, T., Lubbe, A.S., Wilson, M.R., Feringa, B.L., and Leigh, D.A. (2017). Artificial molecular motors. Chem. Soc. Rev. *46*, 2592–2621.

40. Beharry, A.A., and Woolley, G.A. (2011). Azobenzene phwotoswitches for biomolecules. Chem. Soc. Rev. *40*, 4422.

41. Dong, M., Babalhavaeji, A., Samanta, S., Beharry, A.A., and Woolley, G.A. (2015). Red-shifting azobenzene photoswitches for in vivo use. Acc. Chem. Res. *48*, 2662–2670.

42. Kobayashi, S., Yokoyama, H., and Kamei, H. (1987). Substituent and solvent effects on electronic absorption spectra and thermal isomerization of push-pull-substituted cis-azobenzenes. Chem. Phys. Lett. *138*, 333–338.

43. Bléger, D., Schwarz, J., Brouwer, A.M., and Hecht, S. (2012). *o*-fluoroazobenzenes as readily synthesized photoswitches offering nearly quantitative two-way isomerization with visible light. J. Am. Chem. Soc. *134*, 20597–20600.

44. Knie, C., Utecht, M., Zhao, F., Kulla, H., Kovalenko, S., Brouwer, A.M., Saalfrank, P., Hecht, S., and Bléger, D. (2014). *ortho*-Fluoroazobenzenes: visible light switches with very long-lived *Z* isomers. Chem. Eur. J. *20*, 16492–16501.

45. Yang, Y., Hughes, R.P., and Aprahamian, I. (2014). Near-infrared light activated azo-BF_2 switches. J. Am. Chem. Soc. *136*, 13190–13193.

46. Yang, Y., Hughes, R.P., and Aprahamian, I. (2012). Visible light switching of a BF_2 -coordinated azo compound. J. Am. Chem. Soc. *134*, 15221–15224.

47. Greb, L., Eichhöfer, A., and Lehn, J.-M. (2016). Internal C-C bond rotation in photoisomers of α-bisimines: a light-responsive two-step molecular speed regulator based on double imine photoswitching. Eur. J. Org. Chem. *2016*, 1243–1246.

48. Huang, C.-Y., Bonasera, A., Hristov, L., Garmshausen, Y., Schmidt, B.M., Jacquemin, D., and Hecht, S. (2017). *N,N'*-Disubstituted indigos as readily available red-light photoswitches with tunable thermal half-lives. J. Am. Chem. Soc. *139*, 15205–15211.

49. Chaur, M.N., Collado, D., and Lehn, J.-M. (2011). Configurational and constitutional information storage: multiple dynamics in systems based on pyridyl and acyl hydrazones. Chem. Eur. J. *17*, 248–258.

50. van Dijken, D.J., Kovaříček, P., Ihrig, S.P., and Hecht, S. (2015). Acylhydrazones as widely tunable photoswitches. J. Am. Chem. Soc. *137*, 14982–14991.

51. Irie, M., and Mohri, M. (1988). Thermally irreversible photochromic systems. Reversible photocyclization of diarylethene derivatives. J. Org. Chem. *53*, 803–808.

52. Blattmann, H.-R., Meuche, D., Heilbronner, E., Molyneux, R.J., and Boekelheide, V. (1965). Photoisomerization of trans-15,16-dimethyldihydropyrene. J. Am. Chem. Soc. *87*, 130–131.

53. Helmy, S., Leibfarth, F.A., Oh, S., Poelma, J.E., Hawker, C.J., and Read de Alaniz, J. (2014). Photoswitching using visible light: a new class of organic photochromic molecules. J. Am. Chem. Soc. *136*, 8169–8172.

54. Mallory, F.B., Wood, C.S., and Gordon, J.T. (1964). Photochemistry of stilbenes. III. Some aspects of the mechanism of photocyclization to phenanthrenes. J. Am. Chem. Soc. *86*, 3094–3102.

55. Tsivgoulis, G.M., and Lehn, J.-M. (1997). Multiplexing optical systems: multicolor-bifluorescent-biredox photochromic mixtures. Adv. Mater. *9*, 627–630.

56. Klajn, R. (2014). Spiropyran-based dynamic materials. Chem. Soc. Rev. *43*, 148–184.

57. Mitchell, R.H. (1999). The metacyclophanediene-dihydropyrene photochromic π switch. Eur. J. Org. Chem. *1999*, 2695–2703.

58. Klaue, K., Han, W., Liesfeld, P., Berger, F., Garmshausen, Y., and Hecht, S. (2020). Donor–acceptor dihydropyrenes switchable with near-infrared light. J. Am. Chem. Soc. *142*, 11857–11864.

59. Weinstain, R., Slanina, T., Kand, D., and Klán, P. (2020). Visible-to-NIR-light activated release: from small molecules to nanomaterials. Chem. Rev. *120*, 13135–13272.

60. Josa-Culleré, L., and Llebaria, A. (2021). In the search for photocages cleavable with visible light: an overview of recent advances and chemical strategies. ChemPhotoChem *5*, 296–314. https://doi.org/10.1002/cptc.202000253.

61. Barton, D.H.R., Chow, Y.L., Cox, A., and Kirby, G.W. (1962). Photosensitive protection of functional groups. Tetrahedron Lett. *3*, 1055–1057.

62. Patchornik, A., Amit, B., and Woodward, R.B. (1970). Photosensitive protecting groups. J. Am. Chem. Soc. *92*, 6333–6335.

63. Hasan, A., Stengele, K.-P., Giegrich, H., Cornwell, P., Isham, K.R., Sachleben, R.A., Pfleiderer, W., and Foote, R.S. (1997). Photolabile protecting groups for nucleosides: synthesis and photodeprotection rates. Tetrahedron *53*, 4247–4264.

64. Berroy, P., Viriot, M.L., and Carré, M.C. (2001). Photolabile group for 5′-OH protection of nucleosides: synthesis and photodeprotection rate. Sens. Actuators B Chem. *74*, 186–189.

65. García-Fernández, L., Herbivo, C., Arranz, V.S.M., Warther, D., Donato, L., Specht, A., and del Campo, A. (2014). Dual photosensitive polymers with wavelength-selective photoresponse. Adv. Mater. *26*, 5012–5017.

66. Reichmanis, E., Smith, B.C., and Gooden, R. (1985). O-nitrobenzyl photochemistry: solution versus solid-state behavior. J. Polym. Sci. Polym. Chem. Ed. *23*, 1–8.

67. Beier, M. (2000). Production by quantitative photolithographic synthesis of individually quality checked DNA microarrays. Nucleic Acids Res. *28*, 11e–111.

68. Givens, R.S., and Park, C.-H. (1996). p-Hydroxyphenacyl ATP1: a new phototrigger. Tetrahedron Lett. *37*, 6259–6262.

69. Park, C.-H., and Givens, R.S. (1997). New photoactivated protecting groups. 6. *p*-hydroxyphenacyl: a phototrigger for chemical and biochemical probes. J. Am. Chem. Soc. *119*, 2453–2463.

70. Zhang, K., Corrie, J.E.T., Munasinghe, V.R.N., and Wan, P. (1999). Mechanism of photosolvolytic rearrangement of *p*-hydroxyphenacyl esters: evidence for excited-state intramolecular proton transfer as the primary photochemical step. J. Am. Chem. Soc. *121*, 5625–5632.

71. Chen, X., Ma, C., Kwok, W.M., Guan, X., Du, Y., and Phillips, D.L. (2006). A theoretical investigation of *p*-hydroxyphenacyl caged phototrigger compounds: an examination of the excited state photochemistry of *p*-hydroxyphenacyl acetate. J. Phys. Chem. A *110*, 12406–12413.

72. Givens, R.S., Rubina, M., and Wirz, J. (2012). Applications of p-hydroxyphenacyl (pHP) and coumarin-4-ylmethyl photoremovable protecting groups. Photochem. Photobiol. Sci. *11*, 472.

73. Remeš, M., Roithová, J., Schröder, D., Cope, E.D., Perera, C., Senadheera, S.N., Stensrud, K., Ma, C., and Givens, R.S. (2011). Gas-phase fragmentation of deprotonated *p*-hydroxyphenacyl derivatives. J. Org. Chem. *76*, 2180–2186.

74. Arabaci, G., Guo, X.-C., Beebe, K.D., Coggeshall, K.M., and Pei, D. (1999). α-Haloacetophenone derivatives as photoreversible covalent inhibitors of protein tyrosine phosphatases. J. Am. Chem. Soc. *121*, 5085–5086.

75. Zou, K., Cheley, S., Givens, R.S., and Bayley, H. (2002). Catalytic subunit of protein kinase A caged at the activating phosphothreonine. J. Am. Chem. Soc. *124*, 8220–8229.

76. Jana, A., Atta, S., Sarkar, S.K., and Singh, N.D.P. (2010). 1-Acetylpyrene with dual functions as an environment-sensitive fluorophore and fluorescent photoremovable protecting group. Tetrahedron *66*, 9798–9807.

77. Wang, P., Hu, H., and Wang, Y. (2007). Novel photolabile protecting group for carbonyl compounds. Org. Lett. *9*, 1533–1535.

78. Yang, H., Zhang, X., Zhou, L., and Wang, P. (2011). Development of a photolabile carbonyl-protecting group toolbox. J. Org. Chem. *76*, 2040–2048.

79. Givens, R.S., and Matuszewski, B. (1984). Photochemistry of phosphate esters: an efficient method for the generation of electrophiles. J. Am. Chem. Soc. *106*, 6860–6861.

80. Bojtár, M., Kormos, A., Kis-Petik, K., Kellermayer, M., and Kele, P. (2019). Green-light activatable, water-soluble red-shifted coumarin photocages. Org. Lett. *21*, 9410–9414.

81. Lin, Q., Yang, L., Wang, Z., Hua, Y., Zhang, D., Bao, B., Bao, C., Gong, X., and Zhu, L. (2018). Coumarin photocaging groups modified with an electron-rich styryl moiety at the 3-position: long-wavelength excitation, rapid photolysis, and photobleaching. Angew. Chem. Int. Ed. *57*, 3722–3726.

82. Eckardt, T., Hagen, V., Schade, B., Schmidt, R., Schweitzer, C., and Bendig, J. (2002). Deactivation behavior and excited-state properties of (coumarin-4-yl)methyl derivatives. 2. photocleavage of selected (coumarin-4-yl)methyl-caged adenosine cyclic 3′,5′-monophosphates with fluorescence enhancement. J. Org. Chem. *67*, 703–710.

83. Fournier, L., Gauron, C., Xu, L., Aujard, I., Le Saux, T., Gagey-Eilstein, N., Maurin, S., Dubruille, S., Baudin, J.-B., Bensimon, D., et al. (2013). A blue-absorbing photolabile protecting group for *in vivo* chromatically orthogonal photoactivation. ACS Chem. Biol. *8*, 1528–1536.

84. Olson, J.P., Kwon, H.-B., Takasaki, K.T., Chiu, C.Q., Higley, M.J., Sabatini, B.L., and Ellis-Davies, G.C.R. (2013). Optically selective two-photon uncaging of glutamate at 900 nm. J. Am. Chem. Soc. *135*, 5954–5957.

85. Goswami, P.P., Syed, A., Beck, C.L., Albright, T.R., Mahoney, K.M., Unash, R., Smith, E.A., and Winter, A.H. (2015). BODIPY-derived photoremovable protecting groups unmasked with green light. J. Am. Chem. Soc. *137*, 3783–3786.

86. Rubinstein, N., Liu, P., Miller, E.W., and Weinstain, R. (2015). meso-Methylhydroxy BODIPY: a scaffold for photo-labile protecting groups. Chem. Commun. *51*, 6369–6372.

87. Slanina, T., Shrestha, P., Palao, E., Kand, D., Peterson, J.A., Dutton, A.S., Rubinstein, N., Weinstain, R., Winter, A.H., and Klán, P. (2017). In search of the perfect photocage: structure–reactivity relationships in *meso*-methyl BODIPY photoremovable protecting groups. J. Am. Chem. Soc. *139*, 15168–15175.

88. Shrestha, P., Dissanayake, K.C., Gehrmann, E.J., Wijesooriya, C.S., Mukhopadhyay, A., Smith, E.A., and Winter, A.H. (2020). Efficient far-red/near-IR absorbing BODIPY photocages by blocking unproductive conical intersections. J. Am. Chem. Soc. *142*, 15505–15512.

89. Zayat, L., Calero, C., Alborés, P., Baraldo, L., and Etchenique, R. (2003). A new strategy for neurochemical photodelivery: metal-ligand heterolytic cleavage. J. Am. Chem. Soc. *125*, 882–883.

90. Zayat, L., Salierno, M., and Etchenique, R. (2006). Ruthenium(II) bipyridyl complexes as photolabile caging groups for amines. Inorg. Chem. *45*, 1728–1731.

91. Rodgers, Z.L., Hughes, R.M., Doherty, L.M., Shell, J.R., Molesky, B.P., Brugh, A.M., Forbes, M.D.E., Moran, A.M., and Lawrence, D.S. (2015). B_{12}-mediated, long wavelength photopolymerization of hydrogels. J. Am. Chem. Soc. *137*, 3372–3378.

92. Anderson, E.D., Gorka, A.P., and Schnermann, M.J. (2016). Near-infrared uncaging or photosensitizing dictated by oxygen tension. Nat. Commun. *7*, 13378.

93. Wang, X., and Kalow, J.A. (2018). Rapid aqueous photouncaging by red light. Org. Lett. *20*, 1716–1719.

94. Kolb, H.C., Finn, M.G., and Barry Sharpless, K. (2001). Click chemistry: diverse chemical function from a few good reactions. Angew. Chem. Int. Ed. *40*, 2004.

95. Tasdelen, M.A., and Yagci, Y. (2013). Light-induced click reactions. Angew. Chem. Int. Ed. *52*, 5930–5938.

96. Yang, N.C., and Rivas, C. (1961). A new photochemical primary process, the photochemical enolization of o-substituted benzophenones. J. Am. Chem. Soc. *83*, 2213.

97. Arnold, B.J., Mellows, S.M., Sammes, P.G., and Wallace, T.W. (1974). Photochemical reactions. Part II. Cycloaddition reactions with photoenols from 2-methylbenzaldehyde and related systems. J. Chem. Soc. Perkin *1*, 401.

98. Feist, F., Rodrigues, L.L., Walden, S.L., Krappitz, T.W., Dargaville, T.R., Weil, T., Goldmann, A.S., Blinco, J.P., and Barner-Kowollik, C. (2020). Light-induced ligation of *o*-quinodimethanes with gated fluorescence self-reporting. J. Am. Chem. Soc. *142*, 7744–7748.

99. Feist, F., Menzel, J.P., Weil, T., Blinco, J.P., and Barner-Kowollik, C. (2018). Visible light-induced ligation via *o*-quinodimethane thioethers. J. Am. Chem. Soc. *140*, 11848–11854.

100. Clovis, J.S., Eckell, A., Huisgen, R., and Sustmann, R. (1967). 1.3-Dipolare cycloadditionen, XXV. Der Nachweis des freien Diphenylnitrilimins als Zwischenstufe bei Cycloadditionen. Chem. Ber. *100*, 60–70.

101. Song, W., Wang, Y., Qu, J., Madden, M.M., and Lin, Q. (2008). A photoinducible 1,3-dipolar cycloaddition reaction for rapid, selective modification of tetrazole-containing proteins. Angew. Chem. Int. Ed. *47*, 2832–2835.

102. Offenloch, J.T., Gernhardt, M., Blinco, J.P., Frisch, H., Mutlu, H., and Barner-Kowollik, C. (2019). Contemporary photoligation chemistry: the visible light challenge. Chem. Eur. J. *25*, 3700–3709.

103. Padwa, A., Dharan, M., Smolanoff, J., and Wetmore, S.I. (1973). Recent advances in the photochemistry of the carbon-nitrogen double bond. Pure Appl. Chem. *33*, 269–284.

104. Claus, P., Doppler, Th., Gakis, N., Georgarakis, M., Giezendanner, H., Gilgen, P., Heimgartner, H., Jackson, B., Märky, M., Narasimhan, N.S., et al. (1973). Photochemistry of some heterocyclic systems. Pure Appl. Chem. *33*, 339–362.

105. Mueller, J.O., Schmidt, F.G., Blinco, J.P., and Barner-Kowollik, C. (2015). Visible-light-induced click chemistry. Angew. Chem. Int. Ed. *54*, 10284–10288.

106. Vedejs, E., Eberlein, T.H., Mazur, D.J., McClure, C.K., Perry, D.A., Ruggeri, R., Schwartz, E., Stults, J.S., and Varie, D.L. (1986). Thioaldehyde Diels-Alder reactions. J. Org. Chem. *51*, 1556–1562.

107. Fritzsche. (1867). Ueber die festen Kohlenwasserstoffe des Steinkohlentheers. J. Für Prakt. Chem. *101*, 333–343.

108. Bouas-Laurent, H., Desvergne, J.-P., Castellan, A., and Lapouyade, R. (2001). Photodimerization of anthracenes in fluid solutions: (part 2) mechanistic aspects of the photocycloaddition and of the photochemical and thermal cleavage. Chem. Soc. Rev. *30*, 248–263.

109. Dvornikov, A.S., Bouas-Laurent, H., Desvergne, J.-P., and Rentzepis, P.M. (1999). Ultrafast kinetics of 9-decylanthracene photodimers and their application to 3D optical storage. J. Mater. Chem. *9*, 1081–1084.

110. Wells, L.A., Furukawa, S., and Sheardown, H. (2011). Photoresponsive PEG-anthracene grafted hyaluronan as a controlled-delivery biomaterial. Biomacromolecules *12*, 923–932.

111. Rumer, J.W., and McCulloch, I. (2015). Organic photovoltaics: crosslinking for optimal morphology and stability. Mater. Today *18*, 425–435.

112. Kjell, D.P., and Sheridan, R.S. (1984). Photochemical cycloaddition of N-methyltriazolinedione to naphthalene. J. Am. Chem. Soc. *106*, 5368–5370.

113. Houck, H.A., Blasco, E., Du Prez, F.E., and Barner-Kowollik, C. (2019). Light-stabilized dynamic materials. J. Am. Chem. Soc. *141*, 12329–12337.

114. Szymański, W., Beierle, J.M., Kistemaker, H.A.V., Velema, W.A., and Feringa, B.L. (2013). Reversible photocontrol of biological systems by the incorporation of molecular photoswitches. Chem. Rev. *113*, 6114–6178.

115. Xu, D., Bartelt, S.M., Rasoulinejad, S., Chen, F., and Wegner, S.V. (2019). Green light lithography: a general strategy to create active protein and cell micropatterns. Mater. Horiz. *6*, 1222–1229.

116. Kovalenko, N.P., Abdukadirov, A., Gerko, V.I., and Alfimov, M.V. (1980). Some peculiarities of diarylethylenes with 3-pyrenyl fragments. J. Appl. Spectrosc. *32*, 607–612.

117. Kovalenko, N.P., Abdukadyrov, A.T., Gerko, V.I., and Alfimov, M.V. (1980). Luminescent and photochemical behaviour of diarylethylenes with 3-pyrenyl substituents. J. Photochem. *12*, 59–65.

118. Marschner, D.E., Frisch, H., Offenloch, J.T., Tuten, B.T., Becer, C.R., Walther, A., Goldmann, A.S., Tzvetkova, P., and Barner-Kowollik, C. (2018). Visible light [2 + 2] cycloadditions for reversible polymer ligation. Macromolecules *51*, 3802–3807.

119. Kalayci, K., Frisch, H., Truong, V.X., and Barner-Kowollik, C. (2020). Green light triggered [2+2] cycloaddition of halochromic styrylquinoxaline—controlling photoreactivity by pH. Nat. Commun. *11*, 4193.

120. Boase, N.R.B. (2020). Shining a light on bioorthogonal photochemistry for polymer science. Macromol. Rapid Commun. *41*, 2000305.

121. Sangermano, M., Roppolo, I., and Chiappone, A. (2018). New horizons in cationic photopolymerization. Polymers *10*, 136.

122. Zivic, N., Bouzrati-Zerelli, M., Kermagoret, A., Dumur, F., Fouassier, J.-P., Gigmes, D., and Lalevée, J. (2016). Photocatalysts in polymerization reactions. ChemCatChem *8*, 1617–1631.

123. Chen, M., Zhong, M., and Johnson, J.A. (2016). Light-controlled radical polymerization: mechanisms, methods, and applications. Chem. Rev. *116*, 10167–10211.

124. Leibfarth, F.A., Mattson, K.M., Fors, B.P., Collins, H.A., and Hawker, C.J. (2013). External regulation of controlled polymerizations. Angew. Chem. Int. Ed. *52*, 199–210.

125. Michaudel, Q., Kottisch, V., and Fors, B.P. (2017). Cationic polymerization: from photoinitiation to photocontrol. Angew. Chem. Int. Ed. *56*, 9670–9679.

126. Fors, B.P., and Hawker, C.J. (2012). Control of a living radical polymerization of methacrylates by light. Angew. Chem. Int. Ed. *51*, 8850–8853.

127. Treat, N.J., Sprafke, H., Kramer, J.W., Clark, P.G., Barton, B.E., Read de Alaniz, J., Fors, B.P., and Hawker, C.J. (2014). Metal-free atom transfer radical polymerization. J. Am. Chem. Soc. *136*, 16096–16101.

128. Discekici, E.H., Anastasaki, A., Read de Alaniz, J., and Hawker, C.J. (2018). Evolution and future directions of metal-free atom transfer radical polymerization. Macromolecules *51*, 7421–7434.

129. Theriot, J.C., Lim, C.-H., Yang, H., Ryan, M.D., Musgrave, C.B., and Miyake, G.M. (2016). Organocatalyzed atom transfer radical polymerization driven by visible light. Science *352*, 1082–1086.

130. Xu, J., Jung, K., Atme, A., Shanmugam, S., and Boyer, C. (2014). A robust and versatile photoinduced living polymerization of conjugated and unconjugated monomers and its oxygen tolerance. J. Am. Chem. Soc. *136*, 5508–5519.

131. Phommalysack-Lovan, J., Chu, Y., Boyer, C., and Xu, J. (2018). PET-RAFT polymerisation: towards green and precision polymer manufacturing. Chem. Commun. *54*, 6591–6606.

132. Otsu, T., and Yoshida, M. (1982). Role of initiator-transfer agent-terminator (iniferter) in radical polymerizations: polymer design by

organic disulfides as iniferters. Makromol. Chem. Rapid Commun. *3*, 127–132.

133. Otsu, T., Yoshida, M., and Tazaki, T. (1982). A model for living radical polymerization. Makromol. Chem. Rapid Commun. *3*, 133–140.

134. Neilson, B.M., and Bielawski, C.W. (2013). Photoswitchable NHC-promoted ring-opening polymerizations. Chem. Commun. *49*, 5453.

135. Fu, C., Xu, J., and Boyer, C. (2016). Photoacid-mediated ring opening polymerization driven by visible light. Chem. Commun. *52*, 7126–7129.

136. Eisenreich, F., Kathan, M., Dallmann, A., Ihrig, S.P., Schwaar, T., Schmidt, B.M., and Hecht, S. (2018). A photoswitchable catalyst system for remote-controlled (co)polymerization in situ. Nat. Catal. *1*, 516–522.

137. Theunissen, C., Ashley, M.A., and Rovis, T. (2019). Visible-light-controlled ruthenium-catalyzed olefin metathesis. J. Am. Chem. Soc. *141*, 6791–6796.

138. Eivgi, O., Phatake, R.S., Nechmad, N.B., and Lemcoff, N.G. (2020). Light-activated olefin metathesis: catalyst development, synthesis, and applications. Acc. Chem. Res. *53*, 2456–2471.

139. Ogawa, K.A., Goetz, A.E., and Boydston, A.J. (2015). Metal-free ring-opening metathesis polymerization. J. Am. Chem. Soc. *137*, 1400–1403.

140. Lu, P., Kensy, V.K., Tritt, R.L., Seidenkranz, D.T., and Boydston, A.J. (2020). Metal-free ring-opening metathesis polymerization: from concept to creation. Acc. Chem. Res. *53*, 2325–2335.

141. Shanmugam, S., Xu, J., and Boyer, C. (2015). Exploiting metalloporphyrins for selective living radical polymerization tunable over visible wavelengths. J. Am. Chem. Soc. *137*, 9174–9185.

142. Ohtsuki, A., Lei, L., Tanishima, M., Goto, A., and Kaji, H. (2015). Photocontrolled organocatalyzed living radical polymerization feasible over a wide range of wavelengths. J. Am. Chem. Soc. *137*, 5610–5617.

143. Kottisch, V., Michaudel, Q., and Fors, B.P. (2017). Photocontrolled interconversion of cationic and radical polymerizations. J. Am. Chem. Soc. *139*, 10665–10668.

144. Romero, N.A., and Nicewicz, D.A. (2016). Organic photoredox catalysis. Chem. Rev. *116*, 10075–10166.

145. Prier, C.K., Rankic, D.A., and MacMillan, D.W.C. (2013). Visible light photoredox catalysis with transition metal complexes: applications in organic synthesis. Chem. Rev. *113*, 5322–5363.

146. Xu, J., Shanmugam, S., Fu, C., Aguey-Zinsou, K.-F., and Boyer, C. (2016). Selective photoactivation: from a single unit monomer insertion reaction to controlled polymer architectures. J. Am. Chem. Soc. *138*, 3094–3106.

147. Shanmugam, S., Cuthbert, J., Kowalewski, T., Boyer, C., and Matyjaszewski, K. (2018). Catalyst-free selective photoactivation of RAFT polymerization: a facile route for preparation of comblike and bottlebrush polymers. Macromolecules *51*, 7776–7784.

148. Shanmugam, S., Cuthbert, J., Flum, J., Fantin, M., Boyer, C., Kowalewski, T., and Matyjaszewski, K. (2019). Transformation of gels *via* catalyst-free selective RAFT photoactivation. Polym. Chem. *10*, 2477–2483.

149. Zhao, Y., Ma, M., Lin, X., and Chen, M. (2020). Photoorganocatalyzed divergent reversible deactivation radical polymerization toward linear and branched fluoropolymers. Angew. Chem. Int. Ed. *59*, 21470–21474.

150. Frisch, H., Mundsinger, K., Poad, B.L.J., Blanksby, S.J., and Barner-Kowollik, C. (2020). Wavelength-gated photoreversible polymerization and topology control. Chem. Sci. *11*, 2834–2842.

151. Xu, S., Yeow, J., and Boyer, C. (2018). Exploiting wavelength orthogonality for successive photoinduced polymerization-induced self-assembly and photo-crosslinking. ACS Macro Lett. *7*, 1376–1382.

152. Bagheri, A., Yeow, J., Arandiyan, H., Xu, J., Boyer, C., and Lim, M. (2016). Polymerization of a photocleavable monomer using visible light. Macromol. Rapid Commun. *37*, 905–910.

153. Molle, E., Le, D., Norizadeh Abbariki, T., Akdemir, M.S., Takamiya, M., Miceli, E., Kassel, O., and Delaittre, G. (2019). Access to photoreactive core-shell nanomaterials by photoinitiated polymerization-induced self-assembly. ChemPhotoChem *3*, 1084–1089.

154. Delafresnaye, L., Jung, K., Boyer, C., and Barner-Kowollik, C. (2020). Two colours of light drive PET-RAFT photoligation. Polym. Chem. *11*, 6453–6462.

155. Russew, M.-M., and Hecht, S. (2010). Photoswitches: from molecules to materials. Adv. Mater. *22*, 3348–3360.

156. Gohy, J.-F., and Zhao, Y. (2013). Photo-responsive block copolymer micelles: design and behavior. Chem. Soc. Rev. *42*, 7117.

157. Habault, D., Zhang, H., and Zhao, Y. (2013). Light-triggered self-healing and shape-memory polymers. Chem. Soc. Rev. *42*, 7244.

158. Orgiu, E., and Samorì, P. (2014). 25th anniversary article: organic electronics marries photochromism: generation of multifunctional interfaces, materials, and devices. Adv. Mater. *26*, 1827–1845.

159. Abdollahi, A., Roghani-Mamaqani, H., and Razavi, B. (2019). Stimuli-chromism of photoswitches in smart polymers: recent advances and applications as chemosensors. Prog. Polym. Sci. *98*, 101149.

160. Goulet-Hanssens, A., Eisenreich, F., and Hecht, S. (2020). Enlightening materials with photoswitches. Adv. Mater. *32*, 1905966.

161. Nie, H., Self, J.L., Kuenstler, A.S., Hayward, R.C., and Read de Alaniz, J. (2019). Multiaddressable photochromic architectures: from molecules to materials. Adv. Opt. Mater. *7*, 1900224.

162. Pianowski, Z.L. (2019). Recent implementations of molecular photoswitches into smart materials and biological systems. Chem. – Eur. J. *25*, 5128–5144.

163. Ulrich, S., Hemmer, J.R., Page, Z.A., Dolinski, N.D., Rifaie-Graham, O., Bruns, N., Hawker, C.J., Boesel, L.F., and Read de Alaniz, J. (2017). Visible light-responsive DASA-polymer Conjugates. ACS Macro Lett. *6*, 738–742.

164. Kim, S., Yoon, S.-J., and Park, S.Y. (2012). Highly fluorescent chameleon nanoparticles and polymer films: multicomponent organic systems that combine FRET and photochromic switching. J. Am. Chem. Soc. *134*, 12091–12097.

165. Kim, D., Jeong, K., Kwon, J.E., Park, H., Lee, S., Kim, S., and Park, S.Y. (2019). Dual-color fluorescent nanoparticles showing perfect color-specific photoswitching for bioimaging and super-resolution microscopy. Nat. Commun. *10*, 3089.

166. Andersson, P., Robinson, N.D., and Berggren, M. (2005). Switchable charge traps in polymer diodes. Adv. Mater. *17*, 1798–1803.

167. Zacharias, P., Gather, M.C., Köhnen, A., Rehmann, N., and Meerholz, K. (2009). Photoprogrammable organic light-emitting diodes. Angew. Chem. Int. Ed. *48*, 4038–4041.

168. Zhang, Z., Liu, X., Li, Z., Chen, Z., Zhao, F., Zhang, F., and Tung, C.-H. (2008). A smart light-controlled carrier switch in an organic light emitting device. Adv. Funct. Mater. *18*, 302–307.

169. Orgiu, E., Crivillers, N., Herder, M., Grubert, L., Pätzel, M., Frisch, J., Pavlica, E., Duong, D.T., Bratina, G., Salleo, A., et al. (2012). Optically switchable transistor via energy-level phototuning in a bicomponent organic semiconductor. Nat. Chem. *4*, 675–679.

170. Leydecker, T., Herder, M., Pavlica, E., Bratina, G., Hecht, S., Orgiu, E., and Samorì, P. (2016). Flexible non-volatile optical memory thin-film transistor device with over 256 distinct levels based on an organic bicomponent blend. Nat. Nanotechnol. *11*, 769–775.

171. Hou, L., Zhang, X., Cotella, G.F., Carnicella, G., Herder, M., Schmidt, B.M., Pätzel, M., Hecht, S., Cacialli, F., and Samorì, P. (2019). Optically switchable organic light-emitting transistors. Nat. Nanotechnol. *14*, 347–353.

172. Hou, L., Leydecker, T., Zhang, X., Rekab, W., Herder, M., Cendra, C., Hecht, S., McCulloch, I., Salleo, A., Orgiu, E., et al. (2020). Engineering optically switchable transistors with improved performance by controlling interactions of diarylethenes in polymer matrices. J. Am. Chem. Soc. *142*, 11050–11059.

173. Nie, H., Schauser, N.S., Dolinski, N.D., Hu, J., Hawker, C.J., Segalman, R.A., and Read de Alaniz, J. (2020). Light-controllable ionic conductivity in a polymeric ionic liquid. Angew. Chem. Int. Ed. *59*, 5123–5128.

174. Nie, H., Schauser, N.S., Dolinski, N.D., Geng, Z., Oh, S., Chabinyc, M.L., Hawker, C.J., Segalman, R.A., and Read de Alaniz, J. (2021). The role of anions in light-driven conductivity in diarylethene-containing polymeric ionic

liquids. Polym. Chem. *12*, 719–724. https://doi.org/10.1039/D0PY01603A.

175. Nie, H., Schauser, N.S., Self, J.L., Tabassum, T., Oh, S., Geng, Z., Jones, S.D., Zayas, M.S., Reynolds, V.G., Chabinyc, M.L., et al. (2021). Light-switchable and self-healable polymer electrolytes based on dynamic diarylethene and metal-ion coordination. J. Am. Chem. Soc. *143*, 1562–1569.

176. Xie, X., Crespo, G.A., Mistlberger, G., and Bakker, E. (2014). Photocurrent generation based on a light-driven proton pump in an artificial liquid membrane. Nat. Chem. *6*, 202–207.

177. Sperling, L.H. (2006). Introduction to Physical Polymer Science, 4th edition (Wiley).

178. Ikeda, T., and Ube, T. (2011). Photomobile polymer materials: from nano to macro. Mater. Today *14*, 480–487.

179. Zhou, H., Xue, C., Weis, P., Suzuki, Y., Huang, S., Koynov, K., Auernhammer, G.K., Berger, R., Butt, H.-J., and Wu, S. (2017). Photoswitching of glass transition temperatures of azobenzene-containing polymers induces reversible solid-to-liquid transitions. Nat. Chem. *9*, 145–151.

180. Zha, R.H., Vantomme, G., Berrocal, J.A., Gosens, R., de Waal, B., Meskers, S., and Meijer, E.W. (2018). Photoswitchable nanomaterials based on hierarchically organized siloxane oligomers. Adv. Funct. Mater. *28*, 1703952.

181. Kuenstler, A.S., Clark, K.D., Read de Alaniz, J., and Hayward, R.C. (2020). Reversible actuation via photoisomerization-induced melting of a semicrystalline poly(azobenzene). ACS Macro Lett. *9*, 902–909.

182. Accardo, J.V., and Kalow, J.A. (2018). Reversibly tuning hydrogel stiffness through photocontrolled dynamic covalent crosslinks. Chem. Sci. *9*, 5987–5993.

183. Vining, K.H., and Mooney, D.J. (2017). Mechanical forces direct stem cell behaviour in development and regeneration. Nat. Rev. Mol. Cell Biol. *18*, 728–742.

184. Kathan, M., Kovaříček, P., Jurissek, C., Senf, A., Dallmann, A., Thünemann, A.F., and Hecht, S. (2016). Control of imine exchange kinetics with photoswitches to modulate self-healing in polysiloxane networks by light illumination. Angew. Chem. Int. Ed. *55*, 13882–13886.

185. Fuhrmann, A., Göstl, R., Wendt, R., Kötteritzsch, J., Hager, M.D., Schubert, U.S., Brademann-Jock, K., Thünemann, A.F., Nöchel, U., Behl, M., et al. (2016). Conditional repair by locally switching the thermal healing capability of dynamic covalent polymers with light. Nat. Commun. *7*, 13623.

186. Göstl, R., and Hecht, S. (2014). Controlling covalent connection and disconnection with light. Angew. Chem. Int. Ed. *53*, 8784–8787.

187. Gu, Y., Alt, E.A., Wang, H., Li, X., Willard, A.P., and Johnson, J.A. (2018). Photoswitching topology in polymer networks with metal–organic cages as crosslinks. Nature *560*, 65–69.

188. Han, M., Luo, Y., Damaschke, B., Gómez, L., Ribas, X., Jose, A., Peretzki, P., Seibt, M., and Clever, G.H. (2016). Light-controlled interconversion between a self-assembled triangle and a rhombicuboctahedral sphere. Angew. Chem. Int. Ed. *55*, 445–449.

189. Kabb, C.P., O'Bryan, C.S., Deng, C.C., Angelini, T.E., and Sumerlin, B.S. (2018). Photoreversible covalent hydrogels for soft-matter additive manufacturing. ACS Appl. Mater. Interfaces *10*, 16793–16801.

190. Truong, V.X., Li, F., Ercole, F., and Forsythe, J.S. (2018). Wavelength-selective coupling and decoupling of polymer chains via reversible [2 + 2] photocycloaddition of styrylpyrene for construction of cytocompatible photodynamic hydrogels. ACS Macro Lett. *7*, 464–469.

191. Kalayci, K., Frisch, H., Barner-Kowollik, C., and Truong, V.X. (2020). Wavelength-dependent stiffening of hydrogel matrices via redshifted [2+2] photocycloadditions. Adv. Funct. Mater. *30*, 1908171.

192. Rosales, A.M., Vega, S.L., DelRio, F.W., Burdick, J.A., and Anseth, K.S. (2017). Hydrogels with reversible mechanics to probe dynamic cell microenvironments. Angew. Chem. Int. Ed. *56*, 12132–12136.

193. Schenzel, A.M., Moszner, N., and Barner-Kowollik, C. (2017). Disulfone cross-linkers for λ-orthogonal photoinduced curing and degradation of polymeric networks. ACS Macro Lett. *6*, 16–20.

194. Scott, T.F., Draughon, R.B., and Bowman, C.N. (2006). Actuation in crosslinked polymers via photoinduced stress relaxation. Adv. Mater. *18*, 2128–2132.

195. Sowan, N., Song, H.B., Cox, L.M., Patton, J.R., Fairbanks, B.D., Ding, Y., and Bowman, C.N. (2021). Light-activated stress relaxation, toughness improvement, and photoinduced reversal of physical aging in glassy polymer networks. Adv. Mater. *33*, e2007221.

196. Worrell, B.T., McBride, M.K., Lyon, G.B., Cox, L.M., Wang, C., Mavila, S., Lim, C.-H., Coley, H.M., Musgrave, C.B., Ding, Y., et al. (2018). Bistable and photoswitchable states of matter. Nat. Commun. *9*, 2804.

197. Chan, B.P. (2010). Biomedical applications of photochemistry. Tissue Eng. Part B Rev. *16*, 509–522.

198. Rapp, T.L., and DeForest, C.A. (2020). Visible light-responsive dynamic biomaterials: going deeper and triggering more. Adv. Healthc. Mater. *9*, 1901553.

199. Jeong, M., Park, J., and Kwon, S. (2020). Molecular switches and motors powered by orthogonal stimuli. Eur. J. Org. Chem. *2020*, 7254–7283.

200. Azagarsamy, M.A., and Anseth, K.S. (2013). Wavelength-controlled photocleavage for the orthogonal and sequential release of multiple proteins. Angew. Chem. Int. Ed. *52*, 13803–13807.

201. Truong, V.X., Li, F., and Forsythe, J.S. (2017). Photolabile hydrogels responsive to broad spectrum visible light for selective cell release. ACS Appl. Mater. Interfaces *9*, 32441–32445.

202. DeForest, C.A., and Anseth, K.S. (2012). Photoreversible patterning of biomolecules within click-based hydrogels. Angew. Chem. Int. Ed. *51*, 1816–1819.

203. Haydell, M.W., Centola, M., Adam, V., Valero, J., and Famulok, M. (2018). Temporal and reversible control of a DNAzyme by orthogonal photoswitching. J. Am. Chem. Soc. *140*, 16868–16872.

204. Škugor, M., Valero, J., Murayama, K., Centola, M., Asanuma, H., and Famulok, M. (2019). Orthogonally photocontrolled non-autonomous DNA walker. Angew. Chem. Int. Ed. *58*, 6948–6951.

205. Yamano, Y., Murayama, K., and Asanuma, H. (2020). Dual crosslinking photo-switches for orthogonal photo-control of hybridization between serinol nucleic acid and RNA. Chem. Eur. J. Chem. *27*, 4599–4604.

206. Scott, T.F., Kowalski, B.A., Sullivan, A.C., Bowman, C.N., and McLeod, R.R. (2009). Two-color single-photon photoinitiation and photoinhibition for subdiffraction photolithography. Science *324*, 913–917.

207. Li, N., Gattass, R.R., Gershgoren, E., Hwang, H., and Fourkas, J.T. (2009). Achieving 1/20 resolution by one-color initiation and deactivation of polymerization. Science *324*, 910–913.

208. Andrew, T.L., Tsai, H.-Y., and Menon, R. (2009). Confining light to deep subwavelength dimensions to enable optical nanopatterning. Science *324*, 917–921.

209. Cao, Y., Gan, Z., Jia, B., Evans, R.A., and Gu, M. (2011). High-photosensitive resin for super-resolution direct-laser-writing based on photoinhibited polymerization. Opt. Express *19*, 19486.

210. Gan, Z., Cao, Y., Evans, R.A., and Gu, M. (2013). Three-dimensional deep sub-diffraction optical beam lithography with 9 nm feature size. Nat. Commun. *4*, 1–7.

211. Mueller, P., Zieger, M.M., Richter, B., Quick, A.S., Fischer, J., Mueller, J.B., Zhou, L., Nienhaus, G.U., Bastmeyer, M., Barner-Kowollik, C., et al. (2017). Molecular switch for sub-diffraction laser lithography by photoenol intermediate-state cis-trans isomerization. ACS Nano *11*, 6396–6403.

212. Müller, P., Müller, R., Hammer, L., Barner-Kowollik, C., Wegener, M., and Blasco, E. (2019). STED-inspired laser lithography based on photoswitchable spirothiopyran moieties. Chem. Mater. *31*, 1966–1972.

213. Zhang, X., Xi, W., Huang, S., Long, K., and Bowman, C.N. (2017). Wavelength-selective sequential polymer network formation controlled with a two-color responsive initiation system. Macromolecules *50*, 5652–5660.

214. Krappitz, T., Feist, F., Lamparth, I., Moszner, N., John, H., Blinco, J.P., Dargaville, T.R., and Barner-Kowollik, C. (2019). Polymer networks based on photo-caged diene dimerization. Mater. Horiz. *6*, 81–89.

215. Bialas, S., Michalek, L., Marschner, D.E., Krappitz, T., Wegener, M., Blinco, J., Blasco, E., Frisch, H., and Barner-Kowollik, C. (2019). Access to disparate soft matter materials by

curing with two colors of light. Adv. Mater. *31*, 1807288.

216. Michalek, L., Bialas, S., Walden, S.L., Bloesser, F.R., Frisch, H., and Barner-Kowollik, C. (2020). 2D fabrication of tunable responsive interpenetrating polymer networks from a single photoresist. Adv. Funct. Mater. *2005328*, 1–7.

217. Truby, R.L., and Lewis, J.A. (2016). Printing soft matter in three dimensions. Nature *540*, 371–378.

218. Bagheri, A., and Jin, J. (2019). Photopolymerization in 3D printing. ACS Appl. Polym. Mater. *1*, 593–611.

219. Rafiee, M., Farahani, R.D., and Therriault, D. (2020). Multi-material 3D and 4D printing: a Survey. Adv. Sci. *7*, 1–26.

220. Zhou, C., Chen, Y., Yang, Z., and Khoshnevis, B. (2013). Digital material fabrication using mask-image-projection-based stereolithography. Rapid Prototyp. J. *19*, 153–165.

221. Dunn, C.K., Dunn, M.L., Sakhaei, A.H., Fang, N.X., Lee, H., and Ge, Q. (2016). Multimaterial 4D printing with tailorable shape memory polymers. Sci. Rep.

222. Dolinski, N.D., Page, Z.A., Callaway, E.B., Eisenreich, F., Garcia, R.V., Chavez, R., Bothman, D.P., Hecht, S., Zok, F.W., and Hawker, C.J. (2018). Solution mask liquid lithography (SMaLL) for one-step, multimaterial 3D printing. Adv. Mater. *30*, 1800364.

223. Gockowski, L.F., Dolinski, N.D., Chavez, R., Cohen, N., Eisenreich, F., Hecht, S., McMeeking, R.M., Hawker, C.J., and Valentine, M.T. (2020). Engineering crack tortuosity in printed polymer-polymer composites through ordered pores. Mater. Horiz. *7*, 1854–1860.

224. Dolinski, N.D., Callaway, E.B., Sample, C.S., Gockowski, L.F., Chavez, R., Page, Z.A., et al. (2021). Tough Multimaterial Interfaces through Wavelength-Selective 3D Printing. ACS Appl. Mater. Interfaces *13*, 22065–22072.

225. Schwartz, J.J., and Boydston, A.J. (2019). Multimaterial actinic spatial control 3D and 4D printing. Nat. Commun. *10*, 791.

226. Gernhardt, M., Frisch, H., Welle, A., Jones, R., Wegener, M., Blasco, E., and Barner-Kowollik, C. (2020). Multi-material 3D microstructures with photochemically adaptive mechanical properties. J. Mater. Chem. C *8*, 10993–11000.

227. Tumbleston, J.R., Shirvanyants, D., Ermoshkin, N., Janusziewicz, R., Johnson, A.R., Kelly, D., Chen, K., Pinschmidt, R., Rolland, J.P., Ermoshkin, A., et al. (2015). Continuous liquid interface production of 3D objects. Science *347*, 1349–1352.

228. De Beer, M.P., Van Der Laan, H.L., Cole, M.A., Whelan, R.J., Burns, M.A., and Scott, T.F. (2019). Rapid, continuous additive manufacturing by volumetric polymerization inhibition patterning. Sci. Adv. *5*, eaau8723.

229. van der Laan, H.L., Burns, M.A., and Scott, T.F. (2019). Volumetric photopolymerization confinement through dual-wavelength photoinitiation and photoinhibition. ACS Macro Lett. 899–904.

230. Regehly, M., Garmshausen, Y., Reuter, M., König, N.F., Israel, E., Kelly, D.P., Chou, C.-Y., Koch, K., Asfari, B., and Hecht, S. (2020). Xolography for linear volumetric 3D printing. Nature *588*, 620–624.

231. Ichimura, K., and Sakuragi, M. (1988). A spiropyran-iodonium salt system as a two photon radical photoinitiator. J. Polym. Sci. Polym. Lett. Ed. *26*, 185–189.

232. Lee, S.K., and Neckers, D.C. (1991). Two-photon radical-photoinitiator system based on iodinated benzospiropyrans. Chem. Mater. *3*, 858–864.